

Oncology Treatment Discovery

Editors-in-Chief

Vincent J. Cogliano

U.S. Environmental Protection Agency, USA

Chong Li

Chinese Academy of Sciences, China

BIO-BYWORD SCIENTIFIC PUBLISHING PTY LTD

(619 649 400)

Level 10

50 Clarence Street

SYDNEY NSW 2000

Copyright © 2025. Bio-Byword Scientific Publishing Pty Ltd.

Complimentary Copy



Oncology Treatment Discovery

Focus and Scope

Oncology Treatment Discovery is a peer-reviewed, open access journal. It accepts manuscripts relevant to experimental and clinical cancer research. The journal publishes the latest findings in cancer research, including preliminary results, repeated argumentation studies and negative results. The journal welcomes various types of submissions, e.g. research papers, clinical research reports, review articles. Content covers topics that advance clinical practice, challenge the status quo, advocate change in health policy, genomic instability, growth promoting signals, growth inhibitory signals, cell death, tumour microenvironment, carcinogenesis and cancer prevention and tackle issues related to global oncology.

About Publisher

Bio-Byword Scientific Publishing is a fast-growing, peer-reviewed and open access journal publisher, which is located in Sydney, Australia. As a dependable and credible corporation, it promotes and serves a broad range of subject areas for the benefit of humanity. By informing and educating a global community of scholars, practitioners, researchers and students, it endeavors to be the world's leading independent academic and professional publisher. To realize it, it keeps creative and innovative to meet the range of the authors' needs and publish the best of their work.

By cooperating with University of Sydney, University of New South Wales and other world-famous universities, Bio-Byword Scientific Publishing has established a huge publishing system based on hundreds of academic programs, and with a variety of journals in the subjects of medicine, construction, education and electronics.

Publisher Headquarter

BIO-BYWORD SCIENTIFIC PUBLISHING PTY LTD

Level 10

50 Clarence Street

Sydney NSW 2000

Website: www.bbwpublisher.com

Email: info@bbwpublisher.com

Table of Contents

- 1 Clinical Analysis of Endoscopic Esophageal Dilation Combined with Mitomycin in the Treatment of Corrosive Esophageal Stenosis in Children**
Shiwu Yang, Junru Chen, Jun Wu, Fenglong He, Mingxiang Zhang
- 9 Studying the Impact of Skin Dose on Post-Mastectomy Radiotherapy Planning for Breast Cancer**
Wenlan Fu, Yunlong Zhou
- 16 Advances in the Study of mRNA Vaccines and Their Application in Tumor Therapy**
Yuanyuan Zeng
- 24 Establishment and Real-World Application of an Adverse Reaction Monitoring System for Targeted Therapy of Antitumor Drugs**
Xiaoyan Li, Jianfu Zhao, Genshen Ye, Yongjuan Ding, Xi Liu, Zhikun Liang, Qiang Chen
- 30 Research on Ultrasound Diagnosis of Thyroid Nodules: A Bibliometric Analysis**
Xiaodi Chen, Zhiyang Lv
- 41 Investigation of Potential Biological Mechanisms Linking Blood Lipids and Head and Neck Squamous Cell Carcinoma**
Aoxiong Zhou, Jiahao Chen, Yumeng Ou, Jinhai Wu
- 57 Molecular Targets and Developmental Potential of Alkaloid Monomers from Traditional Chinese Medicine as Anticancer Agents**
Beiqi Yang, Tongtong He, Tingting Zhi, Jing Tang
- 66 Esophageal Carcinoma with Small-Cell Neuroendocrine Carcinoma Component and Lymph Node Metastasis Mixed with Poorly Differentiated Squamous Cell Carcinoma: A Rare Case Report**
Binghui Ding, Ling Li
- 73 Exploring the Potential Biological Relationship Between Hypothyroidism and Gastric Cancer: Focus on SH2B3**
Chengju Huang, Aoxiong Zhou, Xin Yang, Xuejun Shen, Jin Wang

Clinical Analysis of Endoscopic Esophageal Dilation Combined with Mitomycin in the Treatment of Corrosive Esophageal Stenosis in Children

Shiwu Yang, Junru Chen, Jun Wu, Fenglong He, Mingxiang Zhang

Kunming Children's Hospital, Kunming 650228, Yunnan, China

Copyright: © 2025 Author(s). This is an open-access article distributed under the terms of the Creative Commons Attribution License (CC BY 4.0), permitting distribution and reproduction in any medium, provided the original work is cited.

Abstract: *Objective:* To explore the clinical application of endoscopic esophageal dilation combined with mitomycin in the treatment of corrosive esophageal stenosis in children. *Methods:* Twenty children with corrosive esophageal stenosis treated in our hospital from August 2023 to March 2025 were selected and divided into an intervention group ($n = 10$, combined with mitomycin) and a control group ($n = 10$, simple dilation) according to the treatment plan. The Stooler swallowing grade, diameter of the stenotic segment, total effective rate, number of dilations, and complications were compared between the two groups before and after treatment. *Results:* After treatment, the swallowing function improved in both groups, but the increase in the diameter of the stenotic segment was greater in the intervention group ($P < 0.05$), and the total effective rate was higher ($P < 0.05$). The average number of dilations in the intervention group (3.20 ± 1.03) was significantly less than that in the control group (5.00 ± 1.63) ($P < 0.05$). There was no statistical difference in the incidence of complications between the two groups, mainly mild bleeding and chest pain. *Conclusion:* Combined mitomycin can improve efficacy, reduce treatment frequency, and has good safety, which is worthy of priority clinical application.

Keywords: Children; Corrosive esophageal stenosis; Endoscopy; Esophageal dilation; Mitomycin

Online publication: September 17, 2025

1. Introduction

As a recognized major public health issue in childhood, corrosive esophageal stricture in children is a serious digestive system disease, mostly caused by accidental ingestion of corrosive substances such as strong acids and alkalis ^[1]. These substances can corrode and invade the esophageal mucosa, inducing inflammatory reactions and ulcers, which can lead to fibrosis and subsequent luminal stenosis, causing feeding difficulties, developmental delays, and even complications such as perforation or mediastinal infection ^[2]. Currently, there are many clinical treatments for corrosive esophageal stricture in children, among which esophageal dilation is one of the commonly used therapeutic methods ^[3]. This method can temporarily relieve the symptoms of dysphagia in children by

mechanically expanding the stenotic esophageal segment ^[4]. However, simple esophageal dilation is prone to recurrence, often requiring repeated procedures, which can increase the physical and psychological suffering of the child and the economic pressure on the family. Mitomycin is an antitumor antibiotic that inhibits fibroblast proliferation and collagen protein synthesis ^[5]. Recent studies have found that mitomycin can inhibit esophageal scar formation and reduce the recurrence rate of stenosis ^[6]. This study focuses on corrosive esophageal stricture in children and evaluates the therapeutic effect of dilation combined with drug therapy to provide a reference for clinical treatment.

2. Materials and methods

2.1. Subjects

This study adopts purposive sampling and selects children with corrosive esophageal stricture who were hospitalized in our hospital from August 2023 to March 2025 and underwent esophageal dilation combined with mitomycin treatment as the research subjects. Inclusion criteria include: (1) meeting the diagnostic criteria and confirmed by endoscopy and imaging; (2) aged 1–12 years old; (3) informed consent from family members. Exclusion criteria include those with severe organ dysfunction, mitomycin allergy, or esophageal perforation/major bleeding. A non-concurrent control design was adopted, with 10 cases in each of the control group and the intervention group based on treatment time. Retrospective analysis showed no significant difference in baseline data between the two groups ($P > 0.05$), as shown in **Table 1**. This study was approved by the Ethics Committee of Kunming Children's Hospital (Approval No.: 2023-03-217-K01).

Table 1. Comparison of clinical data between the two groups

Category	Control group ($n = 10$)	Intervention group ($n = 10$)	t/χ^2	P -value
Age (years old)				
Gender			0.808	0.369
Male	7	4		
Female	3	6		
Stricture location			0.770	0.857
Upper 1/3 esophagus	2	1		
Middle 1/3 esophagus	3	3		
Lower 1/3 esophagus	3	4		
Multiple strictures	1	2		
Stricture length			0.202	0.653
≤ 3 cm	4	5		
> 3 cm	6	5		
Corrosive agent			0.850	0.654
Strong alkali	2	3		
Strong acid	3	4		
Button battery	5	3		

2.2. Research methods

2.2.1. Preoperative preparation

Preoperative preparation and counseling were completed according to the standard protocol for painless gastroscopy, and double-informed consent forms were signed. All pediatric patients underwent endoscopic dilation under general anesthesia with endotracheal intubation, and underwent anesthesia evaluation before surgery. Strict fasting for 8 hours and water deprivation for 4 hours were implemented. A fixed team of senior physicians performed individualized endoscopic diagnosis and treatment based on preoperative imaging results, using balloons (Micro-Tech (Nanjing) Co., Ltd., MBD-0855-18) or bougies (COOK Company, USA) for dilation. The degree of esophageal stenosis was evaluated, and the initial dilator diameter was selected for gradual dilation.

2.2.2. Treatment method for the control group

The control group adopted a standardized protocol, performing bougie/balloon dilation according to the degree of stenosis, with a single target diameter of 10–12 mm. The procedure was repeated every 2–4 weeks until a significant improvement in swallowing function or clinical cure was achieved.

2.2.3. Treatment method for the intervention group

The intervention group received a combined local application of mitomycin (0.4 mg/mL) on the basis of the control treatment. The duration of action was 2–5 minutes, with a frequency of 1–4 times. The drug was applied through endoscopic cotton pad placement or multi-point injection using a needle, and normal saline was used for flushing to ensure safety. Drinking water was allowed 4 hours after surgery, trial feeding was attempted at 6 hours, and oral feeding was resumed the next day without complications, along with concurrent acid suppression therapy.

2.3. Evaluation indicators

2.3.1. Improvement in dysphagia

Dysphagia was evaluated after treatment using the Stooler grading system ^[7]:

- (1) Grade 0: No dysphagia, food can pass smoothly through the mouth, throat, and esophagus to reach the stomach.
- (2) Grade I: Mild dysphagia, food can pass through the mouth and throat but encounters some obstruction in the esophagus, requiring additional effort to swallow.
- (3) Grade II: Moderate dysphagia, food encounters obstruction in both the throat and esophagus, requiring extra effort to swallow.
- (4) Grade III: Complete inability to eat, unable to pass through the mouth and throat, unable to swallow any food, including liquids.
- (5) Grade IV: Severe dysphagia, unable to pass through the mouth and throat, unable to swallow any food, including liquids.

(Note: There seems to be an overlap between Grade III and Grade IV in the original description. Clarification or revision may be needed to distinguish the two grades more clearly.)

2.3.2. Diameter of stenotic segment

Measure the diameter of the narrowest part of the stenotic segment through gastroscopy before and after treatment.

2.3.3 Treatment frequency

Record the total number of dilations required to achieve the criteria for cure after treatment. Clinical efficacy: Evaluate the efficacy after treatment by combining the number of dilation treatments, eating status, and gastroscopy review status. The evaluation is divided into cured, markedly effective, effective, and failed. After treatment evaluation, the total effective rate = (cured + markedly effective + effective) / total number of cases × 100%.

2.3.4. Treatment safety

Record complications during treatment (bleeding, perforation, pain, etc.).

2.4. Statistical analysis

Statistical analysis of the data was performed using SPSS software. Count data are expressed as the number of cases and percentage (%), and the comparison of graded data between the two groups was performed using the Wilcoxon rank-sum test; non-normally distributed measurement data are expressed as median (interquartile range) [M(P25, P75)], and the comparison between the two groups was performed using the Wilcoxon rank-sum test. $P < 0.05$ was considered statistically significant.

3. Results

3.1. Dysphagia grading

After treatment, the Stooler dysphagia grading in the intervention group was significantly better than that in the control group, and the difference was statistically significant ($Z =$, $P < 0.05$). There was no significant difference in the distribution of Stooler grades between the two groups before treatment ($P > 0.05$); after treatment, the grades of both groups were significantly reduced ($P < 0.05$), as shown in **Table 2**.

Table 2. Stooler dysphagia grading before and after treatment in both groups

Time Point	Group	Grade I	Grade II	Grade III	Grade IV	χ^2	P -value
Pre-treatment	Control	2	4	3	1	1.981	0.576
	Intervention	1	3	4	2		
Post-treatment	Control	2	5	3	0	6.363	0.042
	Intervention	6	4	0	0		

3.2. Diameter of stenotic segment

There was no significant difference in the diameter of the stenotic segment between the two groups before treatment ($P > 0.05$); after treatment, the diameter of the intervention group was significantly larger than that of the control group ($P < 0.05$), as shown in **Table 3**.

Table 3. Diameter of the stenotic segment before and after treatment in both groups

Group	n	Pre-treatment	Post-treatment
Control	10	3.90 ± 1.37 mm	8.20 ± 1.32 mm
Intervention	10	3.20 ± 1.03 mm	9.60 ± 1.43 mm
t -value		1.290	3.457
p -value		0.213	0.045

3.3. Treatment frequency

The average number of treatments required in the intervention group was significantly less than that in the control group ($P < 0.05$), as shown in **Table 4**.

Table 4. Total number of treatment sessions for both groups after treatment

Group	n	Post-treatment (times)
Control	10	5.00 ± 1.63
Intervention	10	3.20 ± 1.03
<i>t</i> -value		2.946
<i>p</i> -value		0.009

3.4. Therapeutic effect

The total effective rate of the intervention group was significantly higher than that of the control group, and the cure rate was also significantly higher ($P < 0.05$). See **Table 5** for details.

Table 5. Comparison of treatment efficacy between the two groups after treatment

Group	Cured	Markedly effective	Effective	Ineffective	Total effective rate
Control	1	6	1	2	80%
Intervention	5	2	3	0	100%
χ^2	-	-	-	-	0.823
<i>P</i> -value					0.032

3.5. Treatment safety

Regarding complications, there were 2 cases of bleeding and 1 case of retrosternal pain in the control group; there was 1 case of bleeding and 1 case of retrosternal pain in the intervention group. There was no significant difference in the incidence between the two groups ($P > 0.05$). No serious complications, such as perforation were observed. See **Table 6** for details.

Table 6. Comparison of safety between the two groups after treatment

Group	Bleeding	Retrosternal pain	Severe complications (e.g., Perforation)	Total Incidence
Control	2	1	0	30%
Intervention	1	1	0	20%
χ^2				0.139
<i>p</i> -value				0.709

4. Discussion

4.1. Characteristics and treatment difficulties of corrosive esophageal stenosis in children

Due to the lack of safety education and weak supervision of children in China, corrosive substances are easily accessible, leading to accidental ingestion by children. The most severe complication is esophageal stenosis, which can significantly increase the risk of esophageal cancer in the long term and cause swallowing disorders,

malnutrition, repeated aspiration, and respiratory infections, seriously affecting the quality of life of children ^[8]. Studies have shown that most corrosive injuries are concentrated in the cricoid cartilage, aortic arch area, and inferior margin of the left main bronchus, involving the upper and middle segments of the esophagus ^[9]. Acidic substances cause coagulation necrosis of the mucosa, forming eschars, while alkaline substances cause liquefaction ischemia and thrombosis, both of which can lead to luminal stenosis or even occlusion. The disease ultimately leads to fibrotic stenosis and esophageal shortening ^[10]. The key to treatment lies in precise dilation and inhibition of excessive scar tissue proliferation to reduce the recurrence rate and risk of repeated treatments. Due to the thin esophageal wall and weak elasticity of children, dilation procedures must be performed with extra caution, taking into account physiological characteristics to develop a treatment plan.

4.2. Analysis of the effect of endoscopic esophageal dilation combined with mitomycin treatment

The intervention group had significant efficacy, and the reasons for this result may include:

- (1) The dual effect derived from mitomycin: as a cell cycle non-specific antiproliferative agent, it exerts an alkylating effect by inhibiting DNA and protein synthesis, targets and inhibits fibroblast proliferation, blocks scar tissue regeneration at the source, and effectively improves esophageal stenosis structure ^[11].
- (2) Simple dilation only tears the scar in the short term, leading to restenosis within 3–4 weeks due to continuous fibroblast proliferation. In the intervention group, mitomycin was locally administered during the wound repair phase, which accurately inhibits scar hyperplasia, effectively reduces the recurrence rate, and avoids high surgical risks by blocking DNA/RNA replication and protein synthesis ^[12].
- (3) Children have poor tolerance to endoscopy, and frequent anesthesia and dilation can easily lead to pain and risk of perforation; mitomycin C can reduce the frequency of treatment, which not only reduces medical expenses but also relieves family psychological pressure.
- (4) Safety evaluation showed no significant difference in complication rates between the two groups, confirming that local application of mitomycin C did not increase the risk, which is consistent with domestic and foreign studies ^[13]. In this study, the concentration was strictly controlled to 0.4 mg/mL ^[14], and the cotton pad was applied for 3–5 minutes ^[15] to effectively avoid the risk of high-concentration mucosal injury and drug overdose.

4.3. Research limitations and prospects

This study has the following limitations:

- (1) As a retrospective study, there may be selection bias, and doctors tend to choose combined therapy for severe cases;
- (2) The sample size is small;
- (3) The optimal concentration and duration of action of mitomycin C are not clear, and the applicable age needs to be verified;
- (4) There is a lack of long-term follow-up data for 3–5 years, and the observation period needs to be extended to evaluate the long-term efficacy.

Future research can:

- (1) Conduct multi-center, randomized controlled trials with strict randomization to control bias;
- (2) Expand the sample size, stratified analysis according to the injury object (acid/alkali), stenosis location and degree;

- (3) Set up a dose gradient test of 0.2-0.6mg/mL to determine the optimal concentration for children;
- (4) Explore the combination of other anti-scar drugs to provide new strategies for refractory cases.

5. Conclusion

In summary, endoscopic esophageal dilation combined with local treatment of mitomycin for corrosive esophageal stenosis in children achieves synergistic effects through mechanical dilation and scar-inhibiting medication. This significantly improves efficacy, reduces treatment frequency, lowers the risk of recurrence, and ensures reliable safety. This approach is especially suitable for injuries caused by strong alkalis and stenoses less than 2 cm. For complex cases, it can be incorporated into a comprehensive treatment system. With further research and technological advancements, this approach is expected to become the preferred clinical solution.

Funding

Health Research Project of Kunming Health Commission

Disclosure statement

The authors declare no conflict of interest.

References

- [1] Qi K, Zeng L, Wang C, et al., 2025, Research Progress on Drug Therapy for Corrosive Esophageal Strictures in Children. *International Journal of Pediatrics*, 52(1): 22–26.
- [2] Sarma M, Tripathi P, Arora S, 2021, Corrosive Upper Gastrointestinal Strictures in Children: Difficulties and Dilemmas. *World Journal of Clinical Pediatrics*, 10(6): 124–136.
- [3] Tang L, Lou J, Zhao H, et al., 2023, Clinical Analysis of Endoscopic Esophageal Dilation for the Treatment of Corrosive Esophageal Strictures in Children. *Chinese Journal of Contemporary Pediatrics*, 25(12): 1265–1269.
- [4] Youn B, Kim W, Cheon J, et al., 2010, Balloon Dilatation for Corrosive Esophageal Strictures in Children: Radiologic and Clinical Outcomes. *Korean Journal of Radiology*, 11(2): 203–210.
- [5] Sweed A, Fawaz S, Ezzat W, et al., 2015, A Prospective Controlled Study to Assess the Use of Mitomycin C in Improving the Results of Esophageal Dilatation in Post-Corrosive Esophageal Stricture in Children. *International Journal of Pediatric Otorhinolaryngology*, 79(1): 23–25.
- [6] Isa H, Hasan K, Ahmed H, et al., 2021, Efficacy and Safety of Endoscopic Esophageal Dilatation in Pediatric Patients with Esophageal Strictures. *International Journal of Pediatrics*, 2021: 1277530.
- [7] Yu Y, Xia Q, Liao Y, 2021, Preventive and Therapeutic Effects of Comprehensive Management of Body Position and Drugs on Esophageal Stenosis After Endoscopic Submucosal Dissection. *Minimally Invasive Medicine*, 16(4): 583–585.
- [8] Repici A, Vleggaar F, Hassan C, et al., 2010, Efficacy and Safety of Biodegradable Stents for Refractory Benign Esophageal Strictures: The BEST (Biodegradable Esophageal Stent) Study. *Gastrointestinal Endoscopy*, 72(5): 927–934.
- [9] Tarek S, Mohsen N, Abd El-Kareem D, et al., 2020, Factors Affecting the Outcome of Endoscopic Dilatation in

Refractory Post-Corrosive Oesophageal Stricture in Egyptian Children: A Single-Centre Study. *Esophagus*, 17(3): 330–338.

- [10] Uygun I, 2015, Caustic Oesophagitis in Children: Prevalence, the Corrosive Agents Involved, and Management from Primary Care Through to Surgery. *Current Opinion in Otolaryngology & Head and Neck Surgery*, 23(6): 423–432.
- [11] Dall'Oglio L, Caldaro T, Foschia F, et al., 2016, Endoscopic Management of Esophageal Stenosis in Children: New and Traditional Treatments. *World Journal of Gastrointestinal Endoscopy*, 8(4): 212–219.
- [12] Flor M, Ribeiro I, De Moura D, et al., 2021, Efficacy of Endoscopic Topical Mitomycin C Application in Caustic Esophageal Strictures in the Pediatric Population: A Systematic Review and Meta-Analysis of Randomized Controlled Trials. *Arquivos de Gastroenterologia*, 58(2): 253–261.
- [13] Berger M, Ure B, Lacher M, 2012, Mitomycin C in the Therapy of Recurrent Esophageal Strictures: Hype or Hope? *European Journal of Pediatric Surgery*, 22(2): 109–116.
- [14] El-Asmar K, Hassan M, Abdelkader H, et al., 2013, Topical Mitomycin C Application Is Effective in Management of Localized Caustic Esophageal Stricture: A Double-Blinded, Randomized, Placebo-Controlled Trial. *Journal of Pediatric Surgery*, 48(7): 1621–1627.
- [15] Ghobrial C, Eskander A, 2018, Prospective Study of the Effect of Topical Application of Mitomycin C in Refractory Pediatric Caustic Esophageal Strictures. *Surgical Endoscopy*, 32(12): 4932–4938.

Publisher's note

Bio-Byword Scientific Publishing remains neutral with regard to jurisdictional claims in published maps and institutional affiliations.

Studying the Impact of Skin Dose on Post-Mastectomy Radiotherapy Planning for Breast Cancer

Wenlan Fu, Yunlong Zhou

Department of Oncology, Jiangyou Second People's Hospital, Jiangyou 621702, Sichuan, China

Copyright: © 2025 Author(s). This is an open-access article distributed under the terms of the Creative Commons Attribution License (CC BY 4.0), permitting distribution and reproduction in any medium, provided the original work is cited.

Abstract: *Objective:* To investigate the impact of skin dose on post-mastectomy radiotherapy planning for breast cancer. *Methods:* Sixty patients undergoing radiotherapy after radical mastectomy for breast cancer were collected as research subjects and divided into a traditional group P1 and a newly designed group P2. The traditional method and a new method with the skin as an organ at risk (OAR) for dose limitation were used to set up the plans. The differences between the radiotherapy plans of the two groups were compared. All patients were followed up, focusing on the occurrence of acute skin reactions \geq grade 2, to analyze whether limiting skin dose ultimately benefits patients. *Results:* According to Tables 1, 2, and 3, there was no significant increase in the target dose and the irradiated dose to organs at risk ($P > 0.05$). **Table 4** shows that the maximum skin dose decreased by 1.95%, V107% and V110% decreased by 57.32% and 73.68%, respectively, with statistically significant differences ($P < 0.05$). **Table 5** reveals that among patients without skin dose limitation, 7 developed acute skin reactions \geq grade 2, whereas only 3 developed such reactions after limitation. Although the incidence of acute skin reactions \geq grade 2 decreased by 13.33%, the statistical results showed no significant difference ($P > 0.05$). *Conclusion:* Limiting skin dose by considering it an organ at risk can significantly reduce the irradiated skin dose. However, reducing the skin dose in breast cancer patients does not significantly decrease the incidence of acute skin reactions \geq grade 2. This suggests that reducing the skin dose in breast cancer patients does not significantly benefit them.

Keywords: Radical mastectomy; Radiotherapy; Skin reaction; Dose volume

Online publication: October 16, 2025

1. Introduction

The global number of new breast cancer cases has reached 2.26 million, surpassing lung cancer's 2.2 million cases and becoming the world's leading cancer^[1]. Combination adjuvant radiotherapy after radical mastectomy is an effective means to improve survival rates^[2,3]. However, adjuvant radiotherapy in the treatment of breast cancer may cause acute skin reactions. When the acute skin reaction is grade 2 or higher, it may lead to the interruption of radiotherapy, thereby reducing the tumor control rate. In severe cases, it can even affect the patient's quality of life^[4,5]. Some domestic scholars^[6-8] have attempted to reduce skin toxicity by creating a "skin volume" to limit skin dose. Therefore, this article explores the impact of IMRT technology on skin dose for patients after radical

mastectomy and provides suggestions for addressing skin damage.

2. Materials and methods

2.1. General information

Patients who underwent adjuvant radiotherapy after radical mastectomy for breast cancer at our hospital and Mianyang 404 Hospital from January 2022 to December 2023 were collected. Inclusion criteria: (1) Female, age ≥ 18 years old; (2) Pathologically confirmed breast cancer; (3) Patients underwent adjuvant radiotherapy after radical mastectomy. Exclusion criteria: (1) Only the chest wall area was irradiated; (2) Failed to complete the entire radiotherapy; (3) Only 90% of the target volume of the radiotherapy plan reached the prescribed dose; (4) Patients who could not be medically followed up due to geographical, social, or psychological reasons.

Patients were randomly divided into a traditional group, P_1 and a newly designed group, P_2 . The age range of the traditional group P_1 was 37–82 (median 54), while the age range of the newly designed group P_2 was 34–79 (median 53.7). There was no significant difference ($P > 0.05$), making the two groups comparable.

2.2. Methods

(1) Target Volume Delineation

All patients were positioned supine with both arms crossed in front of the forehead, immobilized using a thermoplastic head-neck-shoulder mask, and underwent contrast-enhanced spiral CT scanning with a slice thickness of 5 mm under quiet breathing. The scanned CT images were transmitted to the physician's workstation (CMS FOCAL 3.0). According to the principles outlined in ICRU Reports No. 50 and 63^[9], the gross tumor volume (GTV), including the primary tumor and positive lymph nodes^[10], was delineated by clinical physicians. The clinical target volume (CTV) was generated by expanding the GTV by 10 mm. The planning target volume (PTV) was then created by expanding the CTV by 5 mm in the anterior, posterior, left, and right directions, and by 10 mm in the superior and inferior directions, followed by retraction to 5 mm beneath the skin surface. All target volumes were delineated slice-by-slice by radiation oncologists with intermediate or higher professional titles and subsequently reviewed and confirmed by the department director with a senior professional title.

A "skin volume" was created by removing the compensator from the external contour and then retracting the resulting volume inward by 3 mm^[6,7]. This volume was used to evaluate the radiation dose delivered to the skin. For all patients, the radiotherapy plan was designed such that the prescribed dose covered 95% of the PTV volume.

(2) Treatment Plan Design

For the conventional group P_1 , an IMRT plan was designed based on the contoured target volume described above. The new design group P_2 was developed on the basis of P_1 by implementing dose constraints to the skin region, primarily restricting high doses. These constraints were progressively intensified until a target volume underdosage occurred. Radiotherapy was delivered using conventional fractionation: 50 Gy in 25 fractions over 5 weeks. It was required that at least 90% of the target volume receive the prescription dose. Dose constraints for organs at risk (OARs) were as follows: Left lung (L-lung): $V_5 < 60\%$, $V_{20} < 30\%$, $V_{30} < 20\%$, $D_{\text{mean}} < 1500$ cGy; Heart: $D_{\text{mean}} < 1000$ cGy, $V_{30} < 15\%$; Spinal cord: Cordmax < 3500 cGy; Femoral head: L-H < 5000 cGy.

(3) Treatment Plan Evaluation

The dose distribution in the target area and normal organs was analyzed based on dose curves and dose-volume histograms. According to ICRU Report 83, the D_{\max} , $D_{2\%}$, $D_{98\%}$, and $D_{50\%}$ for the Planning Target Volume (PTV)/skin volume refer to the doses received by the maximum, 2%, 98%, and 50% volumes of the PTV/skin volume, respectively. Relevant parameters include the Homogeneity Index (HI) and the Conformity Index (CI), where $HI = (D_{2\%} - D_{98\%}) / D_{50\%}$ and $CI = (V_{T,ref} \times V_{T,ref}) / (V_T \times V_{ref})$. Here, V_T is the target volume, V_{ref} is the volume enclosed by the reference isodose line, and $V_{T,ref}$ is the target volume enclosed by the reference isodose line. An HI value closer to 0 indicates a more homogeneous dose distribution, while a CI closer to 1 indicates better conformity between the 95% prescription isodose line and the target volume. Skin volume V_{107} : the absolute volume enclosed by 107% of the prescription dose (i.e., the absolute volume enclosed by 5350 cGy). Similarly, V_{110} .

2.3. Evaluation criteria for acute skin reactions

Skin adverse reactions were evaluated according to the Acute Radiation Morbidity Scoring Criteria by the Radiation Therapy Oncology Group (RTOG) [11]:

- (1) Grade 0: No noticeable change; skin remains normal.
- (2) Grade 1: Faint erythema, dry desquamation, decreased sweating, alopecia.
- (3) Grade 2: Moderate to brisk erythema; patchy moist desquamation, mostly confined to skin folds and creases; moderate edema. On mucosa: marked erythema, pain, inflammatory discharge.
- (4) Grade 3: Confluent moist desquamation other than skin folds and creases; significant edema. On mucosa: ulceration, bleeding, necrosis.
- (5) Grade 4: Life-threatening or functionally severe skin or mucosal necrosis, ulceration, or fistula formation.

Evaluation was performed within 3 months after the start of radiotherapy. All patients applied a protective skin agent before radiotherapy. When acute skin reactions reached Grade 2 or higher, irradiation was immediately stopped. Wound care was provided to prevent infection, and moist burn ointment was applied if necessary. Irradiation was resumed only after the ulcerated area had healed.

2.4. Statistical analysis

Data were analyzed using SPSS 22.0 software. Except for count data, which were analyzed using Fisher's exact test, all other data were analyzed using the paired-sample t-test. All results were expressed as mean \pm standard deviation (SD). A $P < 0.05$ was considered statistically significant.

3. Results

3.1. Occurrence of acute skin reactions of grade 2 or higher

In this study, a total of 77 patients undergoing radiotherapy after radical breast cancer surgery were collected. Seventeen patients were excluded (1 patient with only 90% of the target volume receiving the prescribed dose, 3 patients who did not complete radiation therapy, and 13 patients who only received radiation therapy to the chest wall area). Sixty patients were included in the study (all received radiation therapy to the chest wall and clavicle areas). Fifty-five patients (91.67%) developed acute skin reactions of grade 1, nine patients (15.00%) developed acute skin reactions of grade 2, and one patient (1.67%) developed acute skin reactions of grade 3 or higher. In the conventional plan P_1 , seven patients (23.33%) developed acute skin reactions of grade 2 or higher, while in the skin dose-limiting plan P_2 , three patients (10%) developed acute skin reactions of grade 2 or higher.

3.2. Comparison of the effects of conventional plan P1 and skin dose-limiting plan P2 on target dose

Table 1. Comparison of target doses in the chest wall region

Plan comparison	D _{max} (cGy)	CI	HI	V _{107%} (cm ³)	V _{110%} (cm ³)
P ₁	5534.20 ± 57.67	0.450 ± 0.062	0.08 ± 0.03	52.14 ± 31.68	2.29 ± 5.10
P ₂	5502.90 ± 42.73	0.451 ± 0.063	0.08 ± 0.02	40.83 ± 23.48	0.32 ± 0.60
<i>t</i> -value	2.346	0.254	1.377	3.176	2.090
<i>p</i> -value	0.066	0.601	0.179	0.04	0.046

Table 2. Comparison of target dose in the clavicle region

Plan comparison	D _{max} (cGy)	CI	HI	V _{107%} (cm ³)	V _{110%} (cm ³)
P ₁	5512.06 ± 60.34	0.599 ± 0.071	0.09 ± 0.03	13.11 ± 10.42	1.08 ± 2.38
P ₂	5489.23 ± 34.17	0.593 ± 0.073	0.09 ± 0.02	11.72 ± 8.74	0.19 ± 0.20
<i>t</i> -value	1.889	0.156	1.101	0.691	2.052
<i>p</i> -value	0.069	0.504	0.450	0.495	0.049

3.3. Comparison of the impact of conventional plan P1 and skin dose-limiting plan P2 on organ-at-risk doses

Table 3. Comparison of organ-at-risk doses

Plan comparison	Affected Lung				Heart		Spinal Cord	Esophagus D _{max}
	V ₅	V ₂₀	V ₃₀	D _{mean}	V ₃₀	D _{mean}	D _{max}	
P ₁	57.36 ± 5.11	24.61 ± 2.01	17.20 ± 1.36	1389.90 ± 52.29	6.76 ± 2.23	735.40 ± 138.25	1720.94 ± 975.82	5115.00 ± 308.44
P ₂	56.18 ± 4.56	24.91 ± 2.06	17.69 ± 1.74	1380.13 ± 50.99	6.62 ± 1.72	685.00 ± 161.07	1767.05 ± 948.31	4931.70 ± 542.96
<i>t</i> -value	0.930	-0.518	-1.164	1.322	0.256	1.238	0.296	1.536
<i>p</i> -value	0.360	0.609	0.254	0.193				

3.4. Impact of limiting skin dose on acute skin reactions

Table 4. Comparison of skin region doses

Plan comparison	D _{max}	V _{107%} (cm ³)	V _{110%} (cm ³)
P ₁	5530.47 ± 80.64	8.95 ± 5.89	0.38 ± 0.64
P ₂	5424.67 ± 63.36	3.82 ± 5.07	0.10 ± 0.23
<i>t</i> -value	6.810	3.777	2.285
<i>p</i> -value	0.00	0.01	0.03

Table 5. Impact of limiting skin dose on acute skin reactions

Group	No \geq Grade 2 acute skin toxicity (n)	\geq Grade 2 acute skin toxicity (n)	t-value	p-value
P ₁	23	7	1.920	0.299
P ₂	27	3		

4. Discussion

Currently, adjuvant radiotherapy after radical mastectomy remains the primary treatment for advanced breast cancer^[12–14]. However, adjuvant radiotherapy in the treatment of breast cancer may cause acute skin adverse events. Grade 2 or higher acute skin toxicity can affect patients' quality of life, and severe cases may even lead to treatment interruption, thereby reducing tumor control rates^[15–17]. Therefore, reducing skin dose and determining whether patients can truly benefit from it has always been an issue that medical workers need to pay attention to.

Zhang et al.^[8] generated skin by reducing the outer contour of the neck by 3mm, and set a plan to limit the skin as an organ at risk (OAR). Studies have shown that compared with the control group, the dIMRT technology research group reduced skin D_{mean} , V_{10} - V_{60} by 7%, 8%, 22%, 25%, 38%, 59%, and 85% respectively ($P = 0.00$, 0.00, 0.00, 0.00, 0.00, 0.00, 0.00). The results showed that limiting the dose of neck skin as an OAR could significantly reduce the exposure of neck skin. Wu's^[18] research results showed that the dIMRT technology made the newly designed group lower than the traditional group in terms of neck skin V_{10} - V_{60} and D_{mean} . The conclusion was that limiting the dose by treating the neck skin as an organ at risk could significantly reduce neck skin exposure. According to Tables 1, 2, 3, and 4, the maximum dose in the skin area decreased by 1.95%, $V_{107\%}$ and $V_{110\%}$ decreased by 57.32% and 73.68% respectively, and the differences were statistically significant ($P < 0.05$), while the target dose and the exposed dose of organs at risk did not increase significantly ($P > 0.05$). This indicates that generating skin by reducing the outer contour of breast cancer by 3 mm and limiting the dose of skin as an OAR can also significantly reduce the skin exposure of breast cancer.

Pasquier et al.^[19] designed a two-center prospective clinical study where 36.8% of patients experienced acute skin adverse reactions of grade 2 or higher, and 4 patients developed acute radiation dermatitis of grade 3, with an incidence rate of 1.38%. These findings are generally consistent with the results of this study, where among the 60 enrolled cases, 9 patients developed acute skin adverse reactions of grade 2, and 1 patient developed an acute skin adverse reaction of grade 3.

According to **Table 4**, limiting the dose to the skin as an organ at risk (OAR) can significantly reduce the skin exposure in breast cancer patients. However, as shown in **Table 5**, among patients without skin dose limitations, 7 developed acute skin reactions of grade 2 or higher. After applying the limitations, the number of patients with acute skin reactions of grade 2 or higher decreased to 3. Although the incidence of acute skin reactions of grade 2 or higher decreased by 13.33% ($P > 0.05$), this suggests that while limiting the skin dose as an OAR can significantly reduce skin exposure in breast cancer patients, reducing the skin dose in breast cancer patients does not significantly benefit the patients.

5. Conclusion

In summary, adopting dose limitations to the skin as an OAR in breast cancer can significantly reduce the radiation dose to the skin. However, reducing the skin dose in breast cancer does not significantly decrease the incidence

of acute skin reactions of grade 2 or higher. This indicates that reducing the skin dose in breast cancer does not provide significant benefits to the patients.

Disclosure statement

The authors declare no conflict of interest.

References

- [1] Siegel R, Miller K, Jemal A, 2020, Cancer Statistics, 2020. *CA Cancer J Clin*, 70(1): 7–30.
- [2] Clarke M, Collins R, Darby S, et al., 2005, Effects of Radiotherapy and Differences in the Extent of Surgery for Early Breast Cancer on Local Recurrence and 15-Year Survival: An Overview of the Randomised Trials. *Lancet*, 366(9503): 2087–2106.
- [3] Yang J, 2021, Evaluation of the Application Effect and Safety of Intensity-Modulated Radiotherapy in Adjuvant Therapy After Radical Mastectomy. *Practical Gynecologic Endocrinology Electronic Journal*, 8(16): 21–23.
- [4] Meattini I, Guenzi M, Fozza A, et al., 2017, Overview on Cardiac, Pulmonary and Cutaneous Toxicity in Patients Treated with Adjuvant Radiotherapy for Breast Cancer. *Breast Cancer*, 24(1): 52–62.
- [5] Aoulad N, Massabeau C, de Lafontan B, et al., 2017, Acute Toxicity of Breast Cancer Irradiation with Modulated Intensity by Tomotherapy®. *Cancer Radiother*, 21(3): 180–189.
- [6] Zhang Y, Liao X, Li J, et al., 2017, Dosimetry Study on Neck Skin Exposure in Spiral Tomography for Early Nasopharyngeal Carcinoma. *Chinese Journal of Radiological Medicine and Protection*, 37(12): 906–910.
- [7] Zhang X, Li K, Li N, et al., 2016, Comparison of Skin Exposure Doses Caused by Different External Irradiation Techniques After Breast-Conserving Surgery for Left Breast Cancer. *Modern Oncology*, 24(20): 3213–3216.
- [8] Zhang Y, Liao X, Li J, et al., 2018, Study on the Difference of Set Limit Dose of Neck Skin in Three Radiotherapy Techniques for Early Nasopharyngeal Carcinoma. *Chinese Journal of Radiation Oncology*, 27(2): 199–203.
- [9] Chavaudra J, Bridier A, 2001, Definition of Volumes in External Radiotherapy: ICRU Reports 50 and 62. *Cancer Radiother*, 5(5): 472–478.
- [10] National Cancer Center, National Cancer Quality Control Center, 2022, Guidelines for Target Delineation and Plan Design in Post-Mastectomy Radiotherapy for Breast Cancer. *Chinese Journal of Radiation Oncology*, 31(10): 863–878.
- [11] Huang C, Hou M, Luo K, et al., 2015, RTOG, CTCAE and WHO Criteria for Acute Radiation Dermatitis Correlate with Cutaneous Blood Flow Measurements. *Breast*, 24(3): 230–236.
- [12] Lyu M, Pan X, Wang H, et al., 2019, The Impact of Changes in Circulating Tumor Cell Count on Treatment Efficacy and Prognosis in Patients with HER2-Positive Early Breast Cancer. *Oncology Progress*, 17(14): 1659–1663.
- [13] Drooger J, Akdeniz D, Pignol J, et al., 2015, Adjuvant Radiotherapy for Primary Breast Cancer in BRCA1 and BRCA2 Mutation Carriers and Risk of Contralateral Breast Cancer with Special Attention to Patients Irradiated at Younger Age. *Breast Cancer Res Treat*, 154(1): 171–180.
- [14] Xiao Y, Song L, Fu Y, et al., 2020, Efficacy Analysis of Postoperative Radiotherapy After Modified Radical Mastectomy in Breast Cancer Patients Downstaged by Neoadjuvant Chemotherapy. *Chinese and Foreign Medical Research*, 39(4): 25–28.
- [15] McQuestion M, 2011, Evidence-Based Skin Care Management in Radiation Therapy: Clinical Update. *Semin Oncol Nurs*, 27(2): e1–17.

- [16] Zhuang J, Zhang E, Wang Y, et al., 2020, Recombinant Human Epidermal Growth Factor for the Prevention of Oral Mucositis in Nasopharyngeal Carcinoma Patients Undergoing Concurrent Chemoradiotherapy and Its Effect on Clinical Efficacy. *Journal of Navy Medicine*, 41(1): 50–53.
- [17] Suh O, Flórez M, Sacristán V, et al., Constenla Figueiras M, Pereiro Ferreiros M, 2020, Cutaneous Adverse Events and Quality of Life in Outpatients Receiving Anticancer Agents: Results from an Observational, Cross-Sectional Study. *Drugs Context*, 9: 2020-6-6.
- [18] Wu S, 2020, Study on the Differences in Setting Limit Doses for Neck Skin of Early Nasopharyngeal Carcinoma with Three Radiotherapy Techniques. *Modern Diagnosis and Treatment*, 31(19): 3123–3124.
- [19] Wu Z, Hou L, Li C, et al., 2024, Hypofractionated Versus Conventional Postmastectomy Irradiation for Breast Cancer: Comparison of Acute Skin Toxicity. *Breast Cancer (Dove Med Press)*, 16: 423–432.

Publisher's note

Bio-Byword Scientific Publishing remains neutral with regard to jurisdictional claims in published maps and institutional affiliations.

Advances in the Study of mRNA Vaccines and Their Application in Tumor Therapy

Yuanyuan Zeng*

School of Clinical Medicine, Hangzhou Medical College, Hangzhou 310053, Zhejiang, China

*Corresponding author: Yuanyuan Zeng, YuanYuan_Zeng2004@163.com

Copyright: © 2025 Author(s). This is an open-access article distributed under the terms of the Creative Commons Attribution License (CC BY 4.0), permitting distribution and reproduction in any medium, provided the original work is cited.

Abstract: The active ingredients of traditional vaccines are pathogen antigens, mainly proteins, extracted from cells, and their production relies on large-scale cell culture, which greatly limits the speed of vaccine production and makes it difficult for humans to face large-scale epidemics such as COVID-19. In contrast, mRNA vaccine production technology is a vaccine production technology independent of cell culture. In the 1980s mRNA in vitro transcription methods were invented, in which the mRNA could encode the most effective proteins, which greatly increased the production rate. However, the body's immune system can recognize foreign mRNA, which can trigger an inflammatory response and greatly reduce the amount of mRNA in the body and the efficiency of translation. The nucleotide in mRNA is modified by adding a Cap at 5' end ^[1], adding Poly(A) tail at 3' end, optimization of UTR, optimization of ORF codon, nucleoside, etc., can play a role in protecting the mRNA from being broken down by enzymes, and greatly reduce immune response triggered by mRNA. At present, there are three mRNA tumor vaccines entering the clinical application stage, namely: naked mRNA cancer vaccine, formulation mRNA cancer vaccine and dendritic cell vaccine. In the future, mRNA vaccines are expected to become effective drugs for tumor therapy. This paper reviews the working principle, mechanism and research progress of mRNA vaccines, the base modification of mRNA vaccines, and the application of mRNA vaccines in tumor therapy, with a view to providing theoretical references for the subsequent research on mRNA vaccines.

Keywords: mRNA vaccine; Nucleoside modification; Tumor therapy

Online publication: October 16, 2025

1. Working principles and mechanisms of mRNA vaccines

There are two approaches to vaccine preparation. One is to directly provide or enable the vaccine recipient to produce the target pathogen antigen; the other is to use infection signals that activate the host's immune system. The methods adopted include using intact viruses or bacteria, retaining only the antigenic parts that activate the immune system, and using genetic materials. mRNA vaccines are prepared using genetic materials, utilizing the central dogma where RNA is used to synthesize proteins.

The working principle of mRNA vaccines is that mRNA is encapsulated in lipid nanoparticles (LNPs)^[2]. After the vaccine is injected, it enters cells through fusion endocytosis and releases mRNA, which then combines with ribosomes in the cytoplasm to translate into corresponding proteins. On one hand, these proteins are embedded in the cell membrane to activate B cells and induce them to produce antibodies. On the other hand, the proteins are broken down into small peptide segments by proteases. Some key small peptide segments bind to MHC and are presented on the cell surface to activate T cells (CD8+), thereby inducing cellular immunity^[3].

mRNA vaccines without base modification have safety issues related to inflammatory reactions and the problem of protecting RNA from degradation. The use of liposome technology can prevent RNA degradation. With the development of drug delivery systems, people have developed various materials for in vivo drug delivery^[4,5], such as lipid nanoparticles (LNPs)^[6], polymer nanoparticles^[7], and lipid-polymer hybrid nanoparticles^[8]. Their purpose is to protect mRNA from rapid degradation by the ubiquitous RNases and help it cross multiple biological barriers.

The use of base modification can alleviate the safety issues caused by inflammatory reactions. Common base modifications are the conversion of uridine to pseudouridine and N1-methylpseudouridine. Pseudouridine is connected to ribose at the position of the 5th carbon, and N1-methylpseudouridine is formed by adding the corresponding methyl group to pseudouridine. In the actual synthesis process, inserting modified nucleotides into the raw materials can reduce inflammatory reactions.

2. Research progress on mRNA vaccines

Due to the good tolerability of mRNA vaccines, their ease of degradation, and the fact that they do not integrate into the host genome^[8,9], scientists have never stopped researching mRNA vaccines. The development of mRNA vaccine technology has a history of more than 30 years. In 1961, scientists from the California Institute of Technology successfully extracted mRNA for the first time. In 1990, Wolff's team from the University of Wisconsin^[10] injected RNA and DNA expression vectors containing genes for luciferase, β -galactosidase, and chloramphenicol acetyltransferase into the skeletal muscles of mice, and detected the expressed proteins and the resulting immune response in the muscle cells. In 1992, scientists injected mRNA encoding hormones from normal rat hypothalamic cells into the hypothalamus of rats with diabetes insipidus, and observed a temporary reversal of diabetes insipidus within hours after injection^[11]. In 1995, researchers injected the carcinoembryonic antigen gene into mouse muscles as a cancer vaccine^[12]. In 2002, Heiser's team^[13] found that dendritic cells (DCs) transfected with mRNA encoding prostate-specific antigen could effectively stimulate T cell-mediated anti-tumor immune responses in vitro, and clinical trials were conducted. In 2005, Hungarian biochemist Karikó discovered that the incorporation of modified nucleosides (m5C, m6A, m5U, s2U, or pseudouridine) into mRNA inhibited the potential of RNA to activate DCs, that is, reduced the immunogenicity of mRNA in vivo^[14]. In 2009, Weide et al.^[15] successfully injected protamine-mRNA vaccines into melanoma patients and proved that it was safe and feasible. In 2017, Sahin et al.^[16] demonstrated the clinical feasibility, safety, and anti-tumor activity of targeting individual cancer mutations through RNA neoantigen vaccines. In 2019, the COVID-19 pandemic broke out, and a variety of mRNA vaccines were granted emergency authorization and put into use as COVID-19 vaccines, such as the COVID-19 variant mRNA vaccine jointly developed by Fudan University/Shanghai Lanque/Walvax Biotechnology, and the COVID-19 mRNA vaccine (SYS6006) under CSPC Pharmaceutical Group, as officially announced^[17].

3. Base modification of mRNA vaccines

mRNA plays a crucial role in the process of gene expression. mRNA is derived from DNA through post-transcriptional splicing or modification, carrying the genetic information from DNA and transferring it to ribosomes in the cytoplasm for protein synthesis, thus serving as a bridge between DNA and proteins.

mRNA typically consists of hundreds to thousands of nucleotides, and its structural elements include a 5' cap, a 3' poly A tail (polyadenylate tail), 5' UTR and 3' UTR (untranslated regions), as well as an ORF (open reading frame that encodes proteins).

3.1. Addition of cap at the 5' end

The simplest cap structure is 7-methylguanosine (M7G), which is linked to the triphosphate of the first transcribed nucleotide (M7GpppN) through a 5'-to-5' triphosphate bridge (5'ppp5'), with methylation modification at the 2'-O position (denoted as m7G(5')ppp(5')Xm, where X is the first transcribed nucleotide)^[18,19]. The 5' cap can not only protect mRNA from cleavage by exonucleases but also regulate pre-RNA splicing and nuclear export. It can eliminate free phosphate groups in the mRNA sequence, and after such elimination, the stability of mRNA is enhanced, and the translation of mRNA is accelerated^[20]. Adding a cap at the 5' end can reduce immunogenicity and improve stability.

Up to now, there are two capping methods: one is to add a synthetic Cap analog during in vitro transcription; the other is to perform capping with recombinant vaccinia virus-derived capping enzyme after the end of in vitro transcription. The former is the co-transcriptional capping method, which involves adding anti-reverse cap analogs (ARCA) during transcription; the latter is the enzymatic capping method^[20,21]. ARCA represents an innovative breakthrough in the field of mRNA capping. mRNA transcripts with forward products can be recognized during translation, while those with reverse products cannot be correctly recognized. ARCA avoids the problems encountered in standard caps^[22,23].

3.2. Addition of Poly(A) tail at the 3' end

The 3' end of mRNA has a polyadenylic acid (poly A) tail structure, known as the Poly(A) tail. The generation of a poly A tail on newly synthesized RNA involves the cooperation of many proteins and sequence elements. Almost all eukaryotic animal mRNAs contain a polyadenylation signal (PAS). The PAS and the downstream GU- or U-rich sequences guide the formation of the poly A tail by recruiting protein complexes involved in the initial 3' end processing^[24,25]. Other sequence elements can regulate the efficiency or precise location of polyadenylation. Polyadenylation occurs within 10–30 nt downstream of the PAS, and then poly(A) polymerase (PAP) adds the poly(A) tail. Once 11–14 adenosines are added, nuclear poly(A)-binding proteins can bind to the poly(A) tail in the reaction^[26], after which PAP can rapidly synthesize the full-length polyA tail^[27,28].

The Poly(A) tail plays a role in translation, as it can prevent the synthesized mRNA from being degraded, is of great significance to the stability of mRNA, and promotes its binding to Poly(A) tail-binding proteins, which is beneficial to protein expression^[21]. In many cases, the poly(A) tail protects mRNA. For an enzyme to degrade mRNA starting from the 3' end, it must first degrade the poly(A) tail.

There are currently two recognized tailing methods: one is the transcription of mRNA from a DNA template containing a Poly(A) tail, and the other is enzymatic polyadenylation. The length of the Poly(A) tail has a significant impact on the translation efficiency of mRNA^[20]. Only when the length of the Poly(A) tail is greater than 30 nt can the stability of mRNA translation be ensured^[21]. However, the length of the Poly(A) tail is not as

long as possible. The optimal length of the Poly(A) tail varies among different mRNAs ^[21].

3.3. Optimization of UTR

UTRs are the non-coding parts of mRNA sequences in the upstream and downstream domains of the mRNA coding region. They are related to mRNA stability, specific recognition of mRNA by ribosomes, the translation process, regulation of mRNA secondary structure, as well as regulation of gene translation, half-life, and subcellular localization ^[19]. UTRs play an important regulatory role in the translation process ^[20].

The 5' UTR can directly affect the translation of the ORF. To prevent incorrect initiation and substitution of the ORF during mRNA translation, 5' UTR gene sequences different from the ORF can be used ^[19]. How the 5' UTR regulates translation includes: regulating the translocation of ribosomes on mRNA, and binding to eukaryotic initiation factor 33 (eIF3) to mediate translation initiation ^[20]. As for the 3' UTR, it is a region where unstable factors in mRNA are concentrated. Therefore, when synthesizing the 3' UTR, we can improve mRNA stability and extend its half-life by avoiding the use of unstable sequences or introducing relatively stable elements ^[19]. Since the 3' UTR can regulate translation by binding to microRNAs (miRNAs) ^[20], it has been identified as an important regulator of subcellular mRNA localization ^[29, 30].

3.4. Optimization of ORF codons

The ORF (Open Reading Frame) is the coding sequence for translating proteins. Within this region, using appropriate codons can enhance the translation efficiency of mRNA. Replacing rare codons with similar common codons can increase translation yield ^[19]. We can utilize RNAActive technology to increase the content of guanine and cytosine in the open reading frame of mRNA, thereby improving translation efficiency and delaying mRNA decay.

It is not necessary to replace rare codons with similar common codons for all ORF codons in every mRNA. This is because some proteins require slow translation to fold correctly, effectively, and stably, in which case rare codons should be used. Therefore, different codon optimization strategies should be applied to different mRNAs to improve translation efficiency and quality ^[19].

3.5. Nucleoside modification

Uracil (U) is linked through its N-1 to the C-1' of the pentose sugar, while modified pseudouridine is linked via its C-5 to the C-1' of the pentose sugar. This base modification causes changes in the codons on mRNA. Due to the wobble property of genetic codons, where the first and second bases typically determine the type of amino acid, and the third base allows a certain degree of wobble, simply put, if uracil (U) is at the third position and can be modified to pseudouridine, the tRNA responsible for transport can still recognize this codon. However, RNA enzymes cannot recognize it, enabling escape from the body's innate immunity and resolving the issue of excessive mRNA immunogenicity. Later, people discovered various nucleoside modification methods, such as 5-methylcytidine and N1-methylpseudouridine.

4. Application of mRNA vaccines in tumor therapy

4.1. The mechanism of mRNA vaccines in treating tumors

Like other vaccines, the basic principle of using mRNA vaccines is to stimulate and enhance the anti-tumor immune response in the body ^[31]. The antigens related to tumors encoded in the body are delivered by dendritic

cells and some mRNA injections^[32]. When APCs (Antigen-Presenting Cells) receive antigen signals, mRNA is transported to the cytoplasm, and MHC molecules transduce and process the signals in a cascade manner. APCs present tumor-associated antigens on MHC class I and class II molecules, thereby activating CD8+ and CD4+ T cells. Meanwhile, they can induce the activation of B cells to produce humoral immune responses^[31,33].

4.2. Clinical research progress of mRNA vaccines in tumor therapy

In 1996, the first mRNA-based cancer vaccine study tested dendritic cells pulsed with RNA in vitro^[34]. To date, no mRNA vaccine has been approved for clinical treatment^[21]. However, three major types of tumor vaccines—naked mRNA cancer vaccines, formulated mRNA cancer vaccines, and dendritic cell vaccines—have achieved significant breakthroughs and entered the clinical trial stage.

Naked mRNA vaccines apply the concept of personalized vaccines. Researchers design and manufacture personalized vaccines for each cancer patient by comprehensively identifying individual mutations, calculating, and predicting new epitopes. This marks the first study based on melanoma. Researchers identified mutations expressed in 13 patients with stage III and IV melanoma. Naked mRNA vaccines are generally administered via intradermal or nodular injection^[35,36]. Controlled by ultrasound, the vaccine is injected into the inguinal lymph nodes. In mouse models, the lymph nodes effectively absorb these mRNA antigens, which are then recognized by dendritic cells. All patients developed a T-cell immune response to the vaccine, with two patients showing vaccine-related clinical responses^[37,38]; the remaining specific results have not yet been published.

Formulated mRNA vaccines are optimized versions of naked mRNA vaccines. They refer to mRNA combined with specific carriers or packaging materials to improve stability, delivery efficiency, and immunogenicity^[39]. These carriers or packaging materials can include liposomes, polymers, proteins, etc. This facilitates the recognition of vaccine mRNA antigens by APCs^[38-40]. Clinically, clinical trials for non-small cell carcinoma patients are currently underway. The vaccine CV9201, which encodes five lung cancer tumor-associated antigens, has been designed. It showed good tolerability in 7 patients with stage IIIB and 39 patients with stage IV disease^[41]. In the phase 1b clinical trial of CV9202 vaccine, antigen-specific immunity to CV9202 was detected in 21 out of 25 evaluable patients^[42].

Dendritic cell vaccines are currently the most promising type of mRNA vaccines. Studies have shown that these cells can regulate immune types and induce strong and long-lasting CD8+ and CD4+ T-cell immune responses. In dendritic cell vaccines, a patient's dendritic cells are usually collected, processed, combined with specific antigens (such as antigens from cancer cells), and then reinjected into the patient. A key advantage of dendritic cell vaccines is personalized treatment. By using the patient's own dendritic cells, the vaccine can be customized according to the patient's specific immune system and disease characteristics, improving the targeting of treatment^[43,44]. However, the process of obtaining and preparing suitable dendritic cells is time-consuming and labor-intensive, resulting in a relatively slow development process. The anti-CTLA-4 antibody ipilimumab was combined with TriMix dendritic cells encoding tumor-associated antigens mRNA in patients with advanced melanoma. Among 39 patients who received the vaccine injection, 15 achieved partial or complete immune responses^[45]. Scientists injected dendritic cell vaccines carrying tumor-associated antigen-encoding mRNA into patients with acute myeloid leukemia. The experimental results showed that the 5-year overall survival rate of vaccinated patients was favorable, with approximately 43% of patients experiencing delayed disease recurrence^[46].

In the field of oncology, mRNA tumor vaccines are in the early stages of clinical research. Some preliminary clinical trials have demonstrated the potential of mRNA tumor vaccines to induce immune responses in patients,

but more research is still needed. Therefore, in the design and application of mRNA tumor vaccines, many challenges need to be overcome to ensure their targeting, safety, effectiveness, and other aspects.

5. Conclusion

mRNA vaccine technology represents a breakthrough in vaccine production by eliminating dependence on cell culture, enabling rapid response to pandemics like COVID-19. Through innovations such as 5' capping, Poly(A) tailing, and nucleoside modifications, mRNA stability and translational efficiency have been significantly enhanced while minimizing immune-triggered degradation. Currently, three mRNA cancer vaccines (naked mRNA, formulated mRNA, and dendritic cell vaccines) are in clinical trials, demonstrating promising potential for tumor therapy. This review summarizes the mechanisms, optimization strategies, and therapeutic applications of mRNA vaccines, providing a foundation for future research and development in this transformative field.

Disclosure statement

The authors declare no conflict of interest.

References

- [1] Granot Y, Peer D, 2017, Delivering the Right Message: Challenges and Opportunities in Lipid Nanoparticles-Mediated Modified mRNA Therapeutics—An Innate Immune System Standpoint. *Semin Immunol*, 34: 68–77.
- [2] Muthukrishnan S, Both G, Furuichi Y, et al., 1975, 5'-Terminal 7-Methylguanosine in Eukaryotic mRNA Is Required for Translation. *Nature*, 255(5503): 33–37.
- [3] Zhai T, Liu M, Lei H, 2023, Nucleoside Base Modification Inhibits RNA Immunogenicity and Enables the Development of Novel Coronavirus mRNA Vaccines. *Acta Physiologica Sinica* 23(10): 1–6.
- [4] Karikó K, Muramatsu H, Ludwig J, et al., 2011, Generating the Optimal mRNA for Therapy: HPLC Purification Eliminates Immune Activation and Improves Translation of Nucleoside-Modified, Protein-Encoding mRNA. *Nucleic Acids Res*, 39(21): e142.
- [5] Mitchell M, Billingsley M, Haley R, et al., 2021, Engineering Precision Nanoparticles for Drug Delivery. *Nat Rev Drug Discov*, 20(2): 101–124.
- [6] Patel A, Kaczmarek J, Bose S, et al., 2019, Inhaled Nanoformulated mRNA Polyplexes for Protein Production in Lung Epithelium. *Adv Mater*, 31(8): e1805116.
- [7] Sharp P, 2009, The Centrality of RNA. *Cell*, 136(4): 577–580.
- [8] Karikó K, Muramatsu H, Welsh F, et al., 2008, Incorporation of Pseudouridine into mRNA Yields Superior Nonimmunogenic Vector with Increased Translational Capacity and Biological Stability. *Mol Ther*, 16: 1833–1840.
- [9] Thess A, Grund S, Mui B, et al., 2015, Sequence-Engineered mRNA Without Chemical Nucleoside Modifications Enables an Effective Protein Therapy in Large Animals. *Mol Ther*, 23: 1456–1464.
- [10] Yu D, Ma Y, Wan F, et al., 2023, Research and Application Progress of mRNA Vaccines. *Progress in Biotechnology*, 13(4): 492–498.
- [11] Wolff J, Malone R, Williams P, et al., 1990, Direct Gene Transfer into Mouse Muscle in Vivo. *Science*, 247(4949): 1465–1468.
- [12] Conry R, Lobuglio A, Wright M, et al., 1995, Characterization of a Messenger RNA Polynucleotide Vaccine Vector.

Gland Surg, 55(7): 1397–1400.

- [13] Jirikowski G, Sanna P, Maciejewski-Lenoir D, et al., 1992, Reversal of Diabetes Insipidus in Brattleboro Rats: Intrahypothalamic Injection of Vasopressin mRNA. *Science*, 255(5047): 996–998.
- [14] Heiser A, Coleman D, Dannull J, et al., 2002, Autologous Dendritic Cells Transfected with Prostate-Specific Antigen RNA Stimulate CTL Responses Against Metastatic Prostate Tumors. *J Clin Invest*, 109(3): 409–417.
- [15] Karikó K, Buckstein M, Ni H, et al., 2005, Suppression of RNA Recognition by Toll-Like Receptors: The Impact of Nucleoside Modification and the Evolutionary Origin of RNA. *Immunity*, 23(2): 165–175.
- [16] Weide B, Pascolo S, Scheel B, et al., 2009, Direct Injection of Protamine-Protected mRNA: Results of a Phase 1/2 Vaccination Trial in Metastatic Melanoma Patients. *Journal of Immunotherapy*, 32(5): 498–507.
- [17] Sahin U, Kariko K, Tureci O, 2014, mRNA-Based Therapeutics—Developing a New Class of Drugs. *Nat Rev Drug Discov*, 13(10): 759–780.
- [18] Furuichi Y, 2015, Discovery of m(7)G-Cap in Eukaryotic mRNAs. *Proc Jpn Acad Ser B Phys Biol Sci*, 91(8): 394–409.
- [19] Shatkin A, 1976, Capping of Eucaryotic mRNAs. *Cell*, 9(4 pt 2): 645–653.
- [20] Li Y, Zhu J, Chen J, et al., 2023, Modification Strategies of mRNA Vaccines and Their Applications. *Heilongjiang Journal of Animal Science and Veterinary Medicine*, (13): 36–43.
- [21] Dong W, Zhang X, Chen Y, 2023, Development History and Challenges of Nucleic Acid Modification and Delivery Systems for mRNA Vaccines. *Chinese Journal of Pharmaceuticals*, 54(3): 304–311.
- [22] Stepinski J, Waddell C, Stolarski R, et al., 2001, Synthesis and Properties of mRNAs Containing the Novel “Anti-Reverse” Cap Analogs 7-Methyl (3'-O-Methyl) GpppG and 7-Methyl (3'-Deoxy) GpppG. *RNA*, 7(10): 1486–1495.
- [23] Peng Z, Sharma V, Singleton S, et al., 2002, Synthesis and Application of a Chain-Terminating Dinucleotide mRNA Cap Analog. *Organic Letters*, 4(2): 161–164.
- [24] Proudfoot N, 2011, Ending the Message: Poly(A) Signals Then and Now. *Genes & Development*, 25(17): 1770–1782.
- [25] Tian B, Graber J, 2012, Signals for Pre-mRNA Cleavage and Polyadenylation. *Wiley Interdisciplinary Reviews RNA*, 3(3): 385–396.
- [26] Meyer S, Urbanke C, Wahle E, 2002, Equilibrium Studies on the Association of the Nuclear Poly(A) Binding Protein with Poly(A) of Different Lengths. *Biochemistry*, 41(19): 6082–6089.
- [27] Brawerman G, 1981, The Role of the Poly(A) Sequence in Mammalian Messenger RNA. *CRC Critical Reviews in Biochemistry*, 10(1): 1–38.
- [28] Sheiness D, Darnell J, 1973, Polyadenylic Acid Segment in mRNA Becomes Shorter with Age. *Nature New Biology*, 241(113): 265–268.
- [29] Lawrence J, Singer R, 1986, Intracellular Localization of Messenger RNAs for Cytoskeletal Proteins. *Cell*, 45(3): 407–415.
- [30] Melton D, 1987, Translocation of a Localized Maternal mRNA to the Vegetal Pole of *Xenopus* Oocytes. *Nature*, 328(6125): 80–82.
- [31] Beck J, Reidenbach D, Salomon N, et al., 2021, mRNA Therapeutics in Cancer Immunotherapy. *Molecular Cancer*, 20: 69.
- [32] Boczkowski D, Nair S, Snyder D, et al., 1996, Dendritic Cells Pulsed with RNA Are Potent Antigen-Presenting Cells in Vitro and in Vivo. *Journal of Experimental Medicine*, 184: 465–472.
- [33] Miao L, Zhang Y, Huang L, 2021, mRNA Vaccine for Cancer Immunotherapy. *Molecular Cancer*, 20: 41.

- [34] Sahin U, Derhovanessian E, Miller M, et al., 2017, Personalized RNA Mutanome Vaccines Mobilize Poly-Specific Therapeutic Immunity Against Cancer. *Nature*, 547: 222–226.
- [35] Rittig S, Haentschel M, Weimer K, et al., 2011, Intradermal Vaccinations with RNA Coding for TAA Generate CD8+ and CD4+ Immune Responses and Induce Clinical Benefit in Vaccinated Patients. *Molecular Therapy*, 19: 990–999.
- [36] Hollingsworth R, Jansen K, 2019, Turning the Corner on Therapeutic Cancer Vaccines. *NPJ Vaccines*, 4: 7.
- [37] Hou X, Zaks T, Langer R, et al., 2021, Lipid Nanoparticles for mRNA Delivery. *Nature Reviews Materials*, 6: 1078–1094.
- [38] Hong S, Zhang Z, Liu H, et al., 2018, B Cells Are the Dominant Antigen-Presenting Cells That Activate Naive CD4+ T Cells Upon Immunization with a Virus-Derived Nanoparticle Antigen. *Immunity*, 49: 695–708.e4.
- [39] Guan S, Rosenecker J, 2017, Nanotechnologies in Delivery of mRNA Therapeutics Using Nonviral Vector-Based Delivery Systems. *Gene Therapy*, 24: 133–143.
- [40] Midoux P, Pichon C, 2015, Lipid-Based mRNA Vaccine Delivery Systems. *Expert Review of Vaccines*, 14: 221–234.
- [41] Sebastian M, Schröder A, Scheel B, et al., 2019, A Phase I/IIa Study of the mRNA-Based Cancer Immunotherapy CV9201 in Patients with Stage IIIB/IV Non-Small Cell Lung Cancer. *Cancer Immunology, Immunotherapy*, 68: 799–812.
- [42] Papachristofilou A, Hipp M, Klinkhardt U, et al., 2019, Phase Ib Evaluation of a Self-Adjuvanted Protamine Formulated mRNA-Based Active Cancer Immunotherapy, BI1361849 (CV9202), Combined with Local Radiation Treatment in Patients with Stage IV Non-Small Cell Lung Cancer. *Journal of Immunotherapy of Cancer*, 7: 38.
- [43] Pardi N, Hogan M, Porter F, et al., 2018, mRNA Vaccines—A New Era in Vaccinology. *Nature Reviews Drug Discovery*, 17: 261–279.
- [44] Wykes M, Pombo A, Jenkins C, et al., 1998, Dendritic Cells Interact Directly with Naive B Lymphocytes to Transfer Antigen and Initiate Class Switching in a Primary T-Dependent Response. *Journal of Immunology (Baltimore, Md.: 1950)*, 161(3): 1313–1319.
- [45] De Keersmaecker B, Claerhout S, Carrasco J, et al., 2020, TriMix and Tumor Antigen mRNA Electroporated Dendritic Cell Vaccination Plus Ipilimumab: Link Between T-Cell Activation and Clinical Responses in Advanced Melanoma. *Journal of Immunotherapy of Cancer*, 8: e000329.
- [46] Anguille S, Velde A, Smits E, et al., 2017, Dendritic Cell Vaccination as Postremission Treatment to Prevent or Delay Relapse in Acute Myeloid Leukemia. *Blood*, 130: 1713–1721.

Publisher's note

Bio-Byword Scientific Publishing remains neutral with regard to jurisdictional claims in published maps and institutional affiliations.

Establishment and Real-World Application of an Adverse Reaction Monitoring System for Targeted Therapy of Antitumor Drugs

Xiaoyan Li^{1*†}, Jianfu Zhao^{2†}, Genshen Ye³, Yongjuan Ding^{4†}, Xi Liu⁵, Zhikun Liang¹, Qiang Chen²

¹Pharmacy Department, The Sixth Affiliated Hospital, Sun Yat-sen University, Guangzhou 510655, Guangdong, China

²Oncology Department, The First Affiliated Hospital of Jinan University, Guangzhou 510630, Guangdong, China

³Zhiyan Health Institute of Sciences, Shanghai 510630, China

⁴Pharmacy Department, Affiliated Hospital of Jiangnan University, Wuxi 214122, Jiangsu, China

⁵Pharmacy Department, Zhongshan Torch Development Zone People's Hospital, Zhongshan 528400, Guangdong, China

† These authors contributed equally to this work and share first authorship.

*Corresponding author: Xiaoyan Li, lixian5@mail.sysu.edu.cn

Copyright: © 2025 Author(s). This is an open-access article distributed under the terms of the Creative Commons Attribution License (CC BY 4.0), permitting distribution and reproduction in any medium, provided the original work is cited.

Abstract: This multicenter prospective observational study aims to construct an adverse reaction monitoring system for molecular targeted antitumor drugs and explore its real-world application. By recruiting patients receiving molecular targeted therapy from outpatient, inpatient, and pharmacy settings, we collected comprehensive data including patient demographics, disease information, treatment regimens, and adverse reactions. The adverse reactions were graded according to CTCAE v5.0. With a planned enrollment of at least 100,000 patients over five years, this study will conduct descriptive analysis and build prediction models for adverse reactions. The results will contribute to establishing a national monitoring network and database, updating clinical guidelines, and enhancing the safety of molecular targeted therapy.

Keywords: Adverse reaction monitoring; Molecular targeted antitumor drugs; Real-world study

Online publication: October 16, 2025

1. Introduction

Molecular targeted therapy refers to therapeutic drugs designing for a protein molecule, nucleotide fragment, or gene product in tumor cells that causes tumorigenesis and progression. It is mainly divided into two categories: monoclonal antibodies and small molecule compounds. The advent of molecular targeted therapy has revolutionized cancer treatment. Since the approval of rituximab for CD20-positive non-Hodgkin's lymphoma in 1997 by the US FDA, a plethora of targeted drugs have emerged, such as EGFR inhibitors (e.g., erlotinib, gefitinib), ALK/ROS1 inhibitors (e.g., crizotinib, entrectinib), and HER2 inhibitors (e.g., trastuzumab, pertuzumab), significantly improving patient prognosis across various malignancies including lung cancer, breast cancer, colorectal cancer, leukemia,

lymphoma, melanoma, kidney cancer, gastric cancer, gastrointestinal stromal tumors, liver cancer^[1,2].

Although molecular targeted drugs act on specific targets in tumor cells and have fewer and milder adverse reactions than traditional cytotoxic drugs, since the targets of molecular targeted drugs are also expressed in normal tissues, they can also produce adverse reactions, including systemic, gastrointestinal, skin, liver, kidney, heart, and coagulation adverse reactions. Systemic adverse effects may manifest as fatigue, fever, and joint pain. Gastrointestinal disturbances like diarrhea, vomiting, and liver toxicity (e.g., elevated ALT, AST, and ALP) are common, often attributed to cytochrome-mediated liver metabolism^[3]. Skin toxicities, including rash and itching, can impact patients' quality of life^[4]. Hematological and cardiac toxicities, such as neutropenia and QT interval prolongation, also pose significant clinical concerns^[5-13].

Notably, real-world patients often differ from those in clinical trials, with more complex comorbidities and prior treatment histories, yet existing research, primarily from phase II~III trials and small-sample hospital-based studies, fails to adequately capture this diversity^[14-17]. Therefore, a large-scale real-world study is imperative to comprehensively assess adverse reactions and optimize drug safety management.

2. Materials and methods

2.1. Study design

This is a multicenter, prospective, observational study with no intervention in clinical diagnosis or treatment. It adheres to ethical principles, ensuring patient consent and privacy protection. The duration of the study is 5 years. No randomized or protocol-driven treatment will be administered or provided to subjects during the study. Treatment decisions, if clinically appropriate, will be made at the discretion of the physician.

Patients receiving targeted therapy from outpatient and inpatient wards in the study center voluntarily join the study, sign the informed consent form. Physicians collect baseline characteristics and monitor patients in the hospital to determine whether adverse reactions occur. If adverse reactions occur, record the type, severity of adverse reactions, intervention, and discharge. Outside the hospital, the hospital system follows up regularly, and patients fill out follow-up information, including medication compliance, possible adverse reactions, and researchers follow up accordingly. In the non-study centers, Patients receiving targeted therapy from inpatient and outpatient clinics learn about the project through their doctors or the project's official website, and voluntarily join the project by signing the informed consent form and uploading a baseline character. The regional research team monitors adverse reactions of the patients. Patients complete monthly questionnaires on medication compliance, diet, exercise, disease progression, and any adverse reactions through the patient portal, which are automatically entered into the follow-up database. After patients submit possible adverse reaction information, it will be automatically forwarded to the researchers associated with the patient. The investigator records, grade the AR, and follow up using the intelligent assistance management system. When patients revisit the same center, treatment plans, and examination are automatically collected through the outpatient hospital information system.

The study will rely on modern information technology to establish a nationwide molecular targeted anti-tumor drug adverse reaction monitoring network and long-term monitoring database to provide data support for the subsequent update of the guideline and consensus. At the same time, by collecting patients' disease information, explore the establishment of adverse reaction prediction models for targeted drugs with different mechanisms, and provide reference tools for safe use of drug. During the research process, ethical standards will be strictly obeyed to ensure that the rights of the subjects are fully protected. Subjects will be recruited through the project's official website, and the patient's personal information will be strictly confidential. The research data will be managed

using an electronic medical record system to ensure that the data collection is accurate, complete, and timely.

2.2. Subjects

Patients receiving molecular targeted therapy from outpatient, inpatient, and pharmacy settings voluntarily join the study, sign informed consent, accept follow-up, and report adverse reactions. For patients who experience adverse reactions, researchers follow up on the adverse reaction intervention and outcomes, regularly summarize and analyze the data, and report the occurrence of adverse reactions of different molecular targeted drugs in real world.

2.2.1. Inclusion criteria

- (1) Both male and female patients aged 18 years or older
- (2) Clinically and pathologically diagnosed with malignant tumors (solid and/or hematological).
- (3) Prescribed molecular targeted drugs by clinicians and having received at least one dose.
- (4) Willing and able to undergo long-term follow-up and provide consent.

2.2.2. Exclusion criteria

- (1) Mental disorders or language impairments precluding examination or follow-up.
- (2) Pregnant or lactating women.
- (3) Severe comorbidities with a life expectancy of less than 1 month.
- (4) Other conditions deemed inappropriate by investigators.

2.3. Recruitment

For the study centers, all patients who meet the inclusion and exclusion criteria are monitored for adverse reactions, which include both in-hospital and out-of-hospital monitoring. During in-hospital molecular targeted drug treatment, adverse reactions are promptly reported by clinical physicians, clinical pharmacists, or nursing staff, and relevant information is filled out. After discharge, patients receive regular follow-ups through their mobile devices and self-report any adverse reactions. The pharmacists at the study centers follow up on the adverse reactions reported by patients and fill in the relevant information.

For the non-study centers, Patients who are undergoing molecular targeted drug treatment and are willing to be monitored for adverse reactions can learn about the project from their physicians or the project's official website and voluntarily join the trial. The process is the same as the out-of-hospital monitoring process for patients at study centers.

2.4. Endpoints and definitions

The primary outcome was the spectrum and severity of adverse reactions per SOC and CTCAE v5.0 after molecular targeted drug treatment. Adverse reactions were defined as: not detected before treatment; or stopped before treatment started and reappeared during treatment; or persisted and worsened in severity during treatment compared with the situation before treatment. The spectrum and severity of adverse reactions were summarized according to SOC and CTCAE classifications. The adverse reactions were graded according to Common Terminology Criteria for Adverse Events (CTCAE) v5.0, which is developed by the National Cancer Institute (NCI) of the United States (CTCAE v5.0 is the latest version and was released in November 2017). The preferred terms of the system organ class (SOC) were used to describe adverse events. Secondary outcome was DCR, such as progressive disease (PD), stable disease (SD), complete response (CR), partial response (PR), and death, intervention and outcomes, correlation with molecular targeted drugs, direct or indirect medical costs after AE occurs.

Demographic Information (Age, Gender), Disease (diagnosis, pathological diagnosis, stage, course, comorbidities or complications), Treatment (monotherapy or combination, drugs for related comorbidities), laboratory tests including complete blood count, liver function, renal function, tumor biomarkers, coagulation, imaging examinations including CT/MRI/Ultrasonography/PET-CT, physical examination (blood pressure, heart rate, height, weight), quality of life assessment including SDS/SAS, daily steps, ECOG, medication (DOR and DOT) will also be collected.

2.5. Data management

Researchers input patient baseline information through the EDC platform and collect various data monthly via the patient mobile terminal and other terminals. The adverse reactions were graded according to Common Terminology Criteria for Adverse Events (CTCAE) v5.0. The preferred terms of the system organ class (SOC) were used to describe adverse events. Data is collected through multiple means with minimum manual entry. Logic verification and other functions are added to enhance data quality control, and different data permissions are assigned to researchers. For data preservation, all data is entered into the electronic platform and stored in the cloud, regularly backed up by the main study center and will be preserved for 10 years after the study's end. Patient privacy will be encrypted.

2.6. Sample size and statistical analysis

This study will monitor all molecular targeted drugs. To discover possible rare adverse reactions, at least 100,000 cancer patients will be enrolled, and subgroup analysis will be performed by different mechanisms of the drugs. Statistical methods include descriptive statistics and advanced modeling techniques to analyze adverse reaction patterns and build prediction models. Statistical analysis of adverse reactions will be performed by different treatment, and stratified analysis will be performed by disease, age, gender, and previous treatment. The adverse reactions were graded according to Common Terminology Criteria for Adverse Events (CTCAE) v5.0. The preferred terms of the system organ class (SOC) were used to describe adverse events. The measurable data were described by methods including mean, standard deviation, median, quartile, maximum, minimum, and analyzed by methods such as t-test or rank sum test. The count data will be described by methods such as frequency and frequency (constituent ratio), and analyzed by methods such as chi-square test. Statistical significance is defined as $p < 0.05$. The data will be grouped by disease and stage, and modeled using methods such as generalized linear models. Independent variables were screened, the effects of each variable on adverse reactions were analyzed. Adverse reaction prediction model will be established and fitted.

2.7. List of drugs involved in the study

Table1. Table of drugs involved in the study

Name	Indications
Anlotinib Hydrochloride Capsules	Locally advanced or metastatic non-small cell lung cancer that has progressed or recurred after receiving at least two systemic chemotherapy regimens in the past
Gecacitinib Hydrochloride Tablets	Myelofibrosis (PMF), secondary myelofibrosis due to polycythemia vera (PPV-MF), and secondary myelofibrosis due to essential thrombocythemia (PET-MF)
Almonertinib Mesilate Tablets	Adult patients with locally advanced or metastatic non-small cell lung cancer (NSCLC) who have previously received treatment with epidermal growth factor receptor (EGFR) tyrosine kinase inhibitors (TKIs) and who have a positive T790M mutation
Flumatinib Mesylate Tablets	Adult patients with Philadelphia chromosome-positive chronic myeloid leukemia (Ph+ CML) in the chronic phase

Table 1 (Continued)

Name	Indications
Adebrelimab Injection	First-line treatment for extensive-stage small cell lung cancer, firstline treatment for limited-stage small cell lung cancer, and perioperative treatment for resectable non-small cell lung cancer
Adebrelimab Injection	First-line treatment for extensive-stage small cell lung cancer, firstline treatment for limited-stage small cell lung cancer, and perioperative treatment for resectable non-small cell lung cancer
Cetuximab N01 Injection	Wild-type RAS metastatic colorectal cancer
Famitinib Malate Capsules	Patients with recurrent or metastatic cervical cancer who have failed previous platinum-based chemotherapy but have not received bevacizumab treatment before
Apatinib Mesylate Tablets	Atients with advanced gastric adenocarcinoma or gastric-esophageal junction adenocarcinoma who have experienced progression or recurrence after receiving at least two systemic chemotherapy regimens in the past
Bevacizumab Injection	Metastatic colorectal cancer and advanced, metastatic or recurrent non-small cell lung cancer
Unecritinib Fumarate Capsules	Adult patients with ROS1-positive locally advanced or metastatic non-small cell lung cancer (NSCLC)
Envonalkib Citrate Capsules	The treatment of patients with ALK-positive locally advanced or metastatic non-small cell lung cancer (NSCLC) who have not received treatment with ALK inhibitors

3. Discussion

This multicenter, prospective, observational study provides a comprehensive analysis of the spectrum and severity of adverse reactions (ARs) in patients undergoing molecular targeted therapy (MTT) for malignant tumors. With a large sample size of at least 100,000 participants, our findings will offer valuable insights into the real-world management of ARs associated with MTT. The use of CTCAE v5.0 for grading ARs and SOC for describing adverse events ensures standardization and comparability with other studies in the field. The primary outcome, which focused on the spectrum and severity of ARs post-MTT, should reveal a diverse range of reactions, highlighting the heterogeneity in patient responses to these therapies.

A key strength of this study is its large-scale, multicenter design, which enhances the generalizability of our findings to diverse patient populations. The inclusion of both inpatient and outpatient settings, as well as the integration of non-study centers, further broadens the applicability of our results. However, the study is not without limitations. The observational nature of the study limits causal inferences, and the reliance on physician discretion for treatment decisions may introduce variability in patient management. Additionally, while this study aimed to recruit a large and diverse cohort, the exclusion of patients with mental disorders, language impairments, or severe comorbidities may limit the full representation of the patient population. Selection bias due to voluntary participation also warrants consideration.

4. Conclusion

In conclusion, this study will provide a robust dataset on the spectrum and severity of ARs associated with MTT, and may enhance the personalized approach to manage the adverse reactions. In the future, longer follow-up can be conducted to assess the long-term ARs and evaluate the efficacy of interventions aimed at managing these reactions.

Disclosure statement

The authors declare no conflict of interest.

References

- [1] Sehn LH, Chua N, Mayer J, et al., 2016, Obinutuzumab Plus Bendamustine Versus Bendamustine Monotherapy in Patients With Rituximab-Refractory Indolent Non-Hodgkin Lymphoma (GADOLIN): A Randomised, Controlled, Open-Label, Multicentre, Phase 3 Trial. *Lancet Oncol*, 17(8): 1081–1093.
- [2] Mak JWY, Law AWH, Law KWT, et al., 2023, Prevention and Management of Hepatitis B Virus Reactivation in Patients With Hematological Malignancies in the Targeted Therapy Era. *World J Gastroenterol*, 29(33): 4942–4961.
- [3] Shi Q, Yang X, Ren L, et al., 2020, Recent Advances in Understanding the Hepatotoxicity Associated With Protein Kinase Inhibitors. *Expert Opin Drug Metab Toxicol*, 16(3): 217–226.
- [4] Strumberg D, Awada A, Hirte H, Clark JW, Seeber S, Piccart P, et al., 2006, Pooled Safety Analysis of BAY 43-9006 (Sorafenib) Monotherapy in Patients With Advanced Solid Tumours: Is Rash Associated With Treatment Outcome? *Eur J Cancer*, 42(4): 548–556.
- [5] Funakoshi T, Latif A, Galsky MD, 2013, Risk of Hematologic Toxicities in Cancer Patients Treated With Sunitinib: A Systematic Review and Meta-Analysis. *Cancer Treat Rev*, 39(7): 818–830.
- [6] Zaja F, Tomadini V, Zaccaria A, et al., 2006, CHOP-Rituximab With Pegylated Liposomal Doxorubicin for the Treatment of Elderly Patients With Diffuse Large B-Cell Lymphoma. *Leuk Lymphoma*, 47(10): 2174–2180.
- [7] Tanaka H, Takahashi K, Yamaguchi K, et al., 2018, Hypertension and Proteinuria as Predictive Factors of Effects of Bevacizumab on Advanced Breast Cancer in Japan. *Biol Pharm Bull*, 41(4): 644–648.
- [8] Galvano A, Guarini A, Iacono F, et al., 2019, An Update on the Conquests and Perspectives of Cardio-Oncology in the Field of Tumor Angiogenesis-Targeting TKI-Based Therapy. *Expert Opin Drug Saf*, 18(6): 485–496.
- [9] Je Y, Schutz FA, Choueiri TK, 2009, Risk of Bleeding With Vascular Endothelial Growth Factor Receptor Tyrosine-Kinase Inhibitors Sunitinib and Sorafenib: A Systematic Review and Meta-Analysis of Clinical Trials. *Lancet Oncol*, 10(10): 967–974.
- [10] Choueiri TK, Schutz FA, Je Y, et al., 2010, Risk of Arterial Thromboembolic Events With Sunitinib and Sorafenib: A Systematic Review and Meta-Analysis of Clinical Trials. *J Clin Oncol*, 28(13): 2280–2285.
- [11] Khorana AA, Francis CW, Culakova E, et al., 2007, Thromboembolism Is a Leading Cause of Death in Cancer Patients Receiving Outpatient Chemotherapy. *J Thromb Haemost*, 5(3): 632–634.
- [12] Piper-Vallillo AJ, Sequist LV, 2019, Cardiac Risk-Informed Treatment of EGFR-Mutant Lung Cancer With Osimertinib. *JACC CardioOncol*, 1(2): 179–181.
- [13] Schiefer M, Hendriks LEL, Dinh T, et al., 2018, Current Perspective: Osimertinib-Induced QT Prolongation: New Drugs With New Side-Effects Need Careful Patient Monitoring. *Eur J Cancer*, 91: 92–98.
- [14] Lv B, Chen J, Liu XL, 2022, Anlotinib-Induced Hypertension: Current Concepts and Future Prospects. *Curr Pharm Des*, 28(3): 216–224.
- [15] Leslie I, Boos LA, Larkin J, et al., 2020, Avelumab and Axitinib in the Treatment of Renal Cell Carcinoma: Safety and Efficacy. *Expert Rev Anticancer Ther*, 20(5): 343–354.
- [16] Dikopf A, Wood K, Salgia R, 2015, A Safety Assessment of Crizotinib in the Treatment of ALK-Positive NSCLC Patients. *Expert Opin Drug Saf*, 14(3): 485–493.
- [17] Tamura Y, Tamura Y, 2022, Dasatinib-Induced Pulmonary Hypertension. *Intern Med*, 61(15): 2245–2246.

Publisher's note

Bio-Byword Scientific Publishing remains neutral with regard to jurisdictional claims in published maps and institutional affiliations.

Research on Ultrasound Diagnosis of Thyroid Nodules: A Bibliometric Analysis

Xiaodi Chen^{1,2}, Zhiyang Lv^{1,3*}

¹The First College of Clinical Medical Science, China Three Gorges University, Yichang 443003, Hubei, China

²Department of Ultrasound, Yichang Central People's Hospital, Yichang 443003, Hubei, China

³Department of Cardiology, Yichang Central People's Hospital, Yichang 443003, Hubei, China

*Corresponding author: Zhiyang Lv, lvzhiyang@ctgu.edu.cn

Copyright: © 2025 Author(s). This is an open-access article distributed under the terms of the Creative Commons Attribution License (CC BY 4.0), permitting distribution and reproduction in any medium, provided the original work is cited.

Abstract: *Objective:* To evaluate global research trends and outputs on the ultrasound diagnosis of thyroid nodules using bibliometric analysis. *Methods:* The study searched the Web of Science Core Collection for publications on thyroid nodule ultrasound diagnosis (2000–2025). Relevant literature data (publication year, countries, institutions, authors, journals, keywords, and citations) were extracted. Bibliometric analyses were performed using VOSviewer to map collaboration networks, research hotspots, and co-citation patterns. *Results:* A total of over 8,000 publications were included. Annual output rose from 25 in 2000 to 390 in 2022. The United States and China together contributed more than one-third, with the U.S. leading by citations and China showing rapid growth. Leading institutions were concentrated in East Asia and North America, especially Korea and China. Author networks revealed strong collaboration among Korean radiologists. The thyroid was the most productive and most-cited journal. Keyword co-occurrence clustered around ultrasound risk stratification, FNA cytology and molecular testing, and management strategies. Co-citation analysis highlighted guidelines, particularly the 2015 ATA statement, as central to the knowledge network. *Conclusion:* Research on ultrasound diagnosis of thyroid nodules has expanded rapidly over the past two decades, with Asia and North America at the forefront. Collaboration networks reveal regional clusters and prolific contributor groups. The literature emphasizes differentiating benign from malignant nodules via standardized ultrasound risk stratification and adjunct FNA, while emerging trends include the integration of advanced imaging techniques, artificial intelligence, and nonsurgical therapies. These bibliometric insights map the evolution of this field and can guide future research and international collaboration.

Keywords: Thyroid nodules; Ultrasound diagnosis; Bibliometric analysis; Risk stratification; Artificial intelligence

Online publication: October 16, 2025

1. Introduction

Thyroid nodules are common, with ultrasound detecting them in up to 60% of adults, though only a small fraction is malignant. The widespread adoption of high-resolution ultrasound has markedly increased detection over the

past two decades. Ultrasound remains pivotal for characterizing nodules, guiding fine-needle aspiration (FNA), and stratifying malignancy risk. Standardized reporting systems such as ACR TI-RADS and its international variants have enhanced diagnostic consistency and reduced unnecessary biopsies ^[1]. Research has expanded worldwide, shifting from risk assessment toward management approaches like active surveillance and minimally invasive ablation ^[2]. Meanwhile, artificial intelligence (AI)–assisted interpretation has emerged as a tool to improve diagnostic accuracy ^[3]. Despite this progress, a bibliometric analysis is needed to comprehensively map research trends, collaboration, and emerging hotspots, providing insights into the evolution and future directions of ultrasound-based thyroid nodule diagnosis.

2. Methods

2.1. Data source and search strategy

To capture publications on ultrasound diagnosis of thyroid nodules and used the following Topic Search (TS) query: TS = ((“thyroid nodule” OR “thyroid lesion” OR “thyroid tumor” OR “thyroid carcinoma”) AND (“ultrasound” OR “ultrasonography” OR “sonography”) AND (“diagnosis” OR “differential diagnosis” OR “malignant” OR “benign”) AND (“clinical study” OR “clinical trial” OR “patients”)) This query combined terms related to thyroid nodules and carcinoma, ultrasound/sonography techniques, diagnostic evaluation of benign and malignant nodules, and clinical research settings. The truncation operator was used to include multiple word variations. The search was limited to peer-reviewed articles and reviews published in English from January 2000 to June 2025. Non-article records such as conference abstracts, letters, and editorials were excluded. The search was finalized on June 30, 2025, and all retrieved records were exported with complete bibliographic and citation information for subsequent bibliometric analysis.

2.2. Data analysis tools

Data were analyzed using VOSviewer version 1.6.20 for performance metrics and collaboration maps (authors, institutions, countries, keywords). Standard network algorithms were applied to identify clusters of related items. Key indicators included annual publications, citations, author and institutional productivity, journal output, and keyword frequencies. Visualizations and summary tables were generated to present research patterns and hotspots.

3. Results

3.1. Annual publication trends

Figure 1 illustrates the publication trends from 2000 to 2025, showing an exponential growth pattern ($R^2 = 0.9461$). In the early phase (2000–2009), annual output remained low, but research activity rose sharply after 2010, driven by advances in imaging and increasing thyroid disease incidence. The surge continued, peaking after 2018, with more than 350 publications annually from 2020 to 2022. From 2023 to 2025, cumulative output still increased, but yearly publications fluctuated, with a decline in 2025 likely due to incomplete data or shifting research priorities. Overall, the field demonstrates strong momentum, with growth expected to continue as new technologies drive further innovation.

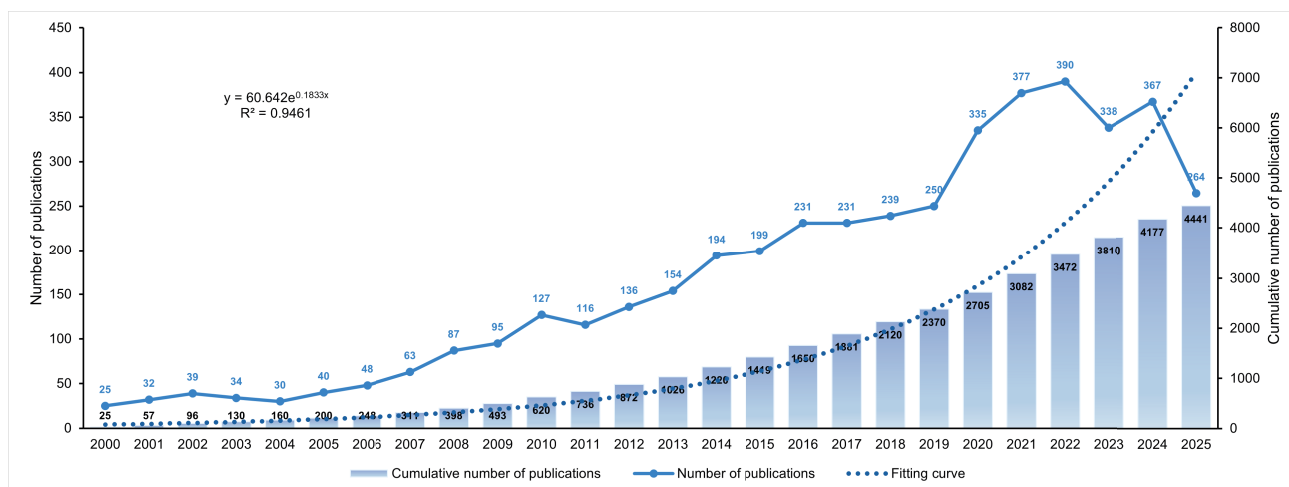


Figure 1. Annual number of publications and citations on ultrasound diagnosis of thyroid nodules, 2000–2025.

3.2. Country and institutional analysis

Global research on thyroid nodule ultrasound is concentrated in a few key regions, with the United States, China, and South Korea occupying central positions in the international collaboration network (**Figure 2**). The U.S. maintains broad partnerships with European countries such as Italy, Germany, and the UK, while China collaborates closely with East Asian neighbors including Japan and South Korea. South Korea, despite its smaller size, plays a pivotal role in advancing thyroid ultrasound, supported by its national screening practices and radiology expertise. European nations contribute actively and often serve as bridges for multinational studies, while countries from the Middle East and South America are gradually entering the global network, indicating the geographic expansion of this field.

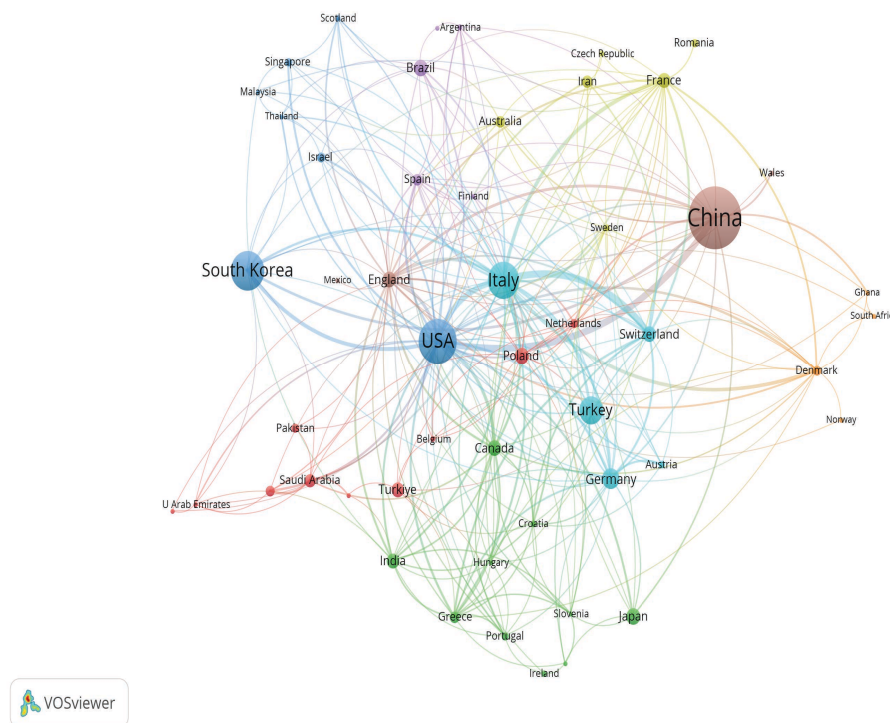


Figure 2. Global collaboration map of countries engaged in ultrasound diagnosis of thyroid nodules research.

At the institutional level (**Figure 3; Table 1**), East Asian universities dominate output. The University of Ulsan (147 publications, 8,436 citations) and Yonsei University (142 publications, 8,264 citations) rank highest, reflecting the strength of Korean radiology groups. Shanghai Jiao Tong University follows with 120 publications, alongside other Chinese centers such as Zhejiang and Tongji University. Sungkyunkwan and Seoul National University further reinforce Korea's leadership. In North America, Mayo Clinic stands out with comparatively fewer papers (58) but exceptionally high citation impact (17,934 citations; around 309 per article), underlining its role in guideline development and influential clinical studies. Overall, collaboration at the institutional level remains regionally clustered, with strong intra-national cooperation but fewer cross-regional ties, suggesting that while global engagement is evident, much research activity remains centered within regional academic hubs.

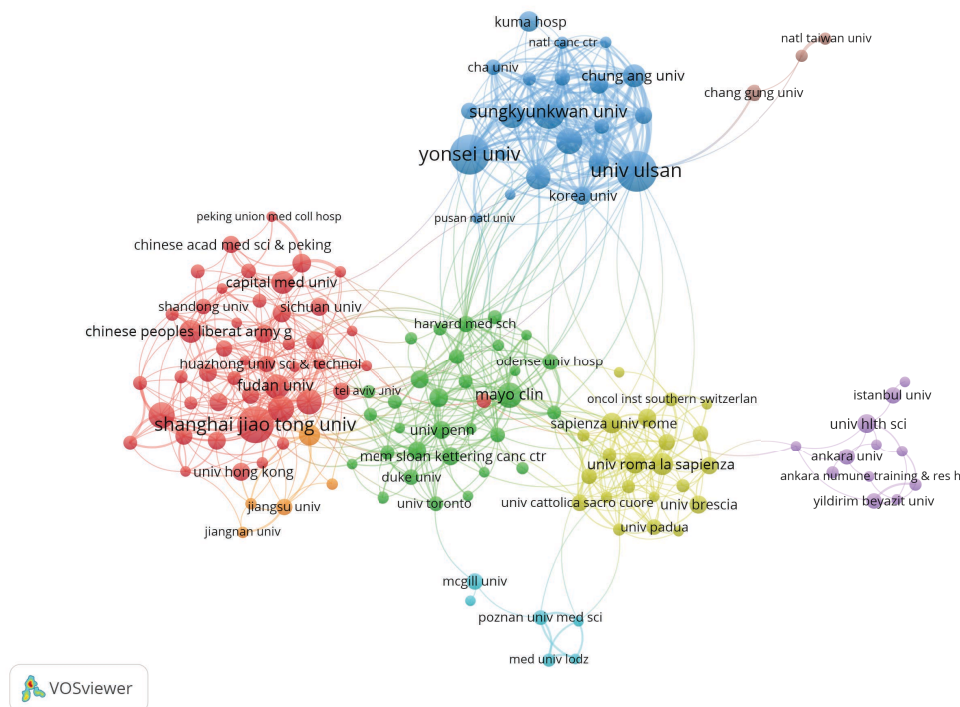


Figure 3. Institutional collaboration network in research on ultrasound diagnosis of thyroid nodules.

Table 1. Top 10 institutions by publication output

Institution name	Total number of articles	Total citations	Average citations
Univ Ulsan	147	8436	57.3878
Yonsei Univ	142	8264	58.1972
Shanghai Jiao Tong Univ	120	1484	12.3667
Sungkyunkwan Univ	93	5580	60
Zhejiang Univ	62	696	11.2258
Tongji Univ	62	1249	20.1452
Seoul Natl Univ	59	4585	77.7119
Sun Yat Sen Univ	58	867	14.9483
Mayo Clin	58	17934	309.2069
Inje Univ	57	2262	39.6842

3.3. Author and co-authorship network

The field of thyroid nodule ultrasound research is dominated by several highly productive author groups, often concentrated within specific countries or institutions. As shown in **Table 2**, the top 10 most prolific authors are overwhelmingly from South Korea. Jung Hwan Baek and Jin Young Kwak rank first with 104 publications each, followed closely by Eun-Kyung Kim with 96 papers. All three are radiologists affiliated with leading Korean medical centers and have made substantial contributions to ultrasound-guided interventions and the development of risk stratification systems. Other Korean radiologists, including Hee Jung Moon, Jeong Hyun Lee, Jung Hyun Yoon, and Jung Hee Shin, also appear in the top 10, each with dozens of publications. This pattern underscores South Korea's leading role in advancing thyroid ultrasound techniques, exemplified by the establishment of the K-TIRADS classification system and pioneering studies on ultrasound-guided ablation.

Table 2. Top 10 authors by publication output

Author name	Total number of articles	Total citations	Average citations
Baek, Jung Hwan	104	5616	54
Kwak, Jin Young	104	5220	50.1923
Kim, Eun-Kyung	96	5308	55.2917
Moon, Hee Jung	76	3328	43.7895
Lee, Jeong Hyun	73	4741	64.9452
Yoon, Jung Hyun	62	2457	39.629
Shin, Jung Hee	53	2171	40.9623
Trimboli, Pierpaolo	46	1437	31.2391
Kim, Dong Wook	42	1574	37.4762
Choi, Young Jun	42	1534	36.5238

The co-authorship network further illustrates the collaborative structure of this field (**Figure 4**). Korean scholars such as Kwak Jin Young, Baek Jung Hwan, and Lee Jeong Hyun form a densely connected cluster, reflecting frequent collaboration and a highly cohesive academic network. In contrast, European researchers such as Pierpaolo Trimboli, Giovanna Luca, and Enrico Papini constitute another cluster, primarily focused on clinical guidelines and follow-up management. Cross-national authors like Cosimo Durante and Erik K. Alexander function as bridging nodes, linking research outcomes from different regions. Overall, the author network exhibits regional clustering: Korean scholars dominate clinical and imaging research, whereas European and North American researchers contribute substantially to guideline development and evidence-based practice. International collaborations, though less frequent, play a crucial role in integrating diverse expertise and ensuring cross-regional knowledge exchange.

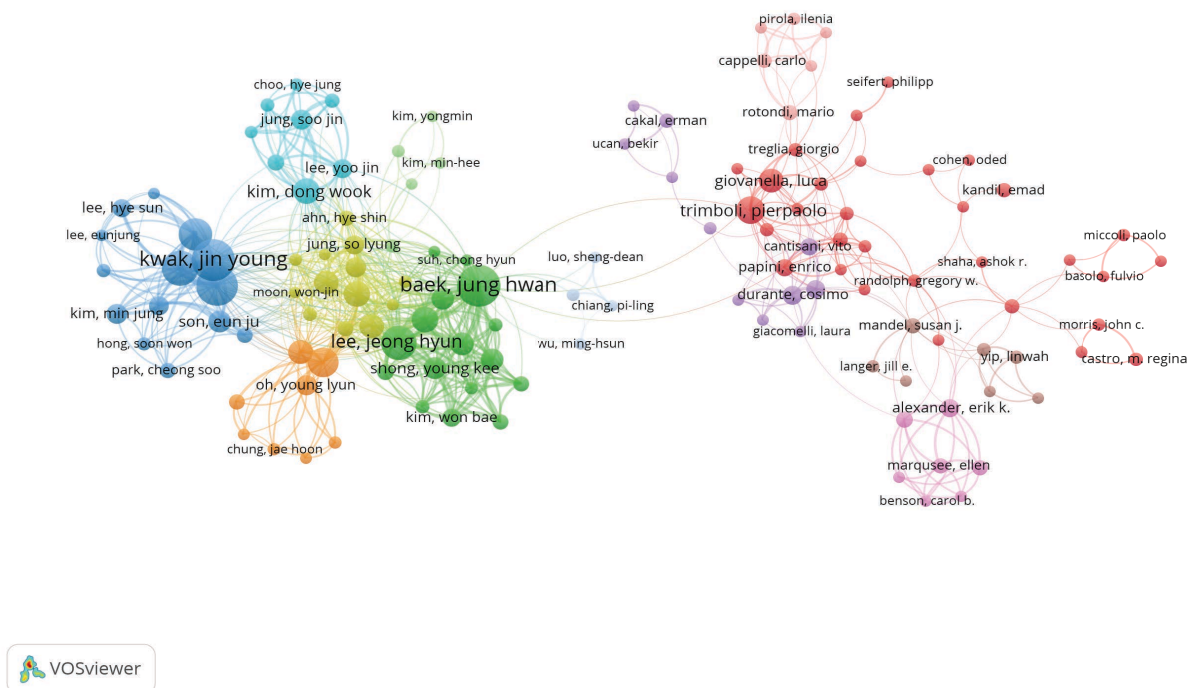


Figure 4. Co-authorship network of leading authors in research on ultrasound diagnosis of thyroid nodules.

3.4. Journal distribution

Publications on thyroid nodule ultrasound were concentrated in a few core journals but spanned across radiology, endocrinology, and multidisciplinary outlets (**Table 3**). Thyroid ranked first, publishing 207 articles with over 26,000 citations, reflecting its role as the leading forum for guidelines and consensus statements. Frontiers in Endocrinology contributed the second-highest number of articles (133), but with relatively low citation averages, likely due to recent publications. Other endocrine journals, such as Endocrine and JCEM, were also major contributors, with JCEM showing particularly high average citations (around 89 per paper). Radiology journals, including European Radiology, Journal of Ultrasound in Medicine, and Korean Journal of Radiology, provided substantial outputs, while Radiology, with only 25 papers, achieved the highest average impact (around 143 citations each). Overall, a few high-impact journals dominate influence, while specialized journals host most of the technical research.

Table 3. Top 10 journals by publication output

Journal name	Total number of articles	Total citations	Average citations
Thyroid	207	26084	126.0097
Frontiers In Endocrinology	133	1205	9.0602
Endocrine	122	2198	18.0164
Journal Of Ultrasound In Medicine	92	2835	30.8152
Journal Of Clinical Endocrinology & Metabolism	91	8130	89.3407
European Radiology	79	3311	41.9114
Clinical Endocrinology	78	2541	32.5769
American Journal Of Roentgenology	63	3441	54.619
Korean Journal Of Radiology	44	2962	67.3182
Radiology	25	3578	143.12

3.5. Keyword co-occurrence and thematic evolution

The author keyword analysis highlights the main research focus in thyroid nodule ultrasound. The most frequent terms were cancer, management, ultrasound, diagnosis, malignancy, and fine-needle aspiration (FNA), which align closely with the central clinical task of distinguishing malignant from benign nodules (**Table 4**).

Table 4. Top 10 keywords by co-occurrence frequency

Rank	Frequency	Centrality	Time	Keyword
1	1681	0	2000	cancer
2	1616	0	2000	management
3	989	0	2000	ultrasound
4	942	0	2000	diagnosis
5	878	0	2000	nodules
6	873	0	2000	carcinoma
7	854	0	2000	thyroid nodule
8	775	0	2000	fine needle aspiration
9	736	0	2002	malignancy
10	694	0	2000	thyroid nodules

The co-occurrence network (**Figure 5**) reveals three thematic clusters. One cluster is centered on imaging and risk stratification, represented by keywords such as ultrasound, TI-RADS, calcifications, and elastography. Another cluster focuses on cytology and molecular diagnosis, with terms including FNA, cytology, the Bethesda system, and BRAF mutation. A third cluster highlights treatment and management, encompassing management, surgery, radiofrequency ablation, and thyroidectomy. Bridging these clusters are recurring terms such as thyroid cancer, malignant, and diagnosis, which appear across contexts and underscore their central role in the literature. Burst keyword analysis further indicates that recent hotspots include guidelines, classification systems (TI-RADS), and radiofrequency ablation, with artificial intelligence emerging as a growing focus in the last five years.

3.6. Reference co-citation analysis

Figure 6 illustrates the co-citation relationships and academic influence among core references. Node size indicates citation frequency, with Haugen (2016) and Cooper (2009) as dominant nodes, underscoring their central role in guideline development for thyroid nodule diagnosis and management. Early foundational works such as Papini (2002) and Moon (2008) laid the groundwork, while Russ (2017) and Durante (2015) reflect more recent advances in diagnostic standards and risk stratification. The network's color-coded clusters capture the thematic evolution of the field: one centered on fine-needle aspiration and cytopathology, another on ultrasound features and malignancy prediction, and a third on guidelines and clinical management. Together, these clusters reveal a developmental trajectory from classic studies to guideline-driven practice and imaging-based approaches, establishing a stable knowledge framework that continues to integrate emerging research findings.

4. Discussion

This bibliometric analysis provides a comprehensive overview of research on ultrasound diagnosis of thyroid nodules, highlighting how the field has evolved in response to clinical needs, guideline development, and technological innovation. The trajectory of publications and citation patterns shows not only growing academic interest but also a gradual convergence toward standardized diagnostic pathways. Interpreting these patterns offers insights into strengths, unresolved challenges, and future directions.

The dominance of guidelines and structured classification systems in the co-citation network underscores their pivotal role in shaping the intellectual foundation of the field. Landmark documents such as the 2015 American Thyroid Association (ATA) guidelines remain central, unifying practice standards across diverse clinical environments. More recently, the updated Bethesda System has refined indeterminate categories and malignancy risk estimates, directly influencing how cytology guides management ^[4]. Comparative validation of major TIRADS frameworks (ACR, EU, K-TIRADS) demonstrates broad agreement but systematic differences in risk allocation ^[5]. This lack of harmonization complicates multinational research and clinical adoption, pointing to the need for global efforts to reconcile thresholds for malignancy prediction and align diagnostic lexicons.

Publication trends also reflect a paradigm shift from diagnosis to management. Earlier studies concentrated on distinguishing benign from malignant nodules, whereas more recent research emphasizes therapeutic strategies. Radiofrequency ablation (RFA) for benign nodules exemplifies this transition. Consensus statements now provide clear recommendations on patient selection, technique, and follow-up, consolidating RFA as a safe and effective alternative to surgery ^[6]. By reducing morbidity compared to thyroidectomy, minimally invasive ablation improves quality of life, recovery time, and cosmetic outcomes. In parallel, active surveillance for low-risk papillary thyroid carcinoma has matured into a validated management pathway. Large cohorts confirm that carefully monitored surveillance can safely avoid overtreatment while maintaining excellent prognosis ^[6]. Together, these strategies represent a shift in oncology toward risk-adapted approaches that balance oncologic safety with patient-centered outcomes.

Artificial intelligence (AI) has rapidly emerged as another defining theme. Deep learning models show promise in augmenting human interpretation, particularly in detecting subtle features such as gross extrathyroidal extension that may be missed by radiologists ^[3]. These technologies could expand access to expert-level interpretation in regions with limited subspecialty expertise. Yet integration into practice faces barriers: variability in image acquisition protocols, equipment, and operator expertise introduces heterogeneity that may limit model generalizability. Moreover, AI must evolve in step with pathology classifications. The 2024 WHO classification and 2023 Bethesda updates have refined diagnostic categories and clarified indeterminate zones ^[3]. Models trained on outdated frameworks risk misalignment with current standards, emphasizing the need for synergy between technological development and evolving diagnostic criteria.

Global collaboration patterns highlight both strengths and limitations. Korean researchers dominate output, especially in radiology-driven studies such as ultrasound-guided interventions and K-TIRADS development. European and North American scholars, though less prolific, have shaped guidelines, cytopathology frameworks, and influential meta-analyses. While this regional specialization has been productive, limited cross-continental collaboration means that findings are often validated locally rather than globally. Building shared image repositories and multinational datasets linking ultrasound features, cytology, and outcomes would enhance reproducibility and generalizability.

The distribution of research across journals reflects the field's dual structure. Specialty outlets such as

the Korean Journal of Radiology and European Radiology publish much of the methodological innovation, while high-impact endocrine journals like *Thyroid* and *JCEM* concentrate the most influential guidelines and practice-changing studies. This two-tiered dissemination suggests that technical advances circulate within specialty readerships, whereas general guidelines reach broader audiences through mainstream journals. For future dissemination, bridging these outlets may ensure that methodological innovations achieve wider clinical translation.

From a clinical perspective, the findings underscore the need to integrate standardized risk stratification with individualized management. Consistent use of ultrasound lexicons and cytology frameworks enhances diagnostic uniformity, while strategies such as RFA and active surveillance expand the therapeutic repertoire beyond surgery. AI holds promise but requires careful validation and interpretability to avoid premature clinical adoption. From a research standpoint, priorities include multinational trials comparing TIRADS frameworks, integration of AI with updated cytology systems, and pragmatic studies evaluating real-world management strategies with attention to patient-reported outcomes and health economics.

This study has limitations. Restriction to the Web of Science Core Collection and English-language publications may underrepresent non-English literature and regional practices. Challenges in author name disambiguation and institutional affiliations could bias productivity metrics. Furthermore, citation-based analyses are limited by time lag, with newer studies not yet accruing influence. Nonetheless, consistent patterns across multiple indicators, such as the centrality of guidelines, dominance of regional clusters, and emergence of AI and minimally invasive management, support the robustness of the findings.

5. Conclusion

In conclusion, the landscape of thyroid nodule ultrasound research reflects both consolidation and innovation. Core guidelines and classification systems provide a stable framework, while minimally invasive therapies, surveillance strategies, and AI are reshaping practice. Recent advances in cytopathology^[4], comparative validation of risk stratification^[5], consensus on ablation therapy^[7], evidence supporting surveillance^[8], AI-driven imaging interpretation^[3], and updated pathology frameworks^[9] together illustrate a field moving toward standardized yet personalized care. Global collaboration and harmonization of diagnostic criteria will be essential to optimize patient outcomes and ensure equitable dissemination of best practices.

Disclosure statement

The authors declare no conflict of interest.

References

- [1] Tessler F, Middleton W, Grant E, et al., 2017, ACR Thyroid Imaging, Reporting and Data System (TI-RADS): White Paper of the ACR TI-RADS Committee. *J Am Coll Radiol*, 14(5): 587–595.
- [2] Chou R, Dana T, Haymart M, et al., 2022, Active Surveillance Versus Thyroid Surgery for Differentiated Thyroid Cancer: A Systematic Review. *Thyroid*, 32(4): 351–367.
- [3] Qi Q, Huang X, Zhang Y, et al., 2023, Ultrasound Image-Based Deep Learning to Assist in Diagnosing Gross Extrathyroidal Extension Thyroid Cancer: A Retrospective Multicenter Study. *EClinicalMedicine*, 58: 101905.

- [4] Ali S, Baloch Z, Cochand-Priollet B, et al., 2023, The 2023 Bethesda System for Reporting Thyroid Cytopathology. *Thyroid*, 33(9): 1039–1044.
- [5] Piticchio T, Russ G, Radzina M, et al., 2024, Head-to-Head Comparison of American, European, and Asian TIRADSs in Thyroid Nodule Assessment: Systematic Review and Meta-Analysis. *Eur Thyroid J*, 13(2): e230242.
- [6] Orloff L, Noel J, Stack B, et al., 2022, Radiofrequency Ablation and Related Ultrasound-Guided Ablation Technologies for Treatment of Benign and Malignant Thyroid Disease: An International Multidisciplinary Consensus Statement of the American Head and Neck Society Endocrine Surgery Section with the Asia Pacific Society of Thyroid Surgery, Associazione Medici Endocrinologi, British Association of Endocrine and Thyroid Surgeons, European Thyroid Association, Italian Society of Endocrine Surgery Units, Korean Society of Thyroid Radiology, Latin American Thyroid Society, and Thyroid Nodules Therapies Association. *Head Neck*, 44(3): 633–660.
- [7] Lui M, Patel K, 2024, Current Guidelines for the Application of Radiofrequency Ablation for Thyroid Nodules: A Narrative Review. *Gland Surg*, 13(1): 59–69.
- [8] Kim M, Moon J, Lee E, et al., 2024, Active Surveillance for Low-Risk Thyroid Cancers: A Review of Current Practice Guidelines. *Endocrinol Metab (Seoul)*, 39(1): 47–60.
- [9] Bychkov A, Jung C, 2024, What's New in Thyroid Pathology 2024: Updates from the New WHO Classification and Bethesda System. *J Pathol Transl Med*, 58(2): 98–101.

Publisher's note

Bio-Byword Scientific Publishing remains neutral with regard to jurisdictional claims in published maps and institutional affiliations.

Investigation of Potential Biological Mechanisms Linking Blood Lipids and Head and Neck Squamous Cell Carcinoma

Aoxiong Zhou^{1*}, Jiahao Chen², Yumeng Ou¹, Jinhai Wu³

¹Department of Radiotherapy V, Guangzhou Institute of Cancer Research, the Affiliated Cancer Hospital, Guangzhou Medical University, Guangzhou, Guangdong, China

²Department of Hepatobiliary Surgery, Guangzhou Institute of Cancer Research, the Affiliated Cancer Hospital, Guangzhou Medical University, Guangzhou, Guangdong, China

³Department of Urology, Guangzhou Institute of Cancer Research, the Affiliated Cancer Hospital, Guangzhou Medical University, Guangzhou, Guangdong, China

**Author to whom correspondence should be addressed.*

Copyright: © 2025 Author(s). This is an open-access article distributed under the terms of the Creative Commons Attribution License (CC BY 4.0), permitting distribution and reproduction in any medium, provided the original work is cited.

Abstract: *Background:* Head and neck squamous cell carcinoma (HNSCC) is a common malignancy with a heterogeneous etiology. Circulating total cholesterol (TC), apolipoprotein A-I (ApoA-I), and low-density lipoprotein cholesterol (LDL-C) may influence tumorigenesis via metabolic, inflammatory, and immune pathways. The causal relationship and molecular mechanisms remain unclear. This study systematically evaluated lipid-related genetic variants and HNSCC risk. *Methods:* Two-sample Mendelian randomization (MR) using genome-wide association study (GWAS) data assessed causal effects of TC, ApoA-I, and LDL-C on head and neck cancer (HNC). Significant single-nucleotide polymorphisms (SNPs) were functionally annotated and subjected to pathway enrichment. Candidate genes were analyzed in GEPIA2, TIMER3.0, and cBioPortal for differential expression (DE), survival, immune infiltration, and clinical stage associations. *Results:* MR revealed no significant causal effects ($P > 0.05$). Positive effect group SNPs are enriched in cytochrome P450 (CYP450)-mediated xenobiotic metabolism; negative effect group SNPs are enriched in monocarboxylic acid and alcohol metabolism pathways, suggesting protective metabolic adaptation. DE analysis showed ADH1B downregulation and FADS1/2, PARP9, and SEMA7A upregulation. Immune infiltration linked these genes to CD8⁺ T cells, M1/M2 macrophages, regulatory T cells (Treg), cancer-associated fibroblasts (CAF), and NK cells, with ADH1B downregulation associated with immunotherapy response. ALDH1A2, EVI5, and LCAT, though not DE, exhibited prognostic value, with expression increasing in advanced stages. *Conclusion:* Lipid-related variants may influence HNSCC via opposing mechanisms: CYP450/inflammation versus metabolic adaptation/alcohol pathways. ADH1B and FADS1/2, PARP9, SEMA7A regulate tumor metabolism and immune microenvironment; ALDH1A2, EVI5, and LCAT hold prognostic potential. These findings provide mechanistic insight and candidate molecular targets for HNSCC prediction and intervention.

Keywords: Lipids; HNSCC; Functional enrichment; Immune infiltration; Prognostic biomarkers

Online publication: October 16, 2025

1. Introduction

Head and neck squamous cell carcinoma (HNSCC) is one of the most common malignancies worldwide and imposes a significant public health burden. HNSCC accounts for hundreds of thousands of new cases and deaths annually worldwide, with highly heterogeneous etiology and carcinogenic mechanisms ^[1]. Beyond traditional risk factors such as smoking, alcohol consumption, and HPV infection, metabolic abnormalities and alterations in lipid profiles have recently attracted increasing attention ^[2]. Circulating lipids, which play essential roles in energy metabolism, cell membrane synthesis, and signaling pathways, are thought to contribute to tumor initiation and progression through inflammation, immune modulation, and endocrine mechanisms ^[3,4].

Multiple clinical and epidemiological studies have reported associations between circulating lipids (total cholesterol [TC], low-density lipoprotein [LDL], high-density lipoprotein [HDL], triglycerides [TG]) and apolipoproteins (ApoA-I, ApoB) with the risk or prognosis of head and neck tumors ^[5-9]. Some studies have further suggested that preoperative or treatment-period lipid and ApoA-I levels may predict responses to immunotherapy or chemoradiotherapy and survival outcomes ^[10]. These observational findings indicate measurable signals between “lipid levels and tumor phenotypes.” However, due to confounding factors (e.g., smoking, nutritional status, concomitant medications—particularly statins), reverse causation, and differences in sample size or tumor subtypes, observational evidence alone is insufficient to establish causality.

Accordingly, we designed a multi-layered research framework: first, two-sample Mendelian randomization (MR) analyses were conducted using publicly available GWAS data to assess the causal effects of high cholesterol, ApoA-I and low-density lipoprotein cholesterol (LDL-C) on head and neck cancer risk; subsequently, single nucleotide polymorphisms (SNPs) exhibiting consistent effect directions in both exposures and outcomes and reaching statistical significance were selected for functional annotation and pathway enrichment analyses to explore the associated metabolic and signaling networks; finally, the identified genes were integrated into multi-omics and online database platforms (GEPIA2, TIMER3.0, and cBioPortal) to perform differential expression, survival, immune infiltration, and clinicopathological association analyses, thereby elucidating potential links between circulating lipids, genetic variation, molecular mechanisms, and clinical phenotypes. This integrative research strategy aims to provide more reliable and systematic evidence regarding the causal relationship between lipid metabolism and HNSCC risk, as well as the underlying molecular pathways, offering new insights for future clinical prediction and intervention.

2. Materials and methods

2.1. Overall study design

The overall study design comprised three sequential steps:

- (1) Conducting two-sample MR analyses using publicly available GWAS summary data to evaluate the potential causal associations of high cholesterol, ApoA-I, and LDL-C with head and neck cancer risk (HNC);
- (2) Based on the significant SNPs identified from the MR analyses, variants exhibiting consistent effect directions across both exposures and outcomes and reaching statistical significance were selected, categorized into positive and negative effect groups, and subjected to functional annotation and enrichment analyses to explore the underlying biological pathways;
- (3) All candidate genes were then integrated into multi-omics and online database platforms, including GEPIA2, TIMER3.0, and cBioPortal, to perform differential expression, survival, immune infiltration,

and clinicopathological association analyses.

2.2. Data sources

This study employed a two-sample MR approach to assess the potential causal relationships between circulating lipid-related exposures and HNC risk. The exposures included high cholesterol (ebi-a-GCST90029021), ApoA-I (ieu-b-107), and LDL-C (ieu-b-110), while the outcome was head and neck cancer (ieu-b-4912). The GWAS summary statistics for these exposures and the outcome were retrieved and downloaded from the OpenGWAS platform (<https://gwas.mrcieu.ac.uk/>)^[11]. All data were derived from previously published studies with appropriate ethical approvals; therefore, no additional ethical approval was required for this study.

2.3. SNP dressing by screening

SNPs significantly associated with high cholesterol, ApoA-I, and LDL-C ($p < 5 \times 10^{-8}$) were selected. SNPs in linkage disequilibrium ($r^2 < 0.001$, window $< 10,000$ kb) were excluded to retain independent variants for subsequent analyses. Subsequently, the F statistic for each SNP was calculated to ensure instrument strength ($F > 10$), and weak instruments were excluded. Finally, the validity and robustness of the selected instruments were further assessed using the MR Steiger filter and the MR-PRESSO test.

For the primary MR analyses, SNPs present in both exposures and outcome with consistent effect directions (i.e., both β_{exposure} and β_{outcome} positive or both negative) and reaching statistical significance in both ($P < 0.05$) were retained as the main analysis set. These SNPs were then categorized into positive and negative effect groups according to effect direction and retained for subsequent functional annotation and enrichment analyses.

2.4. SNP function annotation and gene localization

All SNPs from each group were input into the Ensembl Variant Effect Predictor (VEP; <https://www.ensembl.org/Tools/VEP>) for functional annotation to determine their potential regulatory effects, functional categories, and the candidate genes they mapped to^[12]. VEP is a powerful and flexible tool that annotates the potential biological impact of genomic variants and provides detailed information regarding variant positions, implicated genes, and their possible functions, thereby enabling the identification of genes mapped by SNPs in the positive and negative effect groups. The genes were then organized into two independent gene sets, corresponding to the positive and negative effect groups; finally, all genes mapped by the SNPs were combined into a comprehensive target gene set for subsequent analyses.

2.5. Enrichment analysis

Metascape (<https://metascape.org>) is an integrated bioinformatics platform^[13] that incorporates over 40 distinct biological databases and offers various functional analyses, including interactive analysis and gene annotation. Pathway and functional enrichment analyses were performed separately for the positive and negative gene sets using Metascape, extracting significantly enriched biological processes, signaling pathways, and cellular components.

2.6. Differential expression and survival analysis

GEPIA2 (<http://gepia.cancer-pku.cn/index.html>) is a comprehensive online analysis platform^[14] that leverages RNA-sequencing data from The Cancer Genome Atlas (TCGA) and the Genotype-Tissue Expression (GTEx) projects. All candidate genes mapped by SNPs were input into GEPIA2 for differential expression analysis (tumor

vs. normal) and survival analysis (overall survival and disease-free survival) using the TCGA HNSC dataset. Differential expression analysis was conducted using normalized RNA-seq TPM data, with statistical significance assessed via an ANOVA model. Survival analysis was performed using the Kaplan–Meier method, with samples stratified by median expression levels, and significance tested using the log-rank test.

2.7. Correlation between immune infiltration and immunotherapy

Genes showing significant differential expression in GEPIA2 were further evaluated in TIMER3.0 (<http://timer.cistrome.org/>) for their associations with the tumor immune microenvironment^[15]. TIMER3.0 provides comprehensive immune infiltration analysis and assessment of immunotherapy effects. Analyses included correlations between candidate gene expression and various immune cell types, such as CD8⁺ T cells, regulatory T cells (Tregs), macrophage subtypes (M0, M1, and M2), cancer-associated fibroblasts (CAFs), neutrophils, natural killer (NK) cells, and myeloid-derived suppressor cells (MDSCs), along with an immunotherapy response prediction module to explore the potential immunotherapeutic relevance of these genes.

2.8. Analysis of clinical pathological staging

cBioPortal for Cancer Genomics (<http://cbioportal.org>) is an open-access cancer genomics resource^[16] that provides integrated views of cancer genomic datasets along with associated clinical information. Genes showing significant prognostic associations in survival analyses were queried in cBioPortal to assess the relationships between mRNA expression levels and clinical features, including pathological stage and mutation status, within the TCGA-HNSC dataset. Gene expression distributions were extracted following the default cBioPortal workflow and compared across different pathological stages.

2.9. Statistical analysis

Primary MR analyses were conducted using R version 4.5.1 with the TwoSampleMR package, employing methods such as MR-IVW, weighted median, and MR-Egger, along with MR-PRESSO to detect potential pleiotropy and outliers^[17]. Functional annotation, enrichment, differential expression, immune infiltration, and pathological stage analyses were all performed using the default or recommended parameters of each platform. All statistical tests were two-sided, with $P < 0.05$ considered statistically significant, and multiple testing corrections applied when appropriate.

3. Results

3.1. Mendel randomized analysis of blood lipids and head and neck cancer

This study employed a two-sample MR approach to evaluate the potential causal effects of lipid-related exposures on HNC risk. The results indicated that high cholesterol, ApoA-I, and LDL-C were not significantly associated with head and neck cancer risk (**Table 1**). Estimates obtained from weighted median, MR-Egger, simple mode, and weighted mode methods were directionally consistent, with all P values > 0.05 . The concordant effect directions across different MR methods, coupled with the lack of statistical significance, suggest an absence of robust direct causal evidence linking high cholesterol, ApoA-I, and LDL-C levels to head and neck cancer risk.

Table 1. Mendelian randomization analysis of blood lipids and head and neck cancers

Outcome	Exposure	Method	nSNP	B	se	p - value
Head and neck cancer	High cholesterol	MR Egger	75	-2.01E-03	3.65E-03	0.58
		Weighted median	75	3.22E-03	3.18E-03	0.31
		Inverse variance weighted	75	7.79E-04	2.15E-03	0.72
		Simple mode	75	5.56E-03	5.72E-03	0.33
		Weighted mode	75	2.31E-03	3.43E-03	0.50
	Apolipoprotein A-I	MR Egger	292	2.83E-04	4.66E-04	0.54
		Weighted median	292	9.87E-04	5.44E-04	0.07
		Inverse variance weighted	292	-9.88E-06	3.09E-04	0.97
		Simple mode	292	-6.92E-04	1.34E-03	0.61
		Weighted mode	292	6.82E-04	5.39E-04	0.21
	LDL cholesterol	MR Egger	177	1.38E-04	3.95E-04	0.73
		Weighted median	177	5.43E-04	4.62E-04	0.24
		Inverse variance weighted	177	3.83E-04	2.98E-04	0.20
		Simple mode	177	-1.12E-04	9.61E-04	0.91
		Weighted mode	177	2.66E-04	3.70E-04	0.47

3.2. SNP functional annotation analysis

To further investigate the potential biological mechanisms through which lipid-related genetic variants may influence head and neck cancer, we performed functional annotation on SNPs selected from the MR analysis results. First, based on the effect direction (i.e., concordant beta values for exposure and outcome) and statistical significance ($P < 0.05$), SNPs were classified into a positive effect group (beta > 0, $n = 10$) and a negative effect group (beta < 0, $n = 8$). Subsequently, SNPs from each group were input into the VEP for functional annotation and gene mapping. Functional annotation revealed that the positive effect group SNPs mapped to 11 candidate genes, while the negative effect group SNPs also mapped to 11 candidate genes. The annotation process included the genomic loci of the SNPs, variant types (e.g., exonic nonsynonymous, intronic, regulatory region variants), and predictions of potential regulatory functions.

3.3. Functional enrichment analysis

Considering the potential involvement of complex multi-pathway mechanisms linking lipid metabolism to tumorigenesis, we further performed functional annotation and pathway enrichment analyses on genes grouped by the direction of their beta values.

3.3.1. Positive group SNP enrichment analysis results

Genes mapped from the positive effect group SNPs were significantly enriched in the “Drug metabolism, cytochrome P450” pathway (KEGG), as well as Gene Ontology (GO) biological processes, including “response to xenobiotic stimulus” and “regulation of catalytic activity” (**Figure 1**). These findings suggest that these genes are primarily involved in the metabolism and clearance of exogenous chemicals, such as drugs and environmental carcinogens, and are closely associated with regulating enzymatic activity. DisGeNET disease

phenotype enrichment analysis indicated that these genes were significantly associated with various inflammatory and immune-related disorders (**Figure 2**), including “Allergic Reaction,” “Alcohol-Induced Disorders,” and “Neutrophilia,” and were also highly relevant to tumor phenotypes, such as “Malignant neoplasm of larynx,” “Carcinoma of larynx,” and “Laryngeal Squamous Cell Carcinoma.” PaGenBase tissue-specific expression analysis showed that this gene set was enriched in liver tissue (Count = 3, 27%, Log10(P) = -2.80), suggesting a specific role for these genes in hepatic metabolic processes. Transcription factor target enrichment analysis revealed a significant enrichment of DLX6 target genes (Count = 4, 36%, Log10(P) = -4.40). DLX6 is a transcription factor involved in embryonic development, and its antisense RNA (DLX6-AS1) has been reported to promote cell proliferation and metastasis in laryngeal and other head and neck cancers.

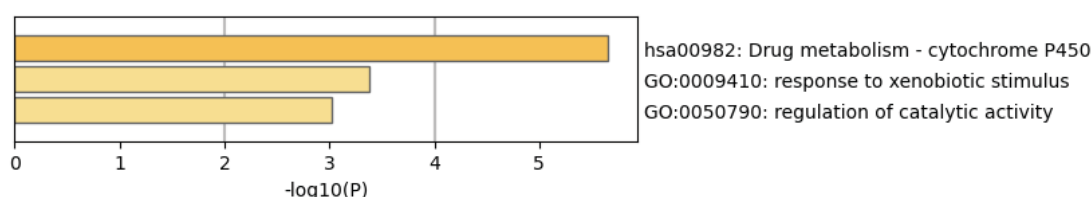


Figure 1. Pathway and process enrichment analysis (+SNP).

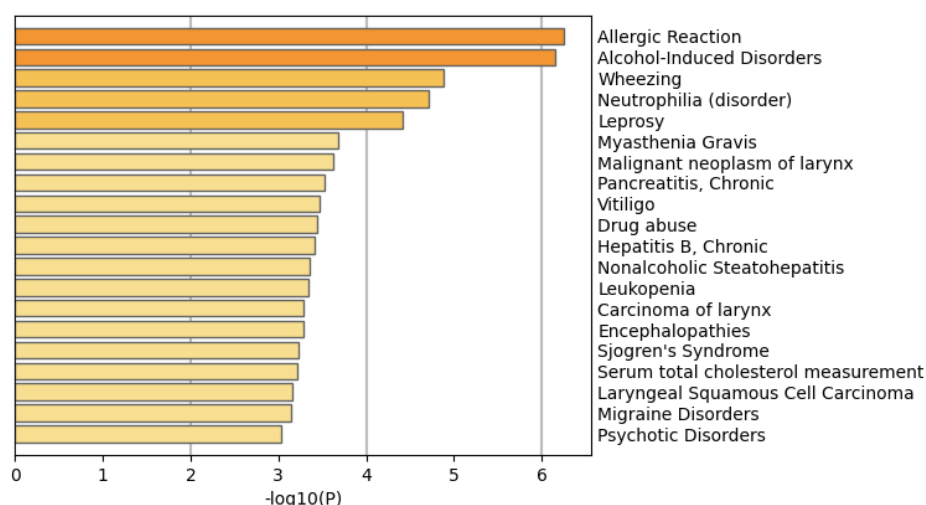


Figure 2. DisGeNET disease association analysis (+SNP).

3.3.2. Negative group SNP enrichment analysis results

Genes mapped from the negative effect group SNPs were primarily enriched in metabolic and adaptive processes, including the “monocarboxylic acid biosynthetic process,” “alcohol metabolic process,” and “response to nutrient levels” (**Table 2**). Among these, monocarboxylic acid metabolism showed the most significant enrichment, encompassing the production and utilization of key metabolites such as lactate and short-chain fatty acids, suggesting a potential role in energy metabolism and tumor microenvironment regulation. DisGeNET disease phenotype enrichment (**Figure 3**) indicated that these genes were closely associated with multiple lipid-related traits, including HDL, LDL, total cholesterol, triglycerides, and metabolic disorders such as hypertriglyceridemia and dyslipidemia. Additionally, they were significantly associated with glucose levels, hematological parameters

(e.g., white blood cell count, hemoglobin), and inflammatory markers (e.g., C-reactive protein, serum albumin). Transcription factor regulatory enrichment highlighted the target gene sets of ZNF507 and ZNF589. These two zinc finger transcription factors are widely involved in gene transcription regulation, chromatin structure maintenance, and cell fate determination, and their downstream regulatory networks may serve as a bridge between lipid metabolism regulation and tumor risk modulation.

Table 2. Pathway and process enrichment analysis (-SNP)

GO	Category	Description	Count	%	Log10(P)	Log10(q)
GO:0072330	GO Biological Processes	monocarboxylic acid biosynthetic process	4	36.36	-6.41	-2.07
GO:0006066	GO Biological Processes	alcohol metabolic process	3	27.27	-3.74	-0.40
GO:0031667	GO Biological Processes	response to nutrient levels	3	27.27	-3.08	0.00

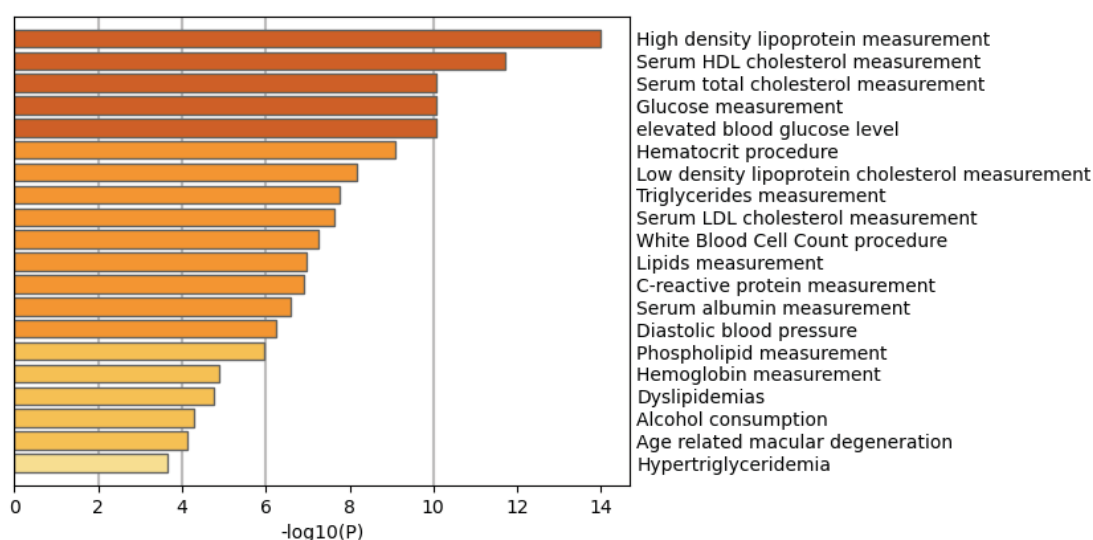


Figure 3. DisGeNET disease association analysis (-SNP).

3.4. Differentially expressed genes

To further investigate the potential roles of genes mapped from relevant SNPs in head and neck squamous cell carcinoma (HNSC), we integrated all genes mapped from both positive and negative effect SNPs as target genes for differential expression analysis. Gene expression data were obtained from the GEPIA2 database, comparing expression levels between HNSC tumor tissues and normal tissues. The analysis revealed that among all target genes, ADH1B, FADS1, FADS2, PARP9, and SEMA7A exhibited significant differential expression in HNSC tissues. Specifically, ADH1B was significantly downregulated in tumor tissues compared to normal tissues, whereas FADS1, FADS2, PARP9, and SEMA7A were significantly upregulated in tumor tissues, exhibiting higher transcriptional levels relative to normal tissues (**Figure 4**). These findings suggest that ADH1B may play a potential protective role in tumorigenesis or tumor-suppressive mechanisms, whereas FADS1, FADS2, PARP9, and SEMA7A may be associated with tumor progression.

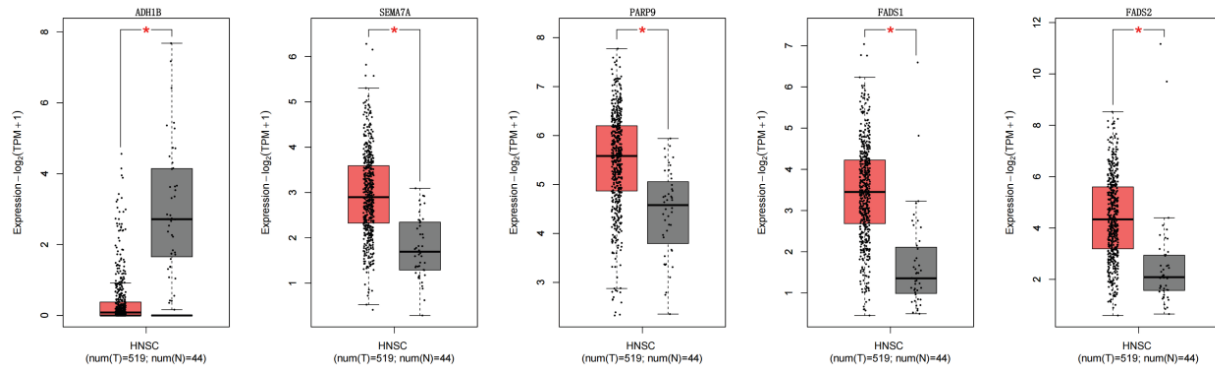


Figure 4. FADS1, FADS2, PARP9 and SEMA7A differential expression analysis.

3.5. Immune infiltration analysis and immune therapy response

3.5.1. Correlation between differentially expressed genes and tumor immune infiltration

Using TIMER3.0 and multiple immune estimation tools, we analyzed the correlations between ADH1B, FADS1, FADS2, PARP9, and SEMA7A and immune cell infiltration, revealing that all these genes were significantly associated with the infiltration levels of multiple immune cell types. ADH1B expression was positively correlated with CD8⁺ T cells ($Rho = 0.292, p = 4.38 \times 10^{-11}$), M1 macrophages ($Rho = 0.332, p = 4.39 \times 10^{-14}$), and NK cells ($Rho = 0.309, p = 2.51 \times 10^{-12}$), but negatively correlated with MDSCs ($Rho = -0.136, p = 2.6 \times 10^{-3}$) and neutrophils ($Rho = -0.257, p = 7.96 \times 10^{-9}$) (**Figure 5**). FADS1 was significantly positively correlated with cancer-associated fibroblasts (CAF, $Rho = 0.382, p = 1.68 \times 10^{-18}$), MDSCs ($Rho = 0.253, p = 1.28 \times 10^{-8}$), M2 macrophages ($Rho = 0.336, p = 2.14 \times 10^{-14}$), and Tregs ($Rho = 0.20, p = 7.84 \times 10^{-6}$), while negatively correlated with CD8⁺ T cells ($Rho = -0.444, p = 4.33 \times 10^{-25}$) (**Figure 6**). FADS2 exhibited strong positive correlations with CAF ($Rho = 0.405, p = 8.18 \times 10^{-21}$), M2 macrophages ($Rho = 0.41, p = 2.67 \times 10^{-21}$), and Tregs ($Rho = 0.303, p = 7.06 \times 10^{-12}$), while negatively correlating with CD8⁺ naïve T cells ($Rho = -0.316, p = 8.27 \times 10^{-13}$) and NK cells ($Rho = -0.226, p = 4.12 \times 10^{-7}$) (**Figure 7**). PARP9 was strongly correlated with M1 macrophages ($Rho = 0.565, p = 1.34 \times 10^{-42}$), M2 macrophages ($Rho = 0.303, p = 7.37 \times 10^{-12}$), Tregs ($Rho = 0.381, p = 2.05 \times 10^{-18}$), neutrophils ($Rho = 0.58, p = 2.27 \times 10^{-45}$), and NK cells ($Rho = 0.433, p = 9.04 \times 10^{-24}$), while negatively correlating with CD8⁺ naïve T cells ($Rho = -0.322, p = 2.85 \times 10^{-13}$) (**Figure 8**). SEMA7A was positively correlated with CAF ($Rho = 0.315, p = 8.94 \times 10^{-13}$), M0/M2 macrophages ($Rho = 0.345, p = 3.84 \times 10^{-15}$; $Rho = 0.199, p = 9.00 \times 10^{-6}$), and neutrophils ($Rho = 0.365, p = 6.34 \times 10^{-17}$), while negatively correlated with CD8⁺ T cells ($Rho = -0.159, p = 4.07 \times 10^{-4}$) and activated NK cells ($Rho = -0.193, p = 1.65 \times 10^{-5}$) (**Figure 9**).

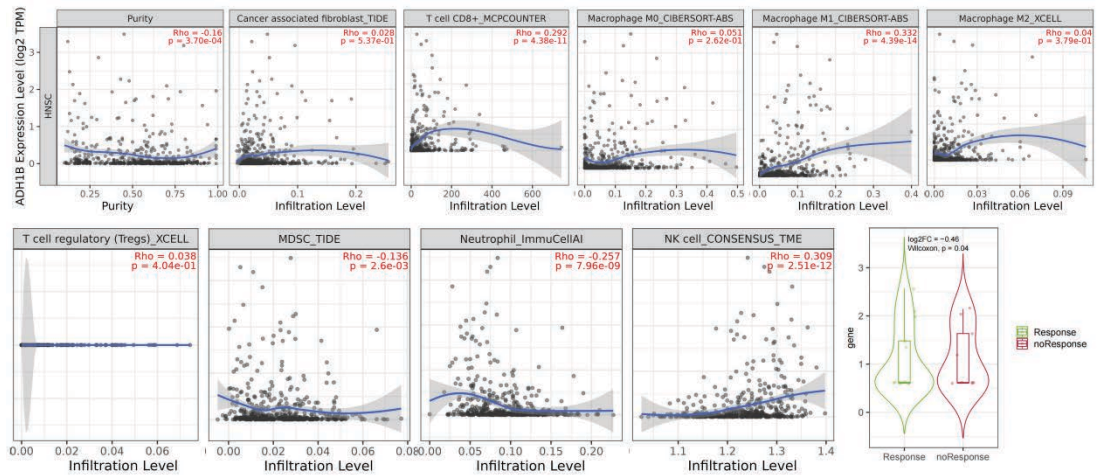


Figure 5. ADH1B Immune infiltration analysis and immune response to therapy.

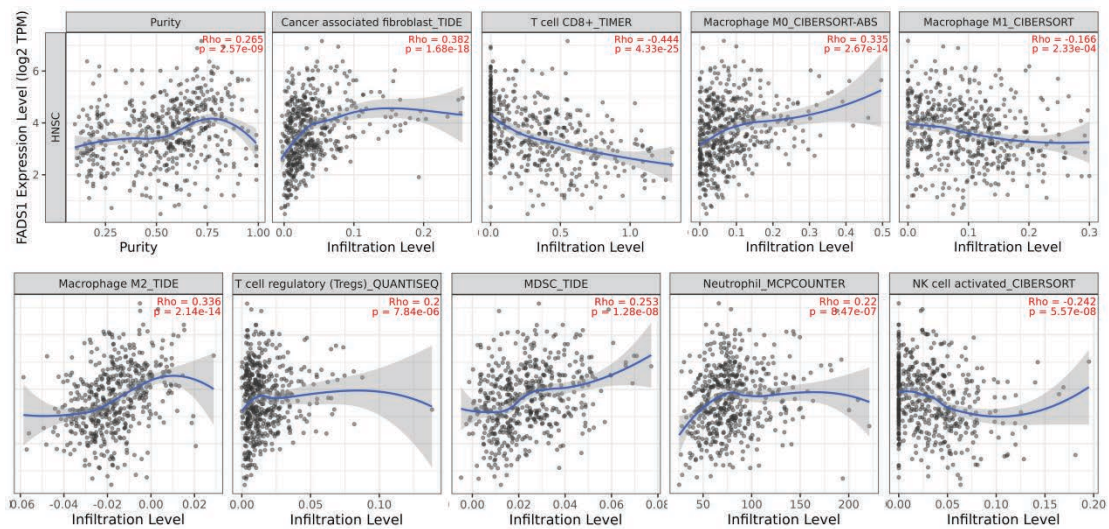


Figure 6. FADS1 Immune infiltration analysis.

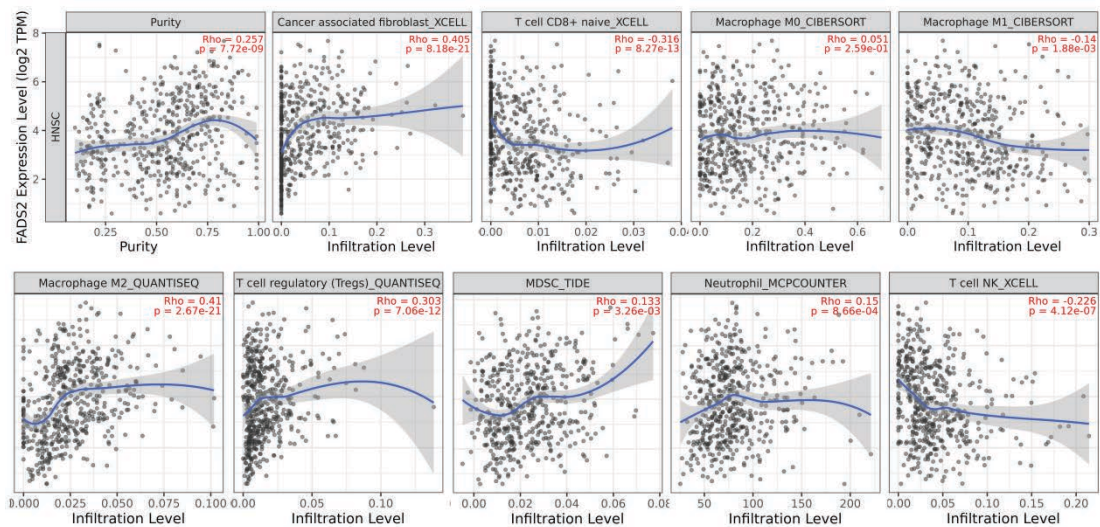


Figure 7. FADS2 Immune infiltration analysis.

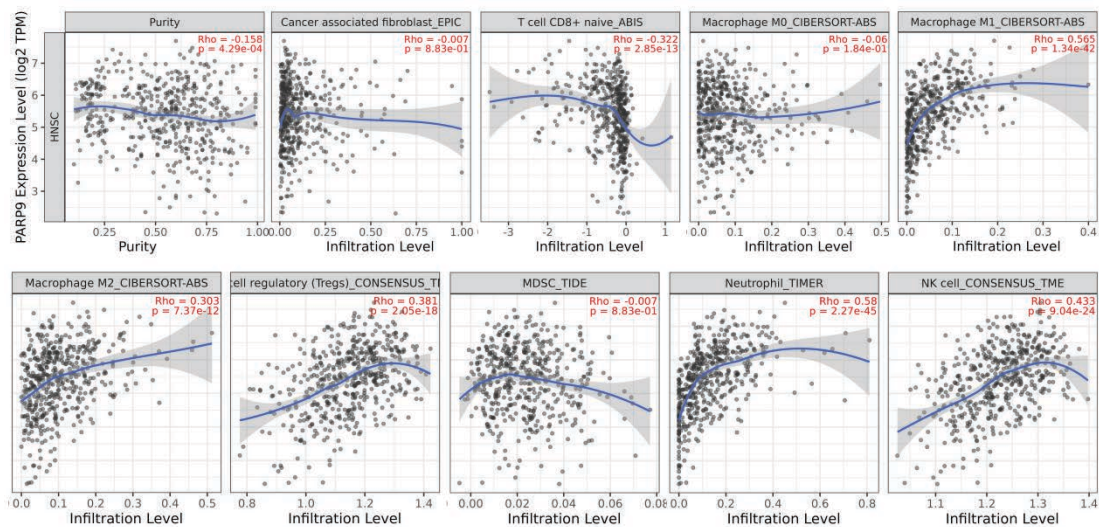


Figure 8. ADH1B Immune infiltration analysis.

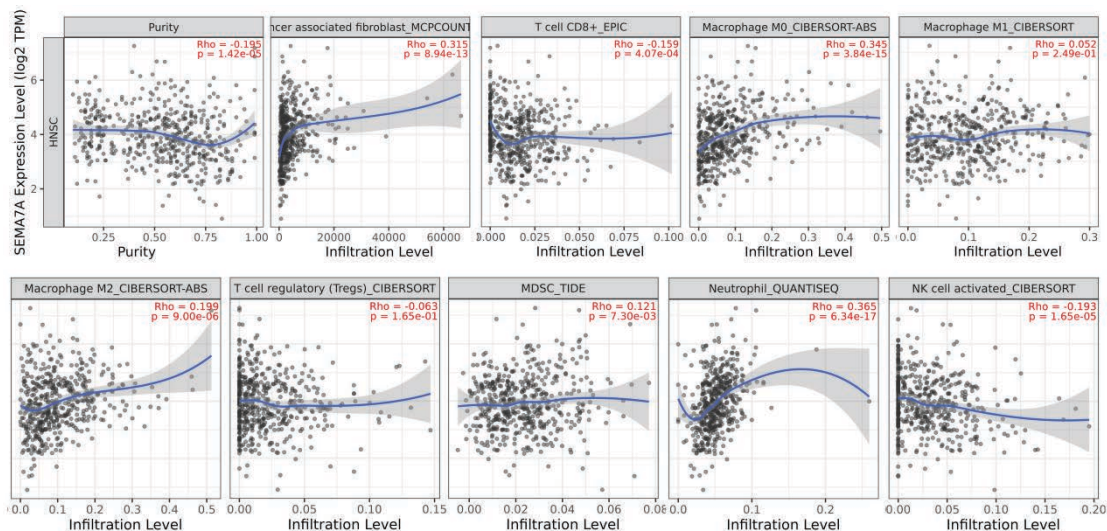


Figure 9. SEMA7A Immune infiltration analysis.

3.5.2. Relationship between genes and immune response to therapy

In the immunotherapy response analysis, ADH1B expression was significantly lower in responders compared with non-responders ($\log_2FC = -0.46$, $p = 0.04$). Further analysis using the Immunotherapy_Gene module revealed that only ADH1B exhibited a statistically significant association with immunotherapy response, whereas the remaining genes did not show significant correlations (**Figure 5**).

3.5. Correlation analysis between survival analysis and clinical pathological staging

To further investigate the clinical relevance of genes that did not exhibit significant differential expression but showed prognostic significance in survival analysis, we integrated the survival results from GEPIA2 with pathological stage data from cBioPortal (**Figure 10**). The results indicated that ALDH1A2, EVI5, and LCAT, although not significantly differentially expressed between tumor and normal tissues, exhibited statistically significant associations with OS or DFS. ALDH1A2 showed significant associations with OS (log-rank $p =$

0.014, $HR = 1.4$, $p = 0.015$) and DFS (log-rank $p = 0.037$, $HR = 1.4$, $p = 0.038$). Its mRNA expression gradually increased with tumor stage (from stage I to stage IVA), with stage IVA samples exhibiting a more concentrated and higher expression distribution. Mutation types included splice variants, missense mutations, shallow deletions, and gene amplifications, with a higher proportion of high-expression samples observed in stage IVA.

EVI5 was significantly associated with OS (log-rank $p = 0.018$, $HR = 0.73$, $p = 0.019$), suggesting that its high expression may confer a protective effect. Stage-wise analysis showed that EVI5 mRNA expression gradually increased from stage I to stage IVA, with overall higher expression levels in stage IVA. Mutation types included splice variants, missense mutations, truncating mutations, in-frame mutations, amplifications, and deletions, with an increased proportion of high-expression samples in stage IVA.

LCAT was significantly associated with DFS (log-rank $p = 0.022$, $HR = 1.5$, $p = 0.023$). Its mRNA expression exhibited a broader distribution in stage IVA, with mutation types including gene amplifications, gains, and shallow deletions. Although its stage-related expression was less pronounced than that of ALDH1A2 and EVI5, some stage IVA samples exhibited high expression levels.

Although ALDH1A2, EVI5, and LCAT did not show significant differential expression, they were closely associated with tumor progression stages and molecular alterations, and exhibited potential prognostic value. Notably, in advanced stage (stage IVA), all three genes displayed more prominent expression patterns, suggesting their involvement in HNSCC progression and potential as clinical prognostic biomarkers.

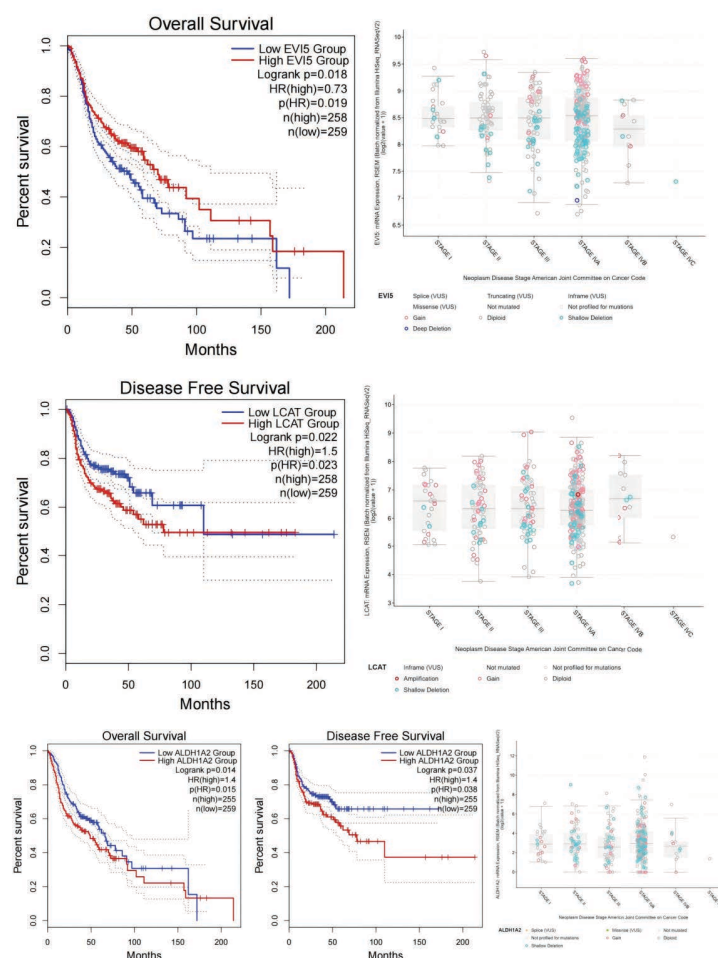


Figure 10. Survival analysis of ALDH1A2, EVI5 and LCAT and correlation with pathological stage.

4. Discussion

This study systematically evaluated the potential causal relationship between blood lipid–related exposures (high cholesterol, ApoA-I, and LDL-C) and head and neck cancer risk using a two-sample Mendelian randomization (MR) approach. Overall, the MR analyses did not reveal a significant causal effect of these lipid traits on HNC risk ($P > 0.05$). It should be noted that the outcome in this MR analysis encompassed broad HNC, including various anatomical sites and histological subtypes, rather than being restricted to head and neck HNSCC. Consequently, potential heterogeneity and the inclusion of other cancer subtypes may partially obscure the localized effects of blood lipid levels on HNSCC.

4.1. Potential mechanisms and enrichment analysis of SNPs associated with blood lipids

The genes mapped by positive effect group SNPs were significantly enriched in cytochrome P450 (CYP450)–related metabolic pathways and xenobiotic metabolism processes, suggesting that blood lipid–associated genetic variants may modulate the function of hepatic CYP450 enzymes, thereby altering the metabolic capacity for exogenous chemicals such as tobacco carcinogens and ethanol metabolites. Previous studies have demonstrated that CYP family members (e.g., CYP1A1, CYP2E1) can convert polycyclic aromatic hydrocarbons and ethanol metabolites into reactive carcinogens, increasing the risk of DNA damage^[18]. Moreover, as the liver serves as the central hub for systemic metabolism, differential expression of these genes may influence the distribution and accumulation of blood lipids and carcinogenic metabolites in circulation, thereby modifying exposure levels in head and neck mucosal tissues. DisGeNET analyses further indicated that genes mapped by positive effect group SNPs are significantly associated with laryngeal cancer and other head and neck malignancies. Enrichment of DLX6 target genes suggests that transcription factor networks may promote malignant behavior by regulating cellular differentiation and proliferation. Notably, DLX6-AS1 has been reported to be overexpressed in laryngeal cancer tissues and associated with tumor progression and metastasis^[19], which aligns closely with the enrichment results of the positive effect group SNPs in this study.

Conversely, genes mapped by negative effect group SNPs were enriched in monocarboxylic acid metabolism, alcohol metabolism, and nutrient response pathways. Key components of monocarboxylic acid metabolism, including lactate and short-chain fatty acids, not only participate in energy metabolism but also function as signaling molecules within the tumor microenvironment to modulate immune cell activity. Variants in these genes may enhance metabolic adaptability under hyperlipidemic or metabolic stress conditions, potentially exerting protective effects against HNSCC. The enrichment of alcohol metabolism–related genes is particularly noteworthy, as acetaldehyde, an intermediate of ethanol metabolism, is a well-established carcinogen^[20]; genetic variants that accelerate acetaldehyde clearance could mitigate mucosal damage in the head and neck. Genes mapped by negative effect group SNPs were also associated with multiple lipid and inflammatory biomarkers, suggesting a role in maintaining lipid homeostasis and modulating inflammation. Enrichment of ZNF507 and ZNF589 target genes reveals a potential transcriptional regulatory network^[21]; these zinc finger transcription factors play pivotal roles in chromatin remodeling and gene expression regulation, potentially bridging lipid metabolism and tumor risk.

Taken together, the enrichment analyses of positive and negative effect group SNPs indicate that blood lipid levels and HNSCC/HNC risk may be co-regulated through two opposing mechanisms. On one hand, lipid-related genetic variants may enhance carcinogen effects via CYP450 metabolism and inflammatory pathways, increasing tumor risk. On the other hand, certain genetic backgrounds may confer metabolic adaptability and enhanced

ethanol metabolism, thereby buffering or mitigating this risk. The counteracting effects of these mechanisms may explain the absence of significant causal associations observed in the overall MR analysis. Furthermore, the broad HNC outcome used in MR analyses may introduce interference from other cancer subtypes, further obscuring the localized effects on HNSCC.

4.2. Differential expression is associated with immune microenvironment

Differential expression analysis of candidate genes mapped by the SNPs revealed that ADH1B was downregulated in HNSC tissues, whereas FADS1, FADS2, PARP9, and SEMA7A were significantly upregulated in tumors. This suggests a potential protective role for ADH1B, while the other genes may be implicated in tumor progression. Previous studies have demonstrated that ADH1B modulates the rate of alcohol metabolism, influencing acetaldehyde accumulation and DNA damage risk ^[22], and its polymorphisms are closely associated with HNSCC susceptibility ^[23], consistent with the differential expression patterns observed in the present study. FADS1 and FADS2, as fatty acid desaturases, participate in polyunsaturated fatty acid biosynthesis, potentially regulating tumor cell membrane fluidity and signal transduction, while also influencing the immune microenvironment via M2 macrophage polarization ^[24]. Upregulation of FADS2 promotes unsaturated fatty acid synthesis, thereby enhancing tumor cell proliferation and chemoresistance ^[25,26]. Although evidence linking PARP9 to HNSC is limited, studies indicate that it is involved in DNA damage response and cell survival signaling, coordinating protein interactions to support cancer cell viability ^[27]. Aberrant glycosylation of SEMA7A can facilitate the formation of an immunosuppressive microenvironment, promoting tumor immune evasion ^[28].

Our immune infiltration analysis showed that ADH1B expression positively correlated with CD8⁺ T cells, M1 macrophages, and NK cells, but negatively correlated with MDSCs and neutrophils, suggesting that ADH1B may exert protective effects by enhancing anti-tumor immunity. In contrast, FADS1, FADS2, PARP9, and SEMA7A were positively associated with cancer-associated fibroblasts, M2 macrophages, and regulatory T cells, while negatively associated with CD8⁺ T cells and NK cells, indicating that these genes may promote tumor progression by modulating an immunosuppressive microenvironment. These findings fill a gap in the current HNSC research by providing integrated immune correlation analysis. Furthermore, immunotherapy response analysis revealed that ADH1B was significantly downregulated in responders compared to non-responders, suggesting its potential utility as a predictive biomarker for immunotherapy efficacy. This observation extends existing knowledge on immunotherapy biomarkers and highlights the clinical relevance of these candidate genes in therapeutic response.

4.3. Correlation between clinical pathological stage and prognosis

Integrating differential expression and survival analyses, ALDH1A2, EVI5, and LCAT did not exhibit significant expression differences between tumor and normal tissues in our HNSC dataset, yet all showed statistically significant associations with OS or DFS. ALDH1A2 was significantly associated with both DFS and OS, with expression levels increasing alongside tumor stage; in advanced-stage tumors (stage IVA), expression was more concentrated and elevated, suggesting a potential role in tumor progression. Although previous studies reported downregulation of ALDH1A2 in HNSC and its association with poor prognosis ^[29], which contrasts with our differential expression results, this discrepancy may be attributable to limited sample size or sample heterogeneity. Nevertheless, combined with stage-stratified analysis, ALDH1A2 appears to be implicated in tumor progression.

Survival analysis indicated that EVI5 high expression may exert a protective effect, although its expression trend increases in advanced-stage tumors. Prior studies in head and neck-related malignancies (including

laryngeal and glottic squamous cell carcinomas) demonstrated that EVI5 is upregulated and promotes tumor cell proliferation and growth by maintaining cell cycle regulators—stabilizing c-MYC, modulating G1→S transition, and inhibiting APC/C activity^[30]. This observation partially conflicts with our survival and differential expression analyses, suggesting that the biological role of EVI5 in HNSC requires further investigation.

LCAT did not show significant differential expression but was significantly associated with DFS. Previous studies indicate that LCAT exhibits context-dependent roles in cancer: it may promote tumor growth in adrenocortical carcinoma (ACC) and colon adenocarcinoma (COAD), while inhibiting progression in low-grade glioma (LGG) and hepatocellular carcinoma (LIHC)^[31]. Currently, data on LCAT in HNSC are limited; however, the elevated expression observed in certain advanced-stage samples, combined with its survival association, suggests that LCAT may serve as a potential biomarker for tumor progression.

4.4. Research limitations and prospects

The limitations of this study should be acknowledged. First, the MR analysis employed a broad HNC outcome encompassing multiple tissue types and pathological subtypes, which may have obscured local effects of blood lipids specifically in HNSC. Second, the sample size for differential expression and immune infiltration analyses was limited, potentially affecting the statistical significance of certain genes (e.g., ALDH1A2, EVI5, and LCAT) and leading to discrepancies with previously reported findings. Additionally, this study did not perform systematic functional experiments, nor did it account for potential confounding factors such as environmental exposures and lifestyle habits, thereby limiting the comprehensiveness and depth of causal interpretation. Future studies should incorporate larger-scale clinical cohorts and functional experiments to validate the mechanistic role and clinical potential of ADH1B, thereby providing key targets for the precision prevention and treatment of HNSC in the context of lipid metabolism.

5. Conclusion

This study systematically evaluated the potential causal relationship between circulating lipid-related traits (TC, ApoA-I, and LDL-C) and HNC risk, while exploring the biological mechanisms and clinical implications of lipid-related genetic variants. The study followed a three-step design. First, two-sample MR using publicly available GWAS data showed no significant causal effect of TC, ApoA-I, or LDL-C on HNC risk. Second, SNPs identified from MR were stratified by effect direction and subjected to functional annotation and pathway enrichment. Positive effect group SNPs were enriched in CYP450-mediated drug and xenobiotic metabolism pathways, whereas negative effect group SNPs were enriched in monocarboxylic acid metabolism, alcohol metabolism, and nutrient response pathways, suggesting HNC/HNSC risk may be modulated by two opposing mechanisms. Third, candidate genes were integrated into multi-omics databases for DE, survival, immune infiltration, and clinical pathological stage analyses. Results showed that ADH1B was downregulated in tumors and may exert a protective effect, indicating its potential as a novel target for tumor immunotherapy. Conversely, FADS1, FADS2, PARP9, and SEMA7A were upregulated and associated with an immunosuppressive TME. Although ALDH1A2, EVI5, and LCAT did not show significant DE, they demonstrated potential prognostic value in OS/DFS and clinical stage analyses.

Disclosure statement

The authors declare no conflict of interest.

References

- [1] Zhou T, Huang W, Wang X, et al., 2024, Global Burden of Head and Neck Cancers from 1990 to 2019. *iScience*, 27(3): 109282.
- [2] Barsouk A, Aluru J, Rawla P, et al., 2023, Epidemiology, Risk Factors, and Prevention of Head and Neck Squamous Cell Carcinoma. *Medical Sciences (Basel, Switzerland)*, 11(2): 42.
- [3] Jin H, Wang J, Wang Z, et al., 2023, Lipid Metabolic Reprogramming in Tumor Microenvironment: From Mechanisms to Therapeutics. *Journal of Hematology & Oncology*, 16(1): 103.
- [4] Liu R, Wang C, Tao Z, et al., 2025, Lipid Metabolism Reprogramming in Cancer: Insights into Tumor Cells and Immune Cells within the Tumor Microenvironment. *Biomedicines*, 13(8): 1895.
- [5] Cioce M, Arbitrio M, Polerà N, et al., 2024, Reprogrammed Lipid Metabolism in Advanced Resistant Cancers: An Upcoming Therapeutic Opportunity. *Cancer Drug Resistance (Alhambra, Calif.)*, 7: 45.
- [6] Liang J, Li L, Li L, et al., 2023, Lipid Metabolism Reprogramming in Head and Neck Cancer. *Frontiers in Oncology*, 13: 1271505.
- [7] Huang Y, Xiao X, Sadeghi F, et al., 2023, Blood Metabolic Biomarkers and the Risk of Head and Neck Cancer: An Epidemiological Study in the Swedish AMORIS Cohort. *Cancer Letters*, 557: 216091.
- [8] Wang S, Wang L, Li H, et al., 2024, Correlation Analysis of Plasma Lipid Profiles and the Prognosis of Head and Neck Squamous Cell Carcinoma. *Oral Diseases*, 30(2): 329–341.
- [9] Wilms T, Boldrup L, Gu X, et al., 2021, High Levels of Low-Density Lipoproteins Correlate with Improved Survival in Patients with Squamous Cell Carcinoma of the Head and Neck. *Biomedicines*, 9(5): 506.
- [10] Feng J, Zhao J, Yang X, et al., 2021, The Prognostic Impact of Preoperative Serum Apolipoprotein A-I in Patients with Esophageal Basaloid Squamous Cell Carcinoma. *Cancer Management and Research*, 13: 7373–7385.
- [11] Elsworth B, Lyon M, Alexander T, et al., 2020, The MRC IEU OpenGWAS Data Infrastructure. *bioRxiv*, 2020.08.10.244293v1.
- [12] McLaren W, Gil L, Hunt SE, et al., 2016, The Ensembl Variant Effect Predictor. *Genome Biology*, 17(1): 122.
- [13] Zhou Y, Zhou B, Pache L, et al., 2019, Metascape Provides a Biologist-Oriented Resource for the Analysis of Systems-Level Datasets. *Nature Communications*, 10(1): 1523.
- [14] Tang Z, Kang B, Li C, et al., 2019, GEPIA2: An Enhanced Web Server for Large-Scale Expression Profiling and Interactive Analysis. *Nucleic Acids Research*, 47(W1): W556–W560.
- [15] Cui H, Zhao G, Lu Y, et al., 2025, TIMER3: An Enhanced Resource for Tumor Immune Analysis. *Nucleic Acids Research*, 53(W1): W534–W541. <https://doi.org/10.1093/nar/gkaf388>
- [16] Cerami E, Gao J, Dogrusoz U, et al., 2012, The cBio Cancer Genomics Portal: An Open Platform for Exploring Multidimensional Cancer Genomics Data. *Cancer Discovery*, 2(5): 401–404.
- [17] Burgess S, Bowden J, Fall T, et al., 2017, Sensitivity Analyses for Robust Causal Inference from Mendelian Randomization Analyses with Multiple Genetic Variants. *Epidemiology (Cambridge, Mass.)*, 28(1): 30–42.
- [18] Malik D, David R, Gooderham N, 2018, Ethanol Potentiates the Genotoxicity of the Food-Derived Mammary Carcinogen PhIP in Human Estrogen Receptor-Positive Mammary Cells: Mechanistic Support for Lifestyle Factors (Cooked Red Meat and Ethanol) Associated with Mammary Cancer. *Archives of Toxicology*, 92(4): 1639–1655.
- [19] An Y, Chen X, Yang Y, et al., 2018, LncRNA DLX6-AS1 Promoted Cancer Cell Proliferation and Invasion by

- Attenuating the Endogenous Function of miR-181b in Pancreatic Cancer. *Cancer Cell International*, 18: 143.
- [20] National Toxicology Program, 2021, 15th Report on Carcinogens. National Toxicology Program, Research Triangle Park (NC). Acetaldehyde: CAS No. 75-07-0, visited on June 12, 2025, https://www.ncbi.nlm.nih.gov/books/NBK590821/?utm_source=chatgpt.com
- [21] Creamer K, Larsen E, Lawrence J, 2022, ZNF146/OZF and ZNF507 Target LINE-1 Sequences. *G3* (Bethesda, Md.), 12(3): jkac002.
- [22] Yukawa Y, Muto M, Hori K, et al., 2012, Combination of ADH1B2/ALDH22 Polymorphisms Alters Acetaldehyde-Derived DNA Damage in the Blood of Japanese Alcoholics. *Cancer Science*, 103(9): 1651–1655.
- [23] Chien H, Tsai C, Young C, et al., 2023, Single-Nucleotide Polymorphism at Alcohol Dehydrogenase 1B: A Susceptible Gene Marker in Oro-/Hypopharyngeal Cancers from Genome-Wide Association Study. *Cancer Medicine*, 12(18): 19174–19187.
- [24] Heravi G, Jang H, Wang X, et al., 2022, Fatty Acid Desaturase 1 (FADS1) Is a Cancer Marker for Patient Survival and a Potential Novel Target for Precision Cancer Treatment. *Frontiers in Oncology*, 12: 942798.
- [25] Gong Q, Li H, Song J, et al., 2023, LncRNA LINC01569 Promotes M2 Macrophage Polarization to Accelerate Hypopharyngeal Carcinoma Progression through the miR-193a-5p/FADS1 Signaling Axis. *Journal of Cancer*, 14(9): 1673–1688.
- [26] Xuan Y, Wang H, Yung M, et al., 2022, SCD1/FADS2 Fatty Acid Desaturases Equipose Lipid Metabolic Activity and Redox-Driven Ferroptosis in Ascites-Derived Ovarian Cancer Cells. *Theranostics*, 12(7): 3534–3552.
- [27] Saleh H, Liloglou T, Rigden D, et al., 2024, KH-Like Domains in PARP9/DTX3L and PARP14 Coordinate Protein-Protein Interactions to Promote Cancer Cell Survival. *Journal of Molecular Biology*, 436(4): 168434.
- [28] Liu Z, Meng X, Zhang Y, et al., 2024, FUT8-Mediated Aberrant N-Glycosylation of SEMA7A Promotes Head and Neck Squamous Cell Carcinoma Progression. *International Journal of Oral Science*, 16(1): 26.
- [29] Seidensaal K, Nollert A, Feige A, et al., 2015, Impaired Aldehyde Dehydrogenase 1 Subfamily Member 2A-Dependent Retinoic Acid Signaling Is Related with a Mesenchymal-Like Phenotype and an Unfavorable Prognosis of Head and Neck Squamous Cell Carcinoma. *Molecular Cancer*, 14: 204.
- [30] Mao C, Zhou X, Jiang Y, et al., 2020, The Evi5 Oncogene Promotes Laryngeal Cancer Cells Proliferation by Stabilizing c-Myc Protein. *Cancer Cell International*, 20: 44.
- [31] Gao M, Zhang W, Li X, et al., 2025, LCAT in Cancer Biology: Embracing Epigenetic Regulation, Immune Interactions, and Therapeutic Implications. *International Journal of Molecular Sciences*, 26(4): 1453.

Publisher's note

Bio-Byword Scientific Publishing remains neutral with regard to jurisdictional claims in published maps and institutional affiliations.

Molecular Targets and Developmental Potential of Alkaloid Monomers from Traditional Chinese Medicine as Anticancer Agents

Beiqi Yang¹, Tongtong He², Tingting Zhi², Jing Tang^{1*}

¹Key Laboratory of Oral Disease Research of Guizhou Provincial Department of Education, School of Stomatology, Zunyi Medical University, Zunyi 563000, Guizhou, China

²The First Clinical Institute, Zunyi Medical University, Zunyi 563006, Guizhou, China

**Author to whom correspondence should be addressed.*

Copyright: © 2025 Author(s). This is an open-access article distributed under the terms of the Creative Commons Attribution License (CC BY 4.0), permitting distribution and reproduction in any medium, provided the original work is cited.

Abstract: Plant-derived alkaloids exhibit significant anticancer potential, yet their multi-target mechanisms, spanning signaling pathways, programmed cell death, immunity, and metabolism, remain fragmented. This narrative review synthesizes recent preclinical evidence on five representative alkaloids: dendrobine (DDB), aloperine (ALO), levo-tetrahydropalmatine (L-THP), solamargine (SM), and cyclovirobuxine D (CVB-D). Using a dual-framework of compound-specific analysis and key regulatory modules (NF- κ B, MAPK, PI3K/AKT/mTOR, JAK/STAT; apoptosis, autophagy, ferroptosis; immune checkpoints; metabolism/microbiota), the study identified convergent anticancer mechanisms with translational relevance. These alkaloids consistently suppress NF- κ B, PI3K/AKT/mTOR, and MAPK pathways, and modulate JAK/STAT signaling. They induce apoptosis and ferroptosis, and block autophagic flux. Notably, EVO and SM downregulate PD-L1 via the MUC1-C/NF- κ B/c-MYC axis, enhancing CD8⁺ T cell function. L-THP activates AMPK and remodels tumor metabolism. These mechanistic insights support rational co-therapies such as L-THP plus metabolic inhibitors, or ALO combined with bispecific immune checkpoint inhibitors. Overall, these alkaloids demonstrate systemic, multi-pathway anticancer efficacy, and represent promising partners in precision combination therapy. Clinical translation should prioritize formulation and pharmacokinetic optimization, biomarker-guided stratification, and preclinical validation of synergistic regimens.

Keywords: Alkaloids; NF- κ B; PI3K/AKT/mTOR; MAPK; Ferroptosis; Autophagy; PD-L1; Combination therapy

Online publication: October 16, 2025

1. Introduction

Cancer remains a leading cause of mortality and poses a major global public health challenge^[1]. Although notable progress has been made in surgery, radiotherapy, targeted therapy, and immunotherapy, the prognosis of many late-

stage cancers remains unsatisfactory ^[2]. Consequently, there is an urgent need to develop safer, more effective, and better-tolerated therapeutic options. In recent years, traditional Chinese medicine (TCM) has attracted increasing attention in oncology due to its unique advantages of multi-component synergy, multi-target modulation, and holistic homeostatic regulation ^[3]. A growing body of pharmacological evidence indicates that active constituents derived from TCM not only directly inhibit tumor cell growth, but also alleviate treatment-related side effects and improve systemic physiological states, thereby serving as complementary or alternative therapies in clinical oncology ^[4]. Among the diverse resources in TCM, alkaloids have emerged as a prominent group of compounds with anti-inflammatory, neuroprotective, and anticancer properties ^[5]. Notably, recent studies suggest that alkaloid monomers may not only exert direct antiproliferative and pro-apoptotic effects, but also provide organ-protective and chemo-sensitizing benefits in combination regimens, thus improving therapeutic tolerance ^[6].

Plant-derived alkaloids are chemically diverse and are supported by substantial preclinical evidence in cancer research ^[7]. Across tumor models in the respiratory, digestive, reproductive, and urinary systems, these alkaloids demonstrate three mechanistic convergences:

- (1) Inhibition of key oncogenic nodes including NF- κ B, MAPK/ERK-JNK-p38, PI3K/AKT/mTOR, and JAK/STAT pathways, limiting proliferation, invasion, metastasis, and therapeutic resistance ^[8–17];
- (2) Reprogramming of cell death and stress response pathways, including apoptosis, ferroptosis, and blockage of autophagic flux, which are particularly relevant in apoptosis-resistant tumors ^[18–23];
- (3) Modulation of the tumor immune microenvironment, such as downregulation of PD-L1 and reactivation of CD8⁺ T cells ^[24–26], alongside remodeling of tumor metabolism and microbiota–metabolism interfaces ^[27–29].

These shared mechanisms suggest that alkaloids possess the potential to counteract pathway crosstalk, one of the key barriers limiting the efficacy of cancer therapies in solid tumors. Nonetheless, their clinical translation faces several obstacles. Therefore, this review systematically summarizes recent preclinical advances of these five alkaloid monomers, highlights their molecular targets and signaling pathways, evaluates their potential in targeted and combination cancer therapies, and discusses key directions for advancing their clinical translation.

2. Representative plant-derived alkaloid monomers

DDB is a sesquiterpene alkaloid primarily derived from *Dendrobium nobile*, representing one of the earliest isolated and most extensively studied active compounds ^[30]. ALO, a quinolizidine alkaloid isolated from *Sophora alopecuroides* L ^[31,32]. L-THP is an isoquinoline alkaloid extracted from *Corydalis yanhusuo*, a plant of the Papaveraceae family ^[33]. SM, a naturally occurring alkaloid extracted from *Solanum nigrum*, exhibits anti-inflammatory, antioxidant, and anticancer properties ^[34]. CVB-D is a steroidal alkaloid isolated from *Buxus microphylla* and related species ^[35].

3. Molecular mechanisms and therapeutic targets of anticancer alkaloids

3.1. NF- κ B signaling pathway

3.1.1. Respiratory system cancers

CVB-D downregulates the expression of phosphorylated p65 (p-p65), interfering with NF- κ B signaling transmission ^[36,37]. SM reduces p65 protein levels, suppressing NF- κ B pathway activation ^[38]. These alkaloids offer novel molecular strategies for lung cancer therapy by intervening at multiple levels of the NF- κ B signaling cascade.

3.1.2. Digestive system cancers

In colorectal cancer, DDB downregulates mRNA expression levels of NF- κ B pathway-related genes such as NF- κ B, COX-2 (Cyclooxygenase-2), and PGE2 (Prostaglandin E2) ^[39].

3.1.3. Reproductive system cancers

In prostate cancer, L-THP enhances phosphorylation of Akt while suppressing NF- κ B expression, thereby inhibiting cancer cell proliferation ^[40].

3.2. MAPK signaling pathway

3.2.1. Respiratory system cancers

SM suppresses the expression of EP4, enhances ERK1/2 phosphorylation, and inhibits lung cancer proliferation ^[41]. DDB increases JNK phosphorylation and induces CHOP, thereby inhibiting the proliferation of lung cancer cells ^[42].

3.2.2. Digestive system cancers

In hepatocellular carcinoma, CVB-D binds to Leukemia Inhibitory Factor at Val145, inducing mitophagy and inhibiting cell invasion and migration ^[43]. In gastric cancer, SM suppresses ERK1/2 phosphorylation while upregulating long non-coding RNAs lncPINT and lncNEAT1_2 ^[44]. In colorectal cancer, CVB-D downregulates phosphorylated ERK1/2, thereby suppressing migration and invasion ^[45]. Moreover, Huangqin Decoction—composed of betulinic acid, L-THP, and quercetin—exerts synergistic effects on HIF-1/MAPK pathways and multiple core targets to inhibit colorectal cancer progression ^[46].

3.3. PI3K/AKT/mTOR signaling pathway

3.3.1. Respiratory system cancers

SM acts via a dual mechanism—reducing Akt phosphorylation at Ser473 and suppressing pathway activation via PDPK1 ^[41,47]. ALO also inhibits the PI3K/Akt/mTOR pathway and decreases transcription and translation of MMP-2 ^[48].

3.3.2. Digestive system cancers

ALO suppresses the expression and release of HMGB1 and its receptor RAGE, leading to inactivation of the PI3K/Akt/mTOR pathway and inhibition of gastric cancer growth ^[49]. In hepatocellular carcinoma, ALO downregulates p110 α , p85, Akt, and p-Akt, thereby inhibiting cell proliferation ^[50]. Both in vitro and in zebrafish tumor models, ALO exerts anticancer effects by suppressing the PI3K/Akt pathway, inducing apoptosis, G2/M cell cycle arrest, mitochondrial membrane potential loss, and changes in cell cycle distribution ^[51]. In colorectal cancer, ALO downregulates Stat3 and PI3KC3, inhibiting pathway activation and tumor cell proliferation ^[31]. SM inhibits PI3K/Akt/mTOR signaling and upregulates PTEN expression, effectively suppressing colorectal cancer cell proliferation and invasion and promoting apoptosis both in vitro and in vivo ^[52].

3.3.3. Reproductive system cancers

In prostate cancer, ALO inhibits Akt phosphorylation, reduces p-Akt expression, and induces apoptosis ^[53]. SM blocks PI3K/Akt signaling, suppresses cell proliferation, and enhances the antitumor effect of docetaxel in vivo ^[54]. In breast cancer, CVB-D exerts its effects by reducing phosphorylation of the autophagy-related suppressors AKT

and mTOR, thus disrupting the autophagic process ^[55].

3.3.4. Urinary system cancers

In renal cell carcinoma, DDB inhibits the expression of p-PI3K, p-Akt, and p-Erk, thereby suppressing the proliferation, migration, and invasion of 786-O and A498 cells ^[8].

3.3.5. Other systemic cancers

In osteosarcoma, ALO significantly reduces PI3K and p-Akt1 levels, thereby inhibiting tumor cell proliferation ^[31]. In thyroid cancer, ALO downregulates p-Akt expression and induces cell death by suppressing the Akt pathway ^[31].

3.4. JAK/STAT signaling pathway

3.4.1. Respiratory system cancers

Aberrant activation of the JAK/STAT pathway is effectively inhibited by several alkaloids. DDB suppresses the expression of PD-L1, p-JAK1/JAK1, and p-JAK2/JAK2 proteins in lung cancer cells, thereby modulating tumor immune escape and progression ^[56].

3.5. Other signaling pathways

3.5.1. Respiratory system cancers

DDB inhibits the SULF2-mediated signaling pathway, thereby reducing ionizing radiation-induced migration and invasion of lung cancer cells ^[42]. ALO targets VPS4A, interfering with autophagosome sealing and autophagosome-lysosome fusion, leading to mitochondrial ROS accumulation, G0/G1 arrest, and apoptosis. It induces autophagy blockade, exhibits strong antitumor activity in lung cancer models, and synergizes with the bispecific PD-L1/TGF- β antibody YM101 ^[18]. DDB downregulates PD-L1 expression and modulates immune cell infiltration, and when combined with PD-L1 blockade, displays synergistic inhibition of tumor growth ^[56]. DDB also synergizes with cisplatin by modulating Treg/Th17 balance, prolonging survival and inhibiting tumor progression in vivo ^[57]. CVB-D activates the p65/BNIP3/LC3 axis to induce mitophagy, enhance apoptosis of A549 and H446 lung cancer cells, and suppress tumor growth in vivo ^[36]. SM enhances the antitumor efficacy of gefitinib in NSCLC by regulating the MALAT1/miR-141-3p/Sp1/IGFBP1 axis and upregulating IGFBP1 expression in vitro and in vivo ^[58]. SM also inhibits STAT1 activation and downregulates PD-L1 expression, thereby enhancing the efficacy of PD-L1 immunotherapy without additional toxicity ^[59]. Furthermore, SM reverses cisplatin resistance by inducing G0/G1 arrest, promoting apoptosis, and inhibiting the Hedgehog pathway, showing synergistic effects with cisplatin ^[60].

3.5.2. Digestive system cancers

L-THP promotes apoptosis in hepatocellular carcinoma by reducing phosphorylated AMPK levels ^[31]. It also activates AMPK-dependent autophagy while inhibiting mitochondrial respiration and glycolysis, inducing “bioenergetic deprivation.” Co-administration with the metabolic inhibitor DPI enhances its therapeutic efficacy ^[11,29,61]. SM modulates the LIF/miR-192-5p/CYR61/AKT axis to induce apoptosis and autophagy, while reprogramming tumor-associated macrophages in liver cancer ^[23]. CVB-D induces ferroptosis by suppressing GPX4 and FSP1, elevating Fe²⁺, MDA, and ROS levels, and apoptosis rates in HepG2 and Huh-7 cells. It also shows strong antitumor efficacy in a C-NKG xenograft model ^[62]. SM inhibits HCC growth and enhances the efficacy of sorafenib by modulating the HOTTIP-TUG1/miR-4726-5p axis and downregulating MUC1

expression ^[63]. In gastric cancer, SM downregulates PD-L1 by inhibiting the STAT3/PD-L1 pathway and reverses IL-6-induced immunosuppression, thereby reducing proliferation, migration, and invasion ^[64].

3.5.3. Reproductive system cancers

In breast cancer, CVB-D binds directly to YAP, suppressing nuclear translocation of YAP/TAZ and downstream oncogenic transcription. It also triggers mitophagy via the FOXO3a/PINK1–Parkin axis, promoting apoptosis ^[65]. ALO suppresses phosphorylation of Ras pathway components ^[31]. In cervical cancer, ALO inhibits the IL-6–JAK1–STAT3 feedback loop, significantly reducing HeLa cell proliferation, migration, invasion, and enhancing apoptosis ^[66]. SM targets CXCL3 and inhibits the ERK pathway, effectively reducing cervical cancer proliferation and metastasis both in vitro and in vivo ^[67].

3.5.4. Urinary system cancers

In bladder cancer, ALO upregulates TIMP-4 while downregulating MMP-2 and MMP-9, thereby inhibiting migration, invasion, and adhesion ^[68]. Nanoparticles co-loaded with solasonine and SM demonstrate synergistic antitumor effects against bladder cancer ^[69].

4. Conclusion and outlook

In summary, plant-based alkaloids hold important supplementary and synergistic potential in modern cancer therapy. By integrating traditional medicinal knowledge with cutting-edge biomedical technologies, particularly multi-omics analysis, targeted delivery systems, and mechanism-driven combination approaches, we can accelerate the translation of these natural compounds into effective, low-toxicity, and personalized cancer treatments.

Funding

This work was supported by grants from the National Science Foundation of China (82104330), Special Project on Scientific and Technological Research of Traditional Chinese Medicine and Ethnic Medicine, Guizhou Provincial Administration of Traditional Chinese Medicine (QZYY-2024-135), Natural Science and Technology Foundation of Guizhou Province (QiankeheJichu-ZK[2022] General 606), and Science and Technology Foundation of Guizhou Health and Health Committee (gzwkj2024-455).

Disclosure statement

The authors declare no conflict of interest.

References

- [1] Liu Y, Yang S, Wang K, et al., 2020, Cellular Senescence and Cancer: Focusing on Traditional Chinese Medicine and Natural Products. *Cell Prolif*, 53(10): e12894.
- [2] Miller K, Nogueira L, Devasia T, et al., 2022, Cancer Treatment and Survivorship Statistics, 2022. *CA Cancer J Clin*, 72(5): 409–436.
- [3] Wang S, Fu J L, Hao H F, et al., 2021, Metabolic Reprogramming by Traditional Chinese Medicine and Its Role in

Effective Cancer Therapy. *Pharmacol Res*, 170: 105728.

- [4] Liu J, Wang S, Zhang Y, et al., 2015, Traditional Chinese Medicine and Cancer: History, Present Situation, and Development. *Thorac Cancer*, 6(5): 561–569.
- [5] Bhambhani S, Kondhare K, Giri A, 2021, Diversity in Chemical Structures and Biological Properties of Plant Alkaloids. *Molecules*, 26(11): 3374.
- [6] Shin H, Kim T, Kim Y, et al., 2017, Protective Effects of *Dendrobium nobile* Against Cisplatin Nephrotoxicity Both In-vitro and In-vivo. *Iran J Pharm Res*, 16(Suppl): 197–206.
- [7] Olofinson K, Abrahamse H, George B, 2023, Therapeutic Role of Alkaloids and Alkaloid Derivatives in Cancer Management. *Molecules*, 28(14): 5578.
- [8] Jia X, Chen Z, Chen X, et al., 2025, Elucidating the Anticancer Potential of Dendrobine in Renal Cell Carcinoma Treatment. *Naunyn Schmiedebergs Arch Pharmacol*, 398(6): 7517–7528.
- [9] Wu Y, Jia Q, Tang Q, et al., 2024, A Specific Super-Enhancer Actuated by Berberine Regulates EGFR-Mediated RAS-RAF1-MEK1/2-ERK1/2 Pathway to Induce Nasopharyngeal Carcinoma Autophagy. *Cell Mol Biol Lett*, 29(1): 92.
- [10] Liu Q, Tang J, Chen S, et al., 2022, Berberine for Gastric Cancer Prevention and Treatment: Multi-Step Actions on the Correa's Cascade Underlie Its Therapeutic Effects. *Pharmacol Res*, 184: 106440.
- [11] Xu M, Ren L, Fan J, et al., 2022, Berberine Inhibits Gastric Cancer Development and Progression by Regulating the JAK2/STAT3 Pathway and Downregulating IL-6. *Life Sci*, 290: 120266.
- [12] Zhang Q, Wang X, Cao S, et al., 2020, Berberine Represses Human Gastric Cancer Cell Growth In Vitro and In Vivo by Inducing Cytostatic Autophagy via Inhibition of MAPK/mTOR/p70S6K and Akt Signaling Pathways. *Biomed Pharmacother*, 128: 110245.
- [13] Li J, Jiang L, Ma Q, et al., 2025, Evodiamine Inhibits Programmed Cell Death Ligand 1 Expression via the PI3K/AKT Signaling Pathway to Regulate Antitumor Immunity in Melanoma. *Sci Rep*, 15(1): 6649.
- [14] Liu J, He L, Zhang W, et al., 2024, Evodiamine Inhibits Proliferation and Induces Apoptosis of Nasopharyngeal Carcinoma Cells via the SRC/ERBB2-Mediated MAPK/ERK Signaling Pathway. *J Transl Med*, 22(1): 859.
- [15] Jung Y, Baek S, Narula A, et al., 2021, Potential Function of Oxymatrine as a Novel Suppressor of Epithelial-to-Mesenchymal Transition in Lung Tumor Cells. *Life Sci*, 284: 119893.
- [16] Chen M, Gu Y, Zhang A, et al., 2021, Biological Effects and Mechanisms of Matrine and Other Constituents of *Sophora flavescens* in Colorectal Cancer. *Pharmacol Res*, 171: 105778.
- [17] Xu B, Qiu T, Yang R, et al., 2024, Oxymatrine Inhibits Migration and Invasion of Esophageal Squamous Cell Carcinoma Cell Lines via the MEK1/ERK/ β -Catenin Pathway. *Chem Biol Interact*, 404: 111270.
- [18] Guo W, Zhou H, Wang J, et al., 2024, Aloperine Suppresses Cancer Progression by Interacting with VPS4A to Inhibit Autophagosome-Lysosome Fusion in NSCLC. *Adv Sci (Weinh)*, 11(31): e2308307.
- [19] Zhang L, Li L, Chen X, et al., 2023, Evodiamine Inhibits ESCC by Inducing M-Phase Cell-Cycle Arrest via CUL4A/p53/p21 Axis and Activating Noxa-Dependent Intrinsic and DR4-Dependent Extrinsic Apoptosis. *Phytomedicine*, 108: 154493.
- [20] Li L, Lu J, Fu S, et al., 2025, Evodiamine Induces Ferroptosis in Prostate Cancer Cells by Inhibiting TRIM26-Mediated Stabilization of GPX4. *Chin Med*, 20(1): 71.
- [21] Hu C, Wu H, Shan Y, et al., 2023, Evodiamine Exhibits Anti-Bladder Cancer Activity by Suppression of Glutathione Peroxidase 4 and Induction of Ferroptosis. *Int J Mol Sci*, 24(7): 6021.
- [22] Wang H, Wei L, Mao D, et al., 2023, Combination of Oxymatrine (Om) and Astragaloside IV (As) Enhances the

- Infiltration and Function of TILs in Triple-Negative Breast Cancer (TNBC). *Int Immunopharmacol*, 125(Pt A): 111026.
- [23] Yin S, Jin W, Qiu Y, et al., 2022, Solamargine Induces Hepatocellular Carcinoma Cell Apoptosis and Autophagy via Inhibiting LIF/miR-192-5p/CYR61/Akt Signaling Pathways and Eliciting Immunostimulatory Tumor Microenvironment. *J Hematol Oncol*, 15(1): 32.
- [24] Hu J, Shi Q, Xue C, Wang Q, 2024, Berberine Protects Against Hepatocellular Carcinoma Progression by Regulating Intrahepatic T Cell Heterogeneity. *Adv Sci (Weinh)*, 11(39): e2405182.
- [25] Jiang Z, Huang J, Xie Y, et al., 2020, Evodiamine Suppresses Non-Small Cell Lung Cancer by Elevating CD8(+) T Cells and Downregulating the MUC1-C/PD-L1 Axis. *J Exp Clin Cancer Res*, 39(1): 249.
- [26] Yu Y, Huang X, Liang C, et al., 2023, Evodiamine Impairs HIF1A Histone Lactylation to Inhibit Sema3A-Mediated Angiogenesis and PD-L1 by Inducing Ferroptosis in Prostate Cancer. *Eur J Pharmacol*, 957: 176007.
- [27] Sun Y, Zhou Q, Chen F, et al., 2023, Berberine Inhibits Breast Carcinoma Proliferation and Metastasis Under Hypoxic Microenvironment Involving Gut Microbiota and Endogenous Metabolites. *Pharmacol Res*, 193: 106817.
- [28] Chen H, Ye C, Wu C, et al., 2023, Berberine Inhibits High Fat Diet-Associated Colorectal Cancer Through Modulation of the Gut Microbiota-Mediated Lysophosphatidylcholine. *Int J Biol Sci*, 19(7): 2097–2113.
- [29] Yin X, Zhang J, Zhao W, et al., 2022, Combined Levo-Tetrahydropalmatine and Diphenyleneiodonium Chloride Enhances Antitumor Activity in Hepatocellular Carcinoma. *Pharmacol Res*, 179: 106219.
- [30] Bhardwaj K, Bhargav R, Patocka J, et al., 2024, Dendrobine: A Neuroprotective Sesquiterpenic Alkaloid for the Prevention and Treatment of Diseases: A Review. *Mini Rev Med Chem*, 24(15): 1395–1408.
- [31] Tahir M, Ali S, Zhang W, et al., 2022, Aloperine: A Potent Modulator of Crucial Biological Mechanisms in Multiple Diseases. *Biomedicines*, 10(4): 905.
- [32] Chen H, Wang S, Chen Q, et al., 2024, Aloperine Ameliorates Acetaminophen-Induced Acute Liver Injury through HMGB1/TLR4/NF- κ B and NLRP3/Inflammasome Pathway. *Mediators Inflamm*, 2024: 3938136.
- [33] Liu L, Liu M, Zhao W, et al., 2021, Levo-tetrahydropalmatine: A New Potential Medication for Methamphetamine Addiction and Neurotoxicity. *Exp Neurol*, 344: 113809.
- [34] Li J, Tang W, Yang Y, et al., 2021, A Programmed Cell-Mimicking Nanoparticle Driven by Potato Alkaloid for Targeted Cancer Chemoimmunotherapy. *Adv Healthc Mater*, 10(13): e2100311.
- [35] Li S, Yan M, Wang Z, et al., 2024, Phytochemistry of Genus *Buxus* and Pharmacology of Cyclovirobuxine D. *Chem Biodivers*, 21(8): e202400494.
- [36] Zeng C, Zou T, Qu J, et al., 2021, Cyclovirobuxine D Induced-Mitophagy through the p65/BNIP3/LC3 Axis Potentiates Its Apoptosis-Inducing Effects in Lung Cancer Cells. *Int J Mol Sci*, 22(11): 5820.
- [37] Xue T, Chen Y, Xu J, et al., 2023, Cyclovirobuxine D Inhibits Growth and Progression of Non-Small Cell Lung Cancer Cells by Suppressing the KIF11-CDC25C-CDK1-CyclinB1 G(2)/M Phase Transition Regulatory Network and the NF κ B/JNK Signaling Pathway. *Int J Oncol*, 62(5): 57.
- [38] Chen Y, Tang Q, Wu J, et al., 2015, Inactivation of PI3-K/Akt and Reduction of SP1 and p65 Expression Increase the Effect of Solamargine on Suppressing EP4 Expression in Human Lung Cancer Cells. *J Exp Clin Cancer Res*, 34: 154.
- [39] Halim C, Xinjing S, Fan L, et al., 2019, Anti-Cancer Effects of Oxymatrine Are Mediated through Multiple Molecular Mechanism(s) in Tumor Models. *Pharmacol Res*, 147: 104327.
- [40] Li P, Ren K, Liang Y, et al., 2020, Aloin Promotes Cell Apoptosis by Targeting HMGB1-TLR4-ERK Axis in Human Melanoma Cells. *Excli J*, 19: 641–651.
- [41] Chen Y, Tang Q, Xiao Q, et al., 2017, Targeting EP4 Downstream c-Jun through ERK1/2-Mediated Reduction of

- DNMT1 Reveals Novel Mechanism of Solamargine-Inhibited Growth of Lung Cancer Cells. *J Cell Mol Med*, 21(2): 222–233.
- [42] Kim Y, Han A, Kim J, et al., 2021, Dendrobine Inhibits γ -Irradiation-Induced Cancer Cell Migration, Invasion and Metastasis in Non-Small Cell Lung Cancer Cells. *Biomedicines*, 9(8): 954.
- [43] Shao Y, Lu D, Jin W, et al., 2025, Targeting LIF With Cyclovirobuxine D to Suppress Tumor Progression via LIF/p38MAPK/p62-Modulated Mitophagy in Hepatocellular Carcinoma. *MedComm* (2020), 6(6): e70227.
- [44] Fu R, Wang X, Hu Y, et al., 2019, Solamargine Inhibits Gastric Cancer Progression by Regulating the Expression of IncNEAT1_2 via the MAPK Signaling Pathway. *Int J Oncol*, 54(5): 1545–1554.
- [45] Jiang F, Chen Y, Ren S, et al., 2020, Cyclovirobuxine D Inhibits Colorectal Cancer Tumorigenesis via the CTHRC1-AKT/ERK-Snail Signaling Pathway. *Int J Oncol*, 57(1): 183–196.
- [46] Li Y, Tang D, Yan H, et al., 2023, Network Pharmacology and Molecular Docking-Based Analyses to Predict the Potential Mechanism of Huangqin Decoction in Treating Colorectal Cancer. *World J Clin Cases*, 11(19): 4553–4566.
- [47] Tang Q, Zheng F, Liu Z, et al., 2019, Novel Reciprocal Interaction of lncRNA HOTAIR and miR-214-3p Contribute to the Solamargine-Inhibited PDPK1 Gene Expression in Human Lung Cancer. *J Cell Mol Med*, 23(11): 7749–7761.
- [48] Liu F, Liu T, Li H, 2021, Aloperine Inhibits the Progression of Non-Small-Cell Lung Cancer through the PI3K/Akt Signaling Pathway. *Cancer Cell Int*, 21(1): 662.
- [49] Tao H, Tang T, Wang S, et al., 2019, The Molecular Mechanisms of Aloin Induce Gastric Cancer Cells Apoptosis by Targeting High Mobility Group Box 1. *Drug Des Devel Ther*, 13: 1221–1231.
- [50] Liu J, Huo C, Cao H, et al., 2021, Corrigendum to Aloperine Induces Apoptosis and G2/M Cell Cycle Arrest in Hepatocellular Carcinoma Cells through the PI3K/Akt Signaling Pathway *Phytomedicine* 61(2019) 152843. *Phytomedicine*, 92: 153731.
- [51] Liu J, Huo C, Cao H, et al., 2019, Aloperine Induces Apoptosis and G2/M Cell Cycle Arrest in Hepatocellular Carcinoma Cells through the PI3K/Akt Signaling Pathway. *Phytomedicine*, 61: 152843.
- [52] Liu A, Liu C, 2024, In Vitro and In Vivo Antineoplastic Activities of Solamargine in Colorectal Cancer through the Suppression of PI3K/AKT Pathway. *Histol Histopathol*, 39(10): 1317–1328.
- [53] Ling Z, Guan H, You Z, et al., 2018, Aloperine Executes Antitumor Effects through the Induction of Apoptosis and Cell Cycle Arrest in Prostate Cancer In Vitro and In Vivo. *Onco Targets Ther*, 11: 2735–2743.
- [54] Ge J, Wang P, Ma H, et al., 2022, Solamargine Inhibits Prostate Cancer Cell Growth and Enhances the Therapeutic Efficacy of Docetaxel via Akt Signaling. *J Oncol*, 2022: 9055954.
- [55] Lu J, Sun D, Gao S, et al., 2014, Cyclovirobuxine D Induces Autophagy-Associated Cell Death via the Akt/mTOR Pathway in MCF-7 Human Breast Cancer Cells. *J Pharmacol Sci*, 125(1): 74–82.
- [56] Li L, Nong J, Li J, et al., 2024, Dendrobine Suppresses Tumor Growth by Regulating the PD-1/PD-L1 Checkpoint Pathway in Lung Cancer. *Curr Cancer Drug Targets*, 25(9): 1108–1117.
- [57] Luo Y, Liu G, Hou P, 2023, Synergism Effect of Dendrobine on Cisplatin in Treatment of H1299 by Modulating the Balance of Treg/Th17. *Anticancer Agents Med Chem*, 23(1): 105–112.
- [58] Tang Q, Zhou Q, Li J, et al., 2023, Solamargine Enhanced Gefitinib Antitumor Effect via Regulating MALAT1/miR-141-3p/Sp1/IGFBP1 Signaling Pathway in Non-Small Cell Lung Cancer. *Carcinogenesis*, 44(6): 497–510.
- [59] Liu Q, Xu M, Qiu M, et al., 2024, Solamargine Improves the Therapeutic Efficacy of Anti-PD-L1 in Lung Adenocarcinoma by Inhibiting STAT1 Activation. *Phytomedicine*, 128: 155538.
- [60] Han Y, Shi J, Xu Z, et al., 2022, Identification of Solamargine as a Cisplatin Sensitizer through Phenotypical Screening in Cisplatin-Resistant NSCLC Organoids. *Front Pharmacol*, 13: 802168.

- [61] Yin X, Li W, Zhang J, et al., 2021, AMPK-Mediated Metabolic Switching Is High Effective for Phytochemical Levo-Tetrahydropalmatine (l-THP) to Reduce Hepatocellular Carcinoma Tumor Growth. *Metabolites*, 11(12): 811.
- [62] Jiang X, Li H, Liu Y, 2024, Cyclovirobuxine D Inhibits Hepatocellular Carcinoma Growth by Inducing Ferroptosis of Hepatocellular Carcinoma Cells. *Discov Oncol*, 15(1): 96.
- [63] Tang Q, Li X, Chen Y, et al., 2022, Solamargine Inhibits the Growth of Hepatocellular Carcinoma and Enhances the Anticancer Effect of Sorafenib by Regulating HOTTIP-TUG1/miR-4726-5p/MUC1 Pathway. *Mol Carcinog*, 61(4): 417–432.
- [64] Liu X, Song L, Liu W, et al., 2025, Solamargine Inhibits Gastric Cancer Progression via Inactivation of STAT3/PD-L1 Signaling. *Mol Med Rep*, 31(2): 35.
- [65] Wang Z, Wu Z, Chen J, et al., 2025, Cyclovirobuxine D Inhibits Triple-Negative Breast Cancer via YAP/TAZ Suppression and Activation of the FOXO3a/PINK1-Parkin Pathway-Induced Mitophagy. *Phytomedicine*, 136: 156287.
- [66] Chen Y, Cai F, Mao Y, et al., 2021, The Anti-Neoplastic Activities of Aloperine in HeLa Cervical Cancer Cells Are Associated with Inhibition of the IL-6-JAK1-STAT3 Feedback Loop. *Chin J Nat Med*, 19(11): 815–824.
- [67] Qu X, Xie J, Zhang Y, et al., 2022, Solamargine Alleviates Proliferation and Metastasis of Cervical Cancer Cells by Blocking the CXCL3-Mediated Erk Signaling Pathway. *Evid Based Complement Alternat Med*, 2022: 7634754.
- [68] Qiu M, Yu L, Liang J, et al., 2023, Aloperine Prevents Migration, Invasion, and Adhesion by Upregulating TIMP-4 in Human Bladder Cancer Cells. *Protein Pept Lett*, 30(3): 250–259.
- [69] Pereira I, Silva L, Luis R, et al., 2024, Evaluation of in Vivo and in Vitro Efficacy of Solasonine/Solamargine-Loaded Lipid-Polymer Hybrid Nanoparticles Against Bladder Cancer. *Int J Pharm*, 661: 124411.

Publisher's note

Bio-Byword Scientific Publishing remains neutral with regard to jurisdictional claims in published maps and institutional affiliations.

Esophageal Carcinoma with Small-Cell Neuroendocrine Carcinoma Component and Lymph Node Metastasis Mixed with Poorly Differentiated Squamous Cell Carcinoma: A Rare Case Report

Binghui Ding*, Ling Li

Department of Thoracic Surgery II, Guangzhou Institute of Cancer Research, the Affiliated Cancer Hospital, Guangzhou Medical University, Guangzhou, China

**Author to whom correspondence should be addressed.*

Copyright: © 2025 Author(s). This is an open-access article distributed under the terms of the Creative Commons Attribution License (CC BY 4.0), permitting distribution and reproduction in any medium, provided the original work is cited.

Abstract: This study reports a case of a 74-year-old male patient with esophageal carcinoma who presented two months before admission with dysphagia and chest pain during meals. Preoperative imaging and biopsy revealed a mixed esophageal neuroendocrine carcinoma and non-neuroendocrine carcinoma (squamous cell carcinoma, SCC), with small-cell neuroendocrine carcinoma (SCNEC) comprising the predominant component (65%). Based on the preferences of the patient and his family, surgical treatment was performed first. Postoperative pathological examination revealed poorly differentiated SCC as the predominant component (approximately 90%), with SCNEC accounting for about 10% and lymph node metastasis present, indicating that the NEC component exhibited marked aggressiveness. This case highlights the importance of multiple deep preoperative biopsies and calls for a reevaluation of the WHO definition of Mixed Neuroendocrine-Non-Neuroendocrine Neoplasm (MiNEN), particularly the 30% threshold. Further clinical studies are warranted to refine the diagnostic criteria and therapeutic strategies for MiNEN to improve patient outcomes.

Keywords: Esophageal cancer; Mixed neuroendocrine-non-neuroendocrine neoplasm (MiNEN); Squamous cell carcinoma (SCC); Neuroendocrine carcinoma (NEC); Lymph node metastasis

Online publication: October 17, 2025

1. Introduction

Esophageal neuroendocrine carcinoma (NEC) is an extremely rare tumor, with an incidence of 3.56 per 100,000 in the United States and European countries; smoking and heavy alcohol consumption are the main risk factors ^[1]. It accounts for only 3.3% of all esophageal malignancies ^[2]. Globally, squamous cell carcinoma (SCC) is the most common type of esophageal cancer, comprising over 90% of cases, particularly in Asia, East Africa, and South

America^[3]. However, mixed tumors containing both NEC and SCC components in the esophagus are even rarer, and their diagnosis and treatment remain highly controversial. Although current treatment strategies include surgery, chemotherapy, radiotherapy, and targeted therapy, no standardized treatment protocol has been established because of the rarity of the disease. Here, we report a case of esophageal carcinoma with mixed NEC and SCC components.

2. Case report

A 74-year-old male presented with a two-week history of dysphagia and retrosternal pain during meals, occasionally accompanied by coughing. He had a 30-year history of smoking approximately 20 cigarettes per day and had quit one year prior to presentation. He also had a 30-year history of alcohol consumption, primarily Chinese liquor (baijiu), averaging 500 mL per day, and had not ceased drinking.

Barium swallow examination showed a narrow, strip-like passage of contrast medium at the level of the eighth to ninth thoracic vertebrae, approximately 5 cm in length, with rigidity of the mid-esophageal wall and poor peristaltic function. Upper abdominal CT (**Figure 1**) demonstrated thickening of the mid-esophageal wall with a maximum thickness of approximately 11 mm and enlarged mediastinal lymph nodes (up to 10 mm × 8 mm) with homogeneous enhancement, raising suspicion of lymph node metastasis.

Endoscopic biopsy (**Figure 2**) revealed a nodular mass located 33–37 cm from the incisors, with an eroded surface, friable texture, and contact bleeding. Histopathological examination with hematoxylin and eosin staining and immunohistochemistry demonstrated features consistent with a mixed neuroendocrine carcinoma–non-neuroendocrine carcinoma, comprising approximately 65% SCNEC and 35% SCC.

On admission, the patient's height was 162.0 cm and weight was 51.5 kg. Because of severe esophageal obstruction that precluded nasogastric feeding, a three-incision (cervical, thoracic, and abdominal) partial esophagectomy with intrathoracic esophagogastrostomy and jejunostomy was performed. Postoperative pathological findings are shown in **Figure 3** and **Figure 4**.

The postoperative clinical course was uneventful, and the patient was discharged without complications. Postoperative follow-up CT is shown in **Figure 1**.

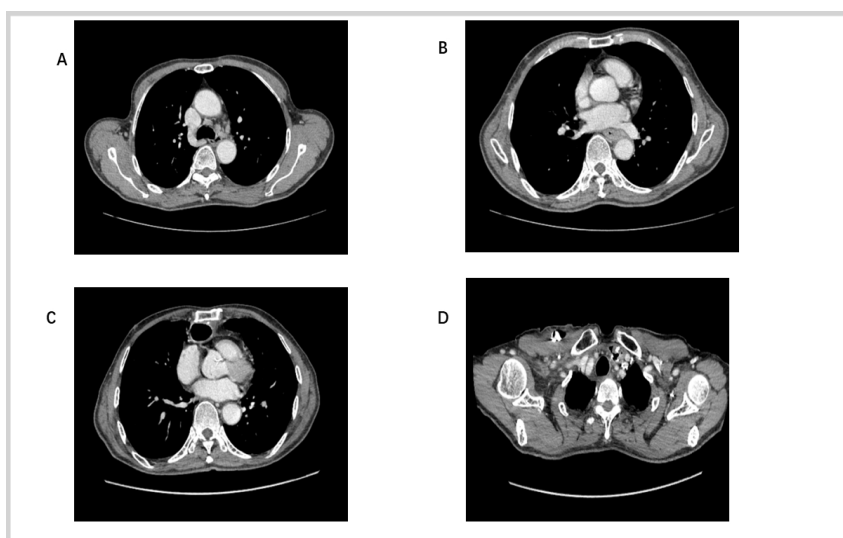


Figure 1. Preoperative and postoperative CT images of the patient. Panels A and B show preoperative CT images, while Panels C and D show postoperative CT images.

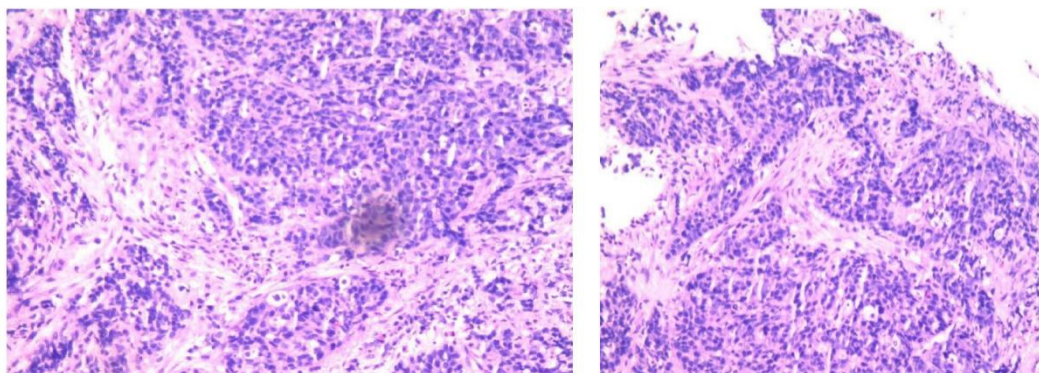


Figure 2. Endoscopic biopsy pathology.

Histopathological section obtained from preoperative endoscopic biopsy of the esophagus showing marked infiltration of atypical cells beneath the squamous epithelium, with some forming nests. Combined with immunohistochemistry, the findings are consistent with a mixed neuroendocrine carcinoma–non-neuroendocrine carcinoma, comprising approximately 65% SCNEC and 35% SCC. The final tumor component ratios will be determined from the postoperative resection specimen. Immunohistochemistry: CK (+), P40 (partial +), P63 (partial +), Synaptophysin (Syn; partial +), Ki-67 ($\approx 75\%$ +), CD56 (partial +), Chromogranin A (CgA; partial +), INSM1 (partial +), CK7 (scattered +), LCA (–), CAM5.2 (–), CK20 (–).

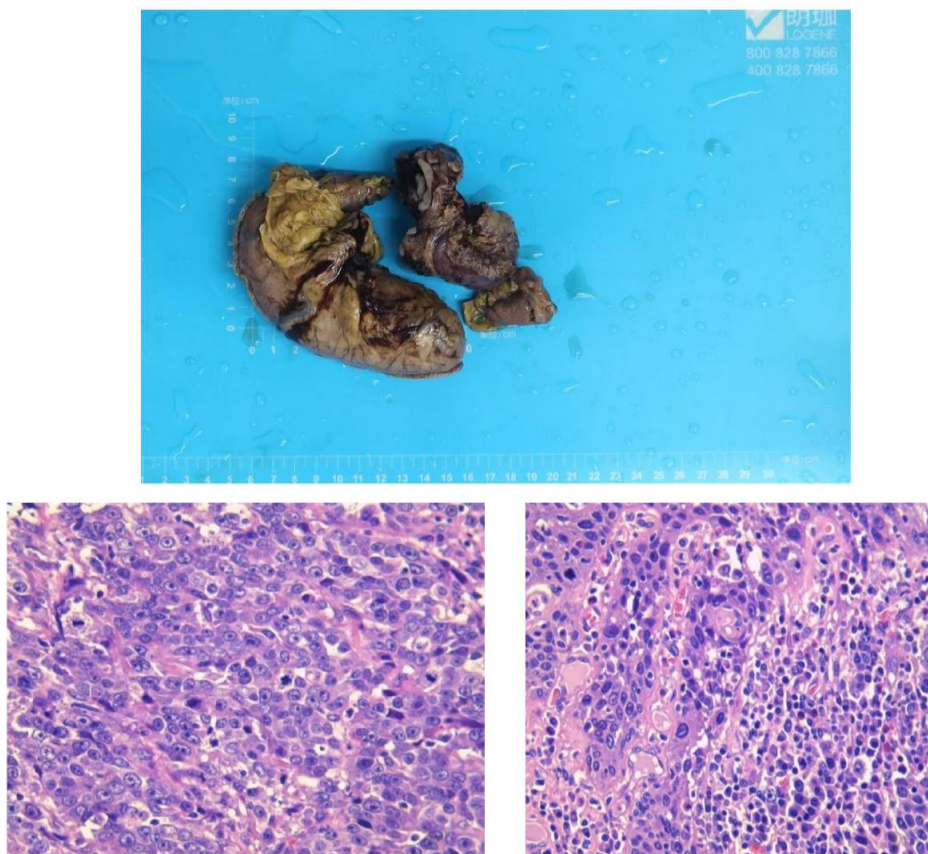


Figure 3. Postoperative specimens of esophageal carcinoma.

Specimens included: paraesophageal lymph nodes of the mid-esophagus, group 7 lymph nodes, proximal margin, distal margin, perigastric lymph nodes near the cardia, lymph nodes along the left gastric artery, esophagus with partial stomach, left supraclavicular lymph nodes, and paraesophageal lymph nodes of the distal esophagus (2 specimens).

Pathological findings: (1) Mid-esophageal paraesophageal lymph nodes: no metastatic carcinoma identified (0/2). (2) Group 7 lymph nodes: no metastatic carcinoma identified (0/6). (3) Proximal resection margin: esophageal tissue free of carcinoma. (4) Distal resection margin: no carcinoma observed in the sampled tissue. (5) Pericardial (cardia) lymph nodes: only fibrous, adipose, and muscular tissue were present; no lymph nodes or carcinoma identified. (6) Lymph nodes along the left gastric artery: no metastatic carcinoma detected (0/1). (7) Esophagus with partial stomach: consistent with a mixed neuroendocrine–non-neuroendocrine carcinoma, comprising approximately 10% SCNEC and 90% poorly differentiated SCC. Tumor infiltrated the full thickness of the esophageal wall into the periesophageal fibroadipose tissue, with suspected intravascular tumor emboli; no definite perineural invasion was observed. Gastric tissue was free of carcinoma. One lymph node identified in the peristomach adipose tissue showed no metastatic carcinoma (0/1). Immunohistochemistry (ID: 148968-018#): CK5/6 (+), P40 (+), Chromogranin A (CgA; –), Synaptophysin (Syn; –), INSM1 (focal +), TTF-1 (–), PD-L1 (22C3; CPS ≈8), PD-L1 (22C3 Neg; –), P53 (~90% +, suggestive of mutant type), Ki-67 (~70% +). (8) Left supraclavicular lymph nodes: no metastatic carcinoma detected (0/2). (9) Paraesophageal lymph nodes of the distal esophagus (2 specimens): no metastatic carcinoma detected (0/2).

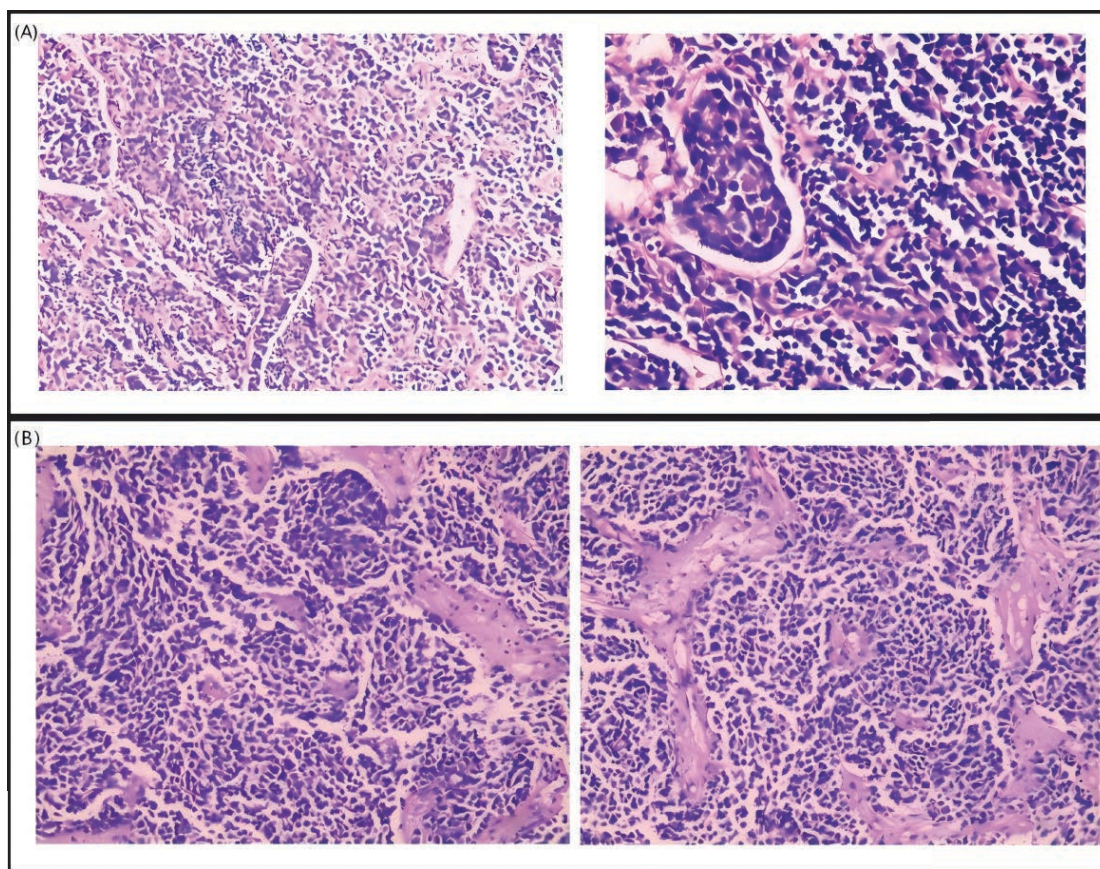


Figure 4. Intraoperative frozen sections. (A) Distal paraesophageal lymph node (intraoperative frozen section). Pathological diagnosis revealed metastatic small cell carcinoma in the examined lymph node (1/1), accompanied by necrosis. (B) Right pararecurrent laryngeal nerve lymph node. Pathological examination revealed metastatic small cell carcinoma in 2 out of 4 examined lymph nodes. Immunohistochemistry showed CK pan (+), Ki-67 (~90%+), Syn (+), and P40 (–).

3. Follow-up and recent examinations

The patient received multiple cycles of adjuvant chemotherapy combined with immunotherapy after surgery. Between November 25, 2023, and February 27, 2024, the patient completed five cycles of cisplatin combined with etoposide and atezolizumab as chemotherapeutic immunotherapy. Subsequently, the patient underwent regular radiotherapy and tolerated treatment well, with no severe adverse reactions observed. Following this, four cycles of albumin-bound paclitaxel chemotherapy were administered on May 29, June 17, July 14, and August 4, 2025, achieving stable disease (SD); all cycles were well tolerated and completed successfully.

Throughout the adjuvant treatment period, the patient remained clinically stable, with no evidence of tumor recurrence or distant metastasis. Repeated imaging studies and clinical follow-up indicated good recovery and a significant improvement in quality of life. During the postoperative and subsequent treatment period, the patient underwent regular imaging and endoscopic follow-up assessments, with findings as follows:

August 2025 follow-up CT (August 4, 2025) of the chest and entire abdomen showed postoperative changes of the esophagus, with no evidence of local tumor recurrence. The anastomosis appeared normal, and no abnormal soft tissue density was observed. Multiple small lymph nodes were seen in the mediastinum and hilar regions, without significant enlargement or signs of metastatic involvement. Chronic inflammatory changes and small pulmonary bullae were noted in both lungs, with no new solid nodules or evidence of metastasis. The liver, gallbladder, spleen, pancreas, and kidneys were unremarkable, and no abnormal fluid collection was observed in the abdominal or pelvic cavities. No evident metastatic lesions were detected in the skeletal system. Overall assessment revealed no evidence of local recurrence or distant metastasis.

July 2024 endoscopy demonstrated a patent anastomosis with well-healed mucosa and no evidence of tumor recurrence. Mucosal congestion and edema were noted in the gastric tube and lumen, suggesting postoperative reflux esophagitis, without stricture, obstruction, or neoplasm. The duodenal bulb mucosa appeared smooth, with no significant abnormalities.

Clinical status and quality of life: According to the most recent hospitalization record (August 2025), the patient reported no significant dysphagia, chest pain, or cough. Nutritional status was stable, body weight was 51 kg, and oral intake was unremarkable, with only occasional reflux symptoms. The patient's mental and physical condition was good, daily activities were independent, vital signs were stable, and overall general condition was satisfactory. Quality of life was significantly improved compared to preoperative status, with normal oral intake and minimal limitations in daily activities. The Karnofsky Performance Status score was estimated at 80–90.

In summary, the patient exhibited good overall recovery during the postoperative and follow-up periods, with no evidence of local recurrence or distant metastasis. Imaging and endoscopic evaluations revealed no tumor progression, nutritional status and quality of life were satisfactory, and the primary complaint was mild reflux symptoms.

4. Discussion

The 2019 World Health Organization (WHO) classification defined mixed neuroendocrine–non-neuroendocrine neoplasms (MiNEN), also referred to as mixed adenoneuroendocrine carcinoma (MANEC), as tumors composed of neuroendocrine (NE) and non-neuroendocrine (non-NE) components, with each component constituting at least 30% of the tumor ^[4]. However, the 30% threshold is primarily based on the assumption that a minor tumor component (< 30%) is unlikely to significantly affect the patient's biological behavior ^[5]. It is noteworthy, however,

that this cutoff is arbitrary and not supported by definitive clinical evidence ^[5]. Therefore, the precise diagnosis of MiNEN remains controversial.

Preoperative biopsy of the patient indicated a mixed neuroendocrine–non-neuroendocrine carcinoma, with small cell neuroendocrine carcinoma comprising approximately 65% and squamous cell carcinoma approximately 35%. Postoperative pathological examination revealed that small cell neuroendocrine carcinoma accounted for only about 10%, whereas poorly differentiated squamous cell carcinoma represented about 90% of the tumor. According to treatment strategies at many centers, MiNEN is often managed using the same approach as pure neuroendocrine carcinoma (NEC) ^[6], typically involving neoadjuvant chemoradiotherapy followed by surgery. However, given the patient's poor nutritional status and severe obstruction at admission, upfront surgical intervention was considered more beneficial. Considering that poorly differentiated squamous cell carcinoma constituted 90% of the postoperative specimens, neoadjuvant chemoradiotherapy would likely have limited effectiveness in symptom relief, functional improvement, or delaying tumor progression.

This case underscores the importance of performing multiple deep biopsies preoperatively to establish an accurate diagnosis ^[6]. Furthermore, although postoperative pathology indicated that small cell neuroendocrine carcinoma comprised only 10% of the tumor, metastases were observed intraoperatively in the right pararecurrent laryngeal nerve and distal paraesophageal lymph nodes. These findings demonstrate the biological activity of this minor component and support a diagnosis of MiNEN.

5. Conclusion

The study reported a rare case of esophageal MiNEN, initially diagnosed via preoperative biopsy as a mixed neuroendocrine–non-neuroendocrine neoplasm in which NEC predominated (~65%). Due to severe obstruction and poor nutritional status, the patient underwent upfront surgical treatment. Postoperative pathology revealed that poorly differentiated SCC predominated (~90%), with NEC comprising a minor component (~10%). Although the NEC component was minor, the presence of lymph node metastases indicated its aggressive biological behavior.

This case highlights the importance of thorough, deep, and multi-site biopsies for accurate diagnosis and emphasizes the need to consider the potential impact of even a minor NEC component on MiNEN biological behavior and clinical management. Although the 30% threshold defining MiNEN remains arbitrary and controversial, the presence of metastasis in this case supports the MiNEN diagnosis and suggests that such tumors can exhibit significant biological aggressiveness regardless of the proportion of each component. Further clinical studies are required to refine the diagnostic criteria and treatment strategies for MiNEN, ultimately aiming to improve patient prognosis.

Disclosure statement

The authors declare no conflict of interest.

References

- [1] Giannetta E, Guarnotta V, Rota F, et al., 2019, A Rare Rarity: Neuroendocrine Tumor of the Esophagus. *Crit Rev Oncol Hematol*, 137: 92–107.
- [2] Kanakasetty G, Dasappa L, Lakshmaiah K, et al., 2016, Clinicopathological Profile of Pure Neuroendocrine

Neoplasms of the Esophagus: A South Indian Center Experience. *J Oncol*, 2016: 2402417.

- [3] Reichenbach Z, Murray M, Saxena R, et al., 2019, Clinical and Translational Advances in Esophageal Squamous Cell Carcinoma. *Adv Cancer Res*, 144: 95–135.
- [4] Scoazec J, Rindi G, 2019, Oesophageal Neuroendocrine Neoplasms. In: WHO Classification of Tumours Editorial Board, ed. *WHO Classification of Tumours of the Digestive System*. 5th ed. International Agency for Research on Cancer, Lyon: 56–58.
- [5] Rosa S, Sessa F, Uccella S, 2016, Mixed Neuroendocrine-Nonneuroendocrine Neoplasms (MiNENs): Unifying the Concept of a Heterogeneous Group of Neoplasms. *Endocr Pathol*, 27(4): 284–311.
- [6] Sulaiman M, Agarwal S, Mandal A, et al., 2022, High-Grade Mixed Neuroendocrine Non-Neuroendocrine Neoplasm of the Gastroesophageal Junction: A Rare Case Report and Review of Literature. *Indian J Pathol Microbiol*, 65(4): 918–920.

Publisher's note

Bio-Byword Scientific Publishing remains neutral with regard to jurisdictional claims in published maps and institutional affiliations.

Exploring the Potential Biological Relationship Between Hypothyroidism and Gastric Cancer: Focus on SH2B3

Chengju Huang¹, Aoxiong Zhou², Xin Yang³, Xuejun Shen¹, Jin Wang^{1*}

¹Department of Gastrointestinal Surgery II, Guangzhou Cancer Institute, Affiliated Cancer Hospital of Guangzhou Medical University, Guangzhou, China

²Department of Radiotherapy V, Guangzhou Institute of Cancer Research, the Affiliated Cancer Hospital, Guangzhou Medical University, Guangzhou, China

³GCP Center, The Eighth Affiliated Hospital, Southern Medical University (The First People's Hospital of Shunde, Foshan), Foshan, 528300, Guangdong, China

*Corresponding author: Jin Wang, gdwjin@126.com

Copyright: © 2025 Author(s). This is an open-access article distributed under the terms of the Creative Commons Attribution License (CC BY 4.0), permitting distribution and reproduction in any medium, provided the original work is cited.

Abstract: *Background:* Gastric cancer (GC) is a common malignancy worldwide, and its development is influenced by genetic, metabolic, and immune microenvironmental factors. Hypothyroidism (HT), characterized by decreased thyroid hormone levels, has been suggested to influence tumor biology, but the molecular mechanisms linking HT to GC remain unclear. *Methods:* Based on Mendelian randomization (MR) studies identifying HT-related single-nucleotide polymorphisms (SNPs), the study annotated candidate genes using the Ensembl database and analyzed their differential expression in GC and normal tissues using GEPIA2. Functional enrichment analysis was performed using Metascape, and survival analysis was conducted with Kaplan–Meier Plotter. The study further evaluated the immune infiltration and clinicopathological associations of prioritized genes to investigate their potential roles in GC progression and therapeutic implications. *Results:* Among 121 candidate genes, 24 were differentially expressed in GC. Functional enrichment analysis revealed that these genes participate in cytokine response, angiogenesis, hemostasis, immune cell regulation, and autoimmune disease pathways. Survival analysis highlighted SH2B3 as a pivotal gene whose high expression correlated with poorer overall survival. Immune infiltration analysis revealed that SH2B3 expression positively correlated with CD8⁺ T cells, neutrophils, and cancer-associated fibroblasts, but negatively with myeloid-derived suppressor cells, suggesting a complex role in shaping the tumor immune microenvironment. Clinicopathological analysis demonstrated an increasing SH2B3 expression with tumor stage, grade, T/N/M classification, and copy number alterations. *Conclusion:* SH2B3 may serve as a key regulator bridging HT and GC by influencing tumor progression and immune microenvironment dynamics. These findings provide novel molecular and immunological insights into the potential protective role of HT in GC and underscore SH2B3 as a promising prognostic biomarker and therapeutic target.

Keywords: Gastric cancer; Hypothyroidism; SH2B3; Tumor immune microenvironment

Online publication: October 16, 2025

1. Introduction

Gastric cancer (GC) is a prevalent malignancy worldwide, with incidence and mortality rates consistently ranking among the highest of digestive system malignancies^[1]. The initiation and progression of GC are regulated by multiple factors, including genetic predisposition, metabolic abnormalities, and alterations in the immune microenvironment^[2]. Hypothyroidism (HT) is a common endocrine disorder characterized by elevated serum thyroid-stimulating hormone (TSH) levels accompanied by reduced synthesis of triiodothyronine (T3) and/or thyroxine (T4); in iodine-sufficient regions, autoimmune diseases such as Hashimoto's thyroiditis represent the primary causes of HT^[3].

Thyroid hormones play key roles in metabolic regulation, the regulation of cell proliferation, and the mediation of immune responses, functions that may directly or indirectly influence tumor initiation and progression^[4]. Previous studies have demonstrated that T3 and T4 can influence the biological behavior of tumor cells through various pathways, such as increasing cellular metabolic rate, inducing angiogenesis, and regulating cyclin expression, thus enhancing the proliferation and invasiveness of certain tumor cells^[5]. In the field of GC research, multiple clinical and experimental studies have reported associations between abnormal thyroid hormone levels and GC patient outcomes, such as prognosis, survival duration, tumor stage, and lymph node metastasis; for example, higher free T4 (fT4) levels and lower T3 levels have been significantly associated with shorter survival in gastroesophageal cancer patients^[6]. However, some studies have not observed significant associations between HT and GC, and the underlying mechanisms—particularly regarding immune regulation, inflammatory signaling pathways, and tumor microenvironmental interactions—remain unclear.

In traditional observational studies investigating the association between HT and GC, confounding factors such as age, *Helicobacter pylori* infection, dietary habits, and comorbid metabolic or autoimmune diseases pose challenges to accurate causal inference. In recent years, large-scale cohort studies have suggested a potential association between HT and GC risk; however, marked heterogeneity persists among study results^[7].

This study aims to systematically investigate the potential biological mechanisms linking HT and GC. The study analyzed the differential expression of genes mapped by HT-related single-nucleotide polymorphisms (SNPs) in GC tissues and evaluated their functional pathways and immune infiltration characteristics; the study further incorporated survival analyses and clinicopathological parameters to identify potential key genes and explore their mechanistic roles in the protective effects of HT on GC. This study seeks to provide molecular and immunological evidence elucidating the intrinsic relationship between HT and GC and to offer novel candidate targets for prognostic evaluation and immunotherapeutic strategies in gastric cancer.

2. Methods and materials

2.1. Experimental Design

Based on previously published Mendelian randomization (MR) studies suggesting a potential protective effect of HT on GC^[8], the study used the Ensembl database to annotate SNPs identified from MR analysis and determine their mapped genes. Subsequently, the study used GEPIA2 to analyze the differential expression of these genes between GC and normal tissues, and conducted functional and pathway enrichment analyses using Metascape to elucidate potential biological processes. The study further assessed the prognostic relevance of candidate genes using the Kaplan–Meier Plotter platform, selecting genes with $P < 0.05$, hazard ratio (HR) > 1 , and expression trends consistent with adverse prognostic outcomes. Finally, the study performed a literature search for the selected genes, giving priority to genes that had not been extensively investigated as potential targets, and analyzed their

immune infiltration characteristics and clinicopathological associations in GC to explore their potential value as therapeutic targets (**Figure 1**).

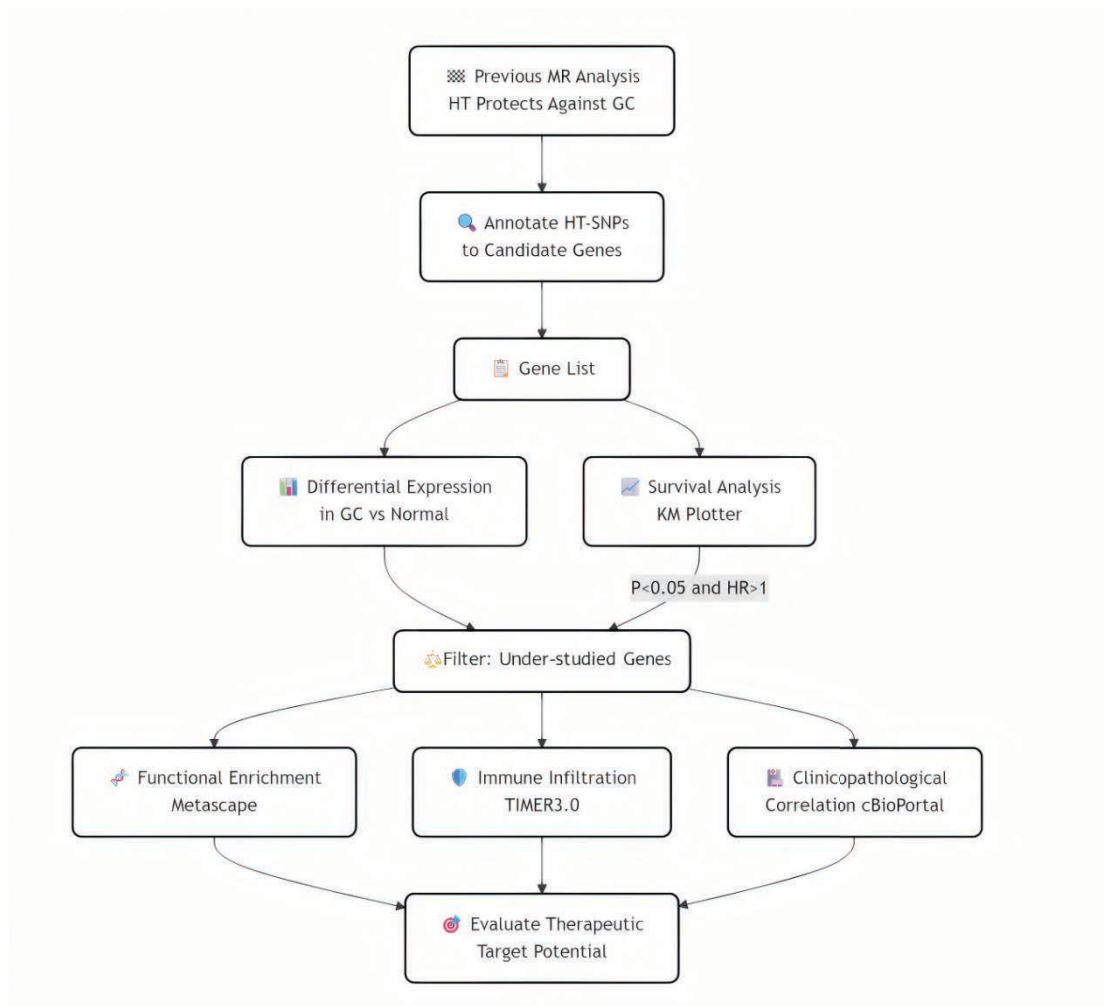


Figure 1. Experimental flow chart.

2.2. Data source

Based on previously published Mendelian randomization (MR) analysis results ^[8], the study further extracted single-nucleotide polymorphisms (SNPs) significantly associated with hypothyroidism (HT) and gastric cancer (GC) identified in the MR analysis and used them as candidate genetic variants for downstream analyses.

2.3. SNP functional annotation

Functional annotation and gene mapping of the candidate SNPs were performed using the Ensembl Genome Browser (<https://www.ensembl.org/>) ^[9]. The study retrieved each variant's chromosomal location and functional category (e.g., missense, synonymous, promoter region, intronic, or regulatory region) and obtained the corresponding target gene information.

2.4. Differential expression analysis

Differential expression analysis of the candidate genes between hepatocellular carcinoma samples (from the

TCGA database) and normal liver tissues (from the GTEx database) was performed using the GEPIA2 platform (<http://gepia2.cancer-pku.cn/>)^[10]. Expression levels were normalized as $\log_2(\text{TPM}+1)$, and a univariate differential test was applied.

2.5. Metascape functional enrichment analysis

Metascape (<http://metascape.org/gp/index.html#/main/step1>) is an integrative bioinformatics tool that integrates more than 40 distinct biological databases and offers interactive analyses, gene annotation, and other functions^[11]. The study used Metascape to perform rapid functional enrichment analyses of the identified differentially expressed genes.

2.6. Survival analysis

The study used the Kaplan–Meier Plotter online database (<https://kmplot.com/analysis>) to conduct survival analyses^[12]. Patients were stratified into high- and low-expression groups based on the median gene expression level. Kaplan–Meier survival curves were generated, and differences between groups were compared using the log-rank test. Hazard ratios (HRs) and 95% confidence intervals (CIs) were calculated. Two-sided P values < 0.05 were considered statistically significant.

2.7. Immune infiltration analysis

To explore the potential role of candidate genes in the tumor immune microenvironment, the study further used the TIMER3.0 database (<http://timer.cistrome.org/>) to analyze correlations between candidate genes and infiltration levels of various immune cell types^[13]. The immune cell types analyzed included CD8⁺ T cells, regulatory T cells (Tregs), macrophage subtypes (M0, M1, and M2), cancer-associated fibroblasts (CAFs), neutrophils, natural killer (NK) cells, and myeloid-derived suppressor cells (MDSCs). Correlations between gene expression and immune cell infiltration levels were evaluated using Spearman's correlation test, with significance set at $p < 0.05$.

2.8. Analysis of clinical pathological staging

cBioPortal for Cancer Genomics (<http://cbioportal.org>) is an open-access cancer genomics resource that provides an integrated view of cancer genomic datasets and associated clinical information^[14]. The study queried our target genes in cBioPortal to evaluate their mRNA expression levels and their relationships with clinical features in the TCGA-HNSC dataset. Gene expression distributions were extracted following cBioPortal's default workflow and compared across different pathological stages.

3. Results

3.1. SNP Functional Annotation

To further explore the potential functions and biological significance of SNPs identified in the MR analysis of hypothyroidism (HT) and gastric cancer (GC), the study used the Variant Effect Predictor (VEP) tool provided by the Ensembl database to perform functional annotation, identifying each SNP's genomic location, potential functional effects, and associations with diseases or phenotypes. After removing duplicates, 121 target genes were ultimately selected for further analysis.

3.2. Differential gene expression

The study analyzed the differential expression of the 121 selected genes between stomach adenocarcinoma (STAD) and normal tissues using the GEPIA2 platform. From this analysis, 24 differentially expressed genes were identified as candidate genes: AGO2, APOBR, ARID5B, C1QTNF6, CD44, CORO2A, DLEU1, GLIS3, HIVEP2, HLA-DPB1, IFIH1, IL2RA, ITGB4, ITPK1, LPP, NEK6, PHF20L1, RAPGEF3, SH2B3, SKAP2, SYN2, TLR3, TMEM86B, and TMOD1.

3.3. Enrichment analysis

To further investigate the potential biological roles of candidate genes in hypothyroidism (HT) and gastric cancer (GC), the study conducted multi-level enrichment analyses, including Pathway & Process, Cell Type Signatures, and disease enrichment using DisGeNET.

In the Pathway & Process enrichment analysis (**Table 1**), the differentially expressed genes were significantly enriched in cellular response to cytokine stimulus (6 genes, 25%), response to wounding (4 genes, 16.7%), positive regulation of angiogenesis (3 genes, 12.5%), hemostasis (4 genes, 16.7%), cell-cell communication (3 genes, 12.5%), and membraneless organelle assembly (3 genes, 12.5%). Additionally, these genes were enriched in the Influenza A pathway (3 genes, 12.5%).

In the Cell Type Signatures analysis (**Figure 2**), the differentially expressed genes were primarily enriched in immune cells and certain tissue-specific cell types. The most significantly enriched cell types included classical monocytes (TRAVAGLINI LUNG OLR1 CLASSICAL MONOCYTE, 5 genes, 21%), B lymphocytes (FAN OVARY CL18 B LYMPHOCYTE, 4 genes, 17%), dendritic cells (TRAVAGLINI LUNG EREG DENDRITIC CELL, 4 genes, 17%), and neutrophils (HAY BONE MARROW NEUTROPHIL, 3 genes, 12%). Additionally, some genes were enriched in midbrain neuronal subtypes (MANNO MIDBRAIN NEUROTYPES HMGL/HPERIC, 5 genes, 21%), embryonic brain myeloid cells (FAN EMBRYONIC CTX BRAIN MYELOID, 3 genes, 12%), and kidney thin ascending limb cells (LAKE ADULT KIDNEY C11 THIN ASCENDING LIMB, 3 genes, 12%). These results suggest that hypothyroidism-associated genes play a key role in immune surveillance and inflammation regulation, potentially enhancing anti-tumor immune responses by modulating the activity of monocytes, B lymphocytes, and dendritic cells. Moreover, the expression of some genes in neuronal and epithelial cells indicates that they may further influence gastric cancer risk through neuro-immune interactions and tissue homeostasis maintenance.

In the DisGeNET disease enrichment analysis (**Figure 3**), the differentially expressed genes were highly enriched in autoimmune diseases and disorders related to thyroid dysfunction. Significantly enriched diseases included hypothyroidism (11 genes, 46%), vitiligo (10 genes, 42%), celiac disease (8 genes, 33%), Graves' disease (8 genes, 33%), dermatomyositis/polymyositis (6–7 genes, 25%–29%), and multi-system autoimmune diseases (6 genes, 25%). Additionally, enrichment was observed for diabetes-related conditions (brittle diabetes, sudden-onset diabetes, ketosis-prone diabetes, 4 genes each, 17%), hematological parameters (eosinophil count, hematocrit), and lipid parameters (triglyceride levels). These findings indicate that hypothyroidism-associated genes are involved not only in autoimmune and endocrine regulation but may also indirectly influence gastric cancer development by modulating metabolic homeostasis.

Table 1. Top 7 clusters with representative enriched terms (one per cluster)

GO	Category	Description	Count	%	Log10(P)	Log10(q)
GO:0071345	GO Biological Processes	Cellular response to cytokine stimulus	6	25	-4.56	-0.22
hsa05164	KEGG Pathway	Influenza A	3	12.5	-3.47	0
GO:0009611	GO Biological Processes	Response to wounding	4	16.67	-3.35	0
GO:0045766	GO Biological Processes	Positive regulation of angiogenesis	3	12.5	-3.34	0
R-HSA-109582	Reactome Gene Sets	Hemostasis	4	16.67	-2.87	0
R-HSA-1500931	Reactome Gene Sets	Cell-cell communication	3	12.5	-2.64	0
GO:0140694	GO Biological Processes	Membraneless organelle assembly	3	12.5	-2.51	0

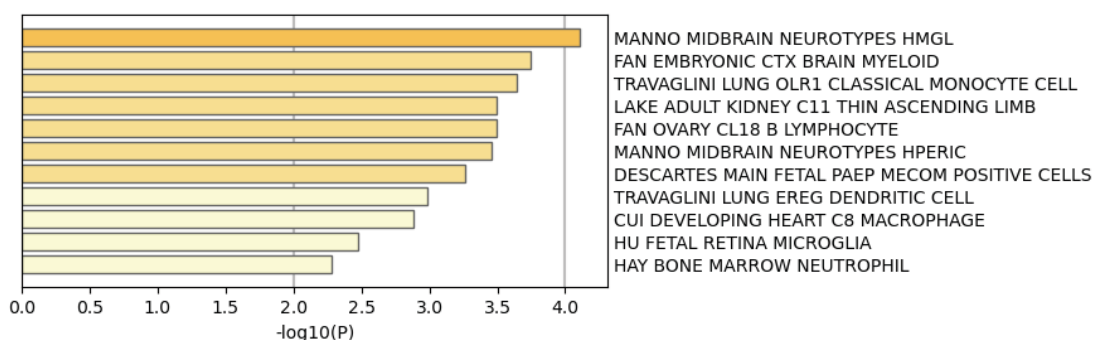


Figure 2. Enrichment of differentially expressed genes in various cell type signatures.

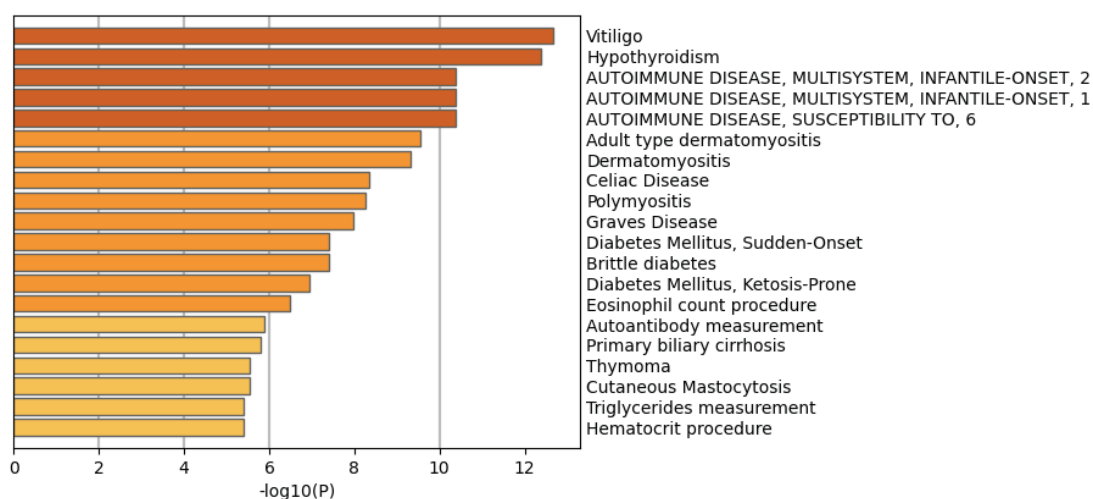


Figure 3. Disease enrichment analysis of differentially expressed genes based on DisGeNET.

3.4. Survival analysis of candidate genes and selection of target gene SH2B3

The 24 differentially expressed candidate genes in gastric cancer tissues were subjected to survival analysis using the Kaplan–Meier Plotter platform to evaluate their association with overall survival (OS). Genes with $P < 0.05$, hazard ratio (HR) > 1 , and expression trends consistent with prognostic outcomes were selected. Ultimately, six genes—AGO2 ($HR = 1.8$), C1QTNF6 ($HR = 2.25$), GLIS3 ($HR = 1.28$), ITGB4 ($HR = 1.62$), LPP ($HR =$

1.73), and SH2B3 ($HR = 1.62$)—were identified. All were highly expressed in gastric cancer tissues, and higher expression was associated with poorer OS. Subsequently, literature searches were performed for these six genes, revealing that SH2B3 has been relatively understudied in gastric cancer, although studies in other cancer types suggest it may have tumor-suppressive roles. Therefore, SH2B3 was selected as the target gene in this study for further analysis of its potential functions and clinical significance in gastric cancer (**Figure 4**).

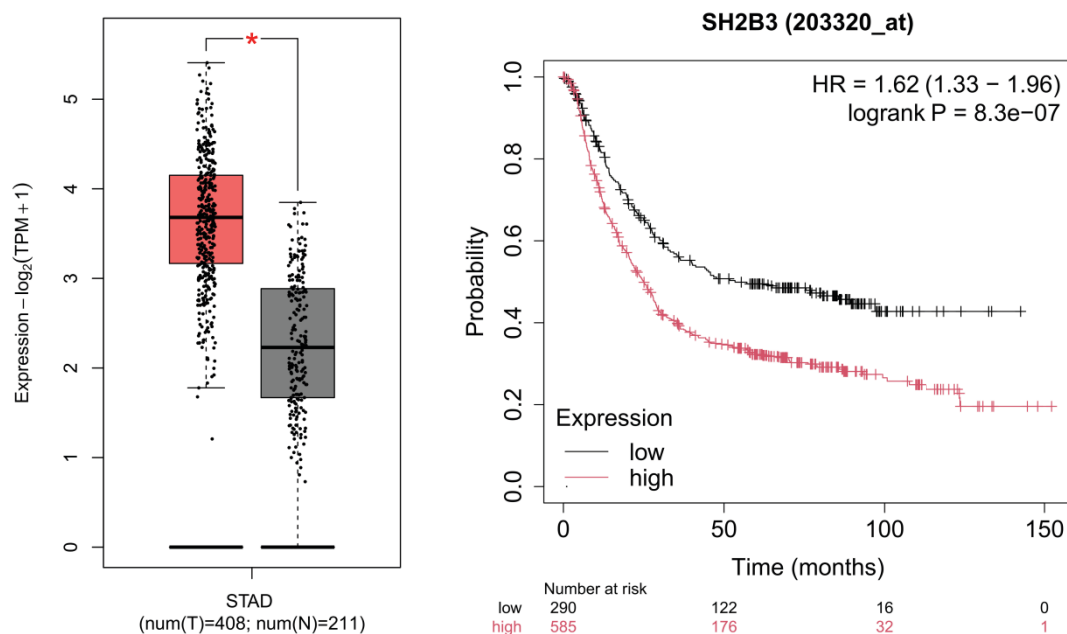


Figure 4. Expression difference and survival analysis of SH2B3 in STAD.

3.5. Immune infiltration analysis of SH2B3

To further investigate the role of SH2B3 in the tumor immune microenvironment, the study conducted a comprehensive analysis of its correlation with the infiltration levels of various immune cells (**Figure 5**). The results indicated that SH2B3 expression was significantly positively correlated with CD8⁺ T cells ($Rho = 0.595$, $p = 2.43 \times 10^{-37}$), as well as with neutrophils and cancer-associated fibroblasts ($Rho = 0.519$, $p = 3.16 \times 10^{-27}$; $Rho = 0.422$, $p = 1.32 \times 10^{-17}$), suggesting that high SH2B3 expression may be associated with increased recruitment of antitumor effector T cells and may influence the inflammatory status and stromal remodeling within the tumor microenvironment.

Additionally, SH2B3 showed mild positive correlations with M2 macrophages ($Rho = 0.148$, $p = 4.13 \times 10^{-3}$) and M1 macrophages ($Rho = 0.119$, $p = 2.14 \times 10^{-2}$), indicating that SH2B3 may contribute to a complex balance between inflammation and immune suppression within the tumor microenvironment. Notably, SH2B3 was significantly negatively correlated with myeloid-derived suppressor cells (MDSCs) ($Rho = -0.251$, $p = 8.51 \times 10^{-7}$), whereas its correlations with regulatory T cells (Tregs), activated natural killer (NK) cells, and M0 macrophages were not significant, suggesting that SH2B3 has limited or potentially negative regulatory effects on certain immunosuppressive cell subsets.

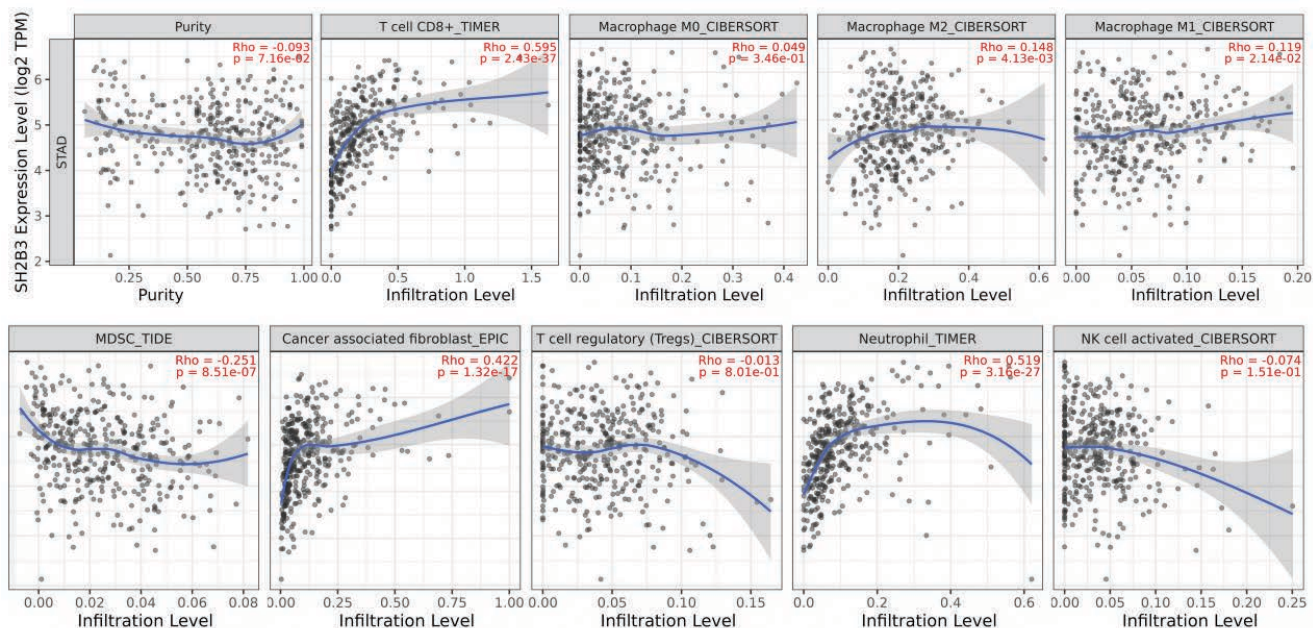


Figure 5. Correlation analysis between SH2B3 expression and tumor purity as well as immune cell infiltration levels in STAD.

3.6. Clinicopathological association analysis of SH2B3

To further investigate the association between SH2B3 and clinicopathological features in gastric cancer, the study systematically analyzed multiple dimensions, including tumor stage, histologic grade, T stage, lymph node stage, metastasis stage, and gene alteration types (**Figure 6**). The results indicated that SH2B3 expression in gastric cancer tissues displayed a progressively increasing trend with tumor progression.

In tumor stage analysis (based on Neoplasm Disease Stage American Joint Committee on Cancer Code), SH2B3 expression was generally low in STAGE I samples and gradually increased from STAGE IA. During mid-to-late STAGE II and STAGE III, expression levels were more dispersed, with some samples showing high expression; high-expression samples were still present in STAGE IV. Significant differences were observed among the tumor stage groups, indicating that SH2B3 expression may be closely associated with tumor progression.

In histologic grade analysis (based on Neoplasm Histologic Grade), G₁ tissues exhibited dispersed SH2B3 expression with a predominance of low-to-moderate levels; in G₂ tissues, the number of high-expression samples increased; in G₃ tissues, high-expression samples were more concentrated with overall elevated expression; GX tissues showed intermediate expression levels. Significant differences were also observed among histologic grade groups, suggesting that SH2B3 expression may reflect the differentiation status of gastric cancer tissues.

Regarding T stage (based on American Joint Committee on Cancer Tumor Stage Code), T₁ samples predominantly displayed low-to-moderate SH2B3 expression; expression gradually increased with T₂, T₃, and T₄ stages, with higher expression samples becoming more concentrated in T₃ and T₄. Notable differences were observed among T-stage groups, indicating that SH2B3 may be closely related to tumor invasion depth.

In lymph node stage analysis (based on Neoplasm Disease Lymph Node Stage American Joint Committee on Cancer Code), N₀ samples showed relatively low SH2B3 expression with few high-expression samples; expression increased progressively with lymph node involvement (N₁–N₃B), with high-expression samples significantly enriched in N₃A and N₃B; NX samples displayed a wide distribution. Significant differences were

observed among lymph node stage groups, suggesting that SH2B3 expression may be associated with lymph node metastasis.

In metastasis stage analysis (based on American Joint Committee on Cancer Metastasis Stage Code), M₀ samples mostly exhibited low-to-moderate expression; M₁ samples had a marked increase in high-expression proportion; MX samples showed a wide distribution, with some high-expression samples still present. Significant differences were observed among metastasis stage groups, indicating that SH2B3 expression may be related to distant metastasis.

Furthermore, SH2B3 expression was influenced by different gene alteration types. Missense (VUS) samples exhibited moderate and broadly distributed expression; amplification samples displayed overall higher expression, with several showing marked upregulation; shallow deletion samples had relatively low expression; gain-type samples exhibited moderate-to-high expression levels. Significant differences in expression were observed among different alteration types, suggesting that gene alterations may influence gastric cancer development and progression by modulating SH2B3 expression.

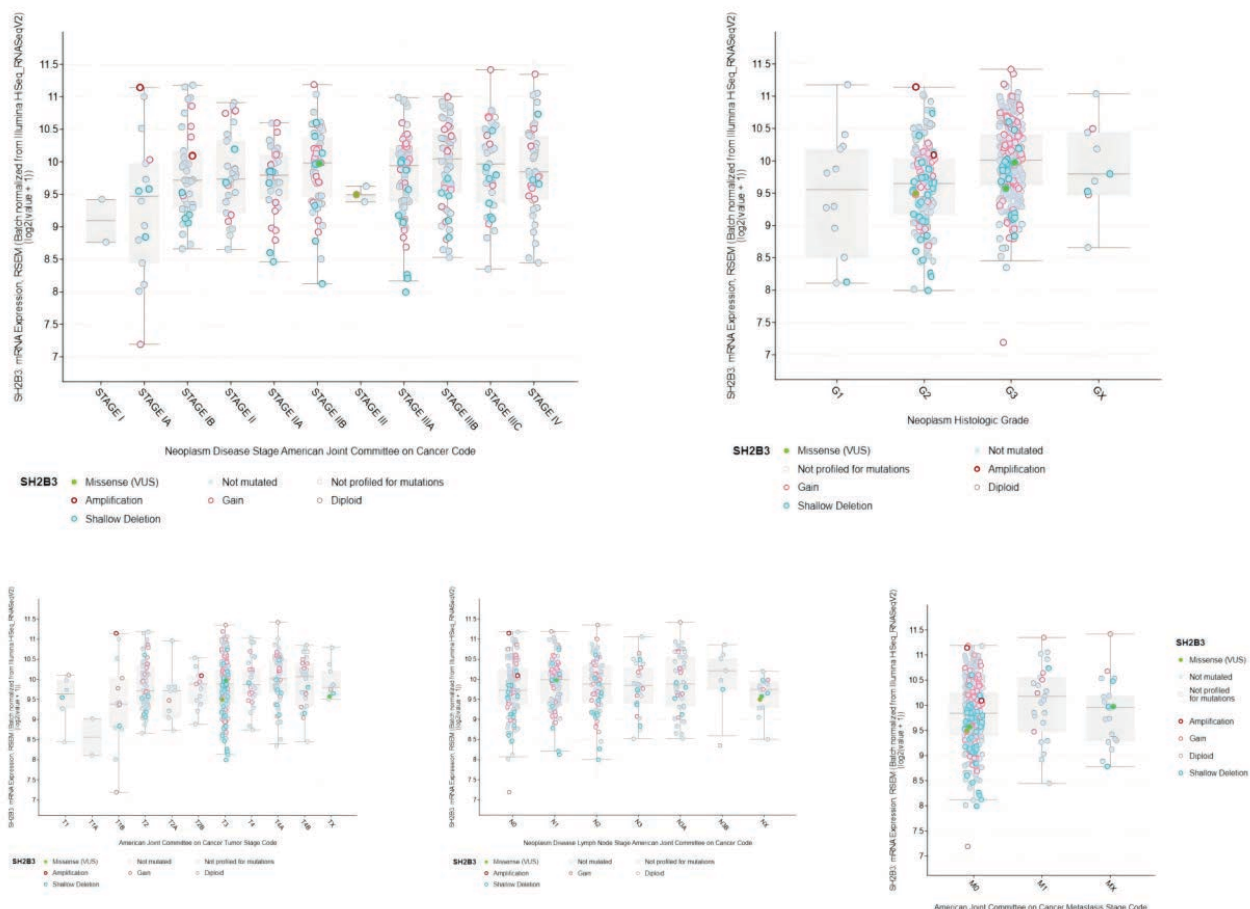


Figure 6. Correlation analysis between SH2B3 expression and clinicopathological features in STAD.

4. Discussion

This study utilized MR analysis as a starting point, combined with multidimensional bioinformatics tools, to explore the potential molecular mechanisms linking HT and GC. Based on candidate gene selection, differential

expression, functional pathway enrichment, and prognostic analyses, the study ultimately focused on SH2B3. This gene has not been extensively studied in the context of GC.

Functional enrichment analysis revealed that the candidate genes were primarily involved in cytokine response, hemostasis, angiogenesis, and immune cell-specific pathways, providing insights into potential mechanisms underlying the association between HT and GC. Cytokine-mediated responses are closely associated with gastric carcinogenesis; previous studies have shown that elevated levels of IL-6 and TNF- α in the gastric tumor microenvironment can activate the STAT3 and NF- κ B signaling pathways, promoting tumor cell proliferation and therapy resistance^[15,16]. HT, as an autoimmune disease, is characterized by chronic inflammation and cytokine imbalance^[17]. For example, IL-2 levels are significantly increased in HT patients, which may enhance antigen presentation and immune surveillance, potentially exerting a protective effect against tumor development^[18]. In our enrichment analysis, the “cellular response to cytokine stimulus” pathway was highly significant, suggesting that HT-related genes may reduce GC risk by maintaining or enhancing immune surveillance.

Additionally, the enrichment of angiogenesis and hemostasis pathways warrants attention. Angiogenesis is a critical factor in tumor growth and metastasis, particularly in GC, where VEGF signaling is closely associated with prognosis^[19]. Some studies have reported that thyroid hormone deficiency can inhibit VEGF-mediated angiogenesis^[20], potentially slowing tumor progression. In our study, the enrichment of “positive regulation of angiogenesis” and “hemostasis” pathways suggests that HT-related genes may indirectly influence GC development by modulating angiogenic and coagulation processes. Immune cell-specific analysis revealed that the candidate genes were significantly enriched in monocytes, B lymphocytes, and dendritic cells, indicating that HT may exert protective effects by promoting antigen presentation and adaptive immune responses. Activated dendritic cells are critical for inducing anti-tumor T cell responses, yet their function is often impaired in GC patients^[21]. Therefore, HT-related genes may partially restore or enhance this immune mechanism.

Disease enrichment analysis further indicated that the candidate genes are closely associated with multiple autoimmune disorders, including celiac disease, Graves’ disease, and vitiligo, consistent with the autoimmune nature of HT and suggesting a potential link to GC via a “shared immunogenetic background.” For instance, IL2RA is both a susceptibility gene for autoimmune diseases and a participant in immune evasion mechanisms in GC^[22,23].

SH2B3 (Src homology 2B adaptor protein 3, also known as LNK) is an intracellular signaling adaptor protein that plays critical roles in hematopoietic homeostasis, autoimmune responses, and inflammation regulation^[24]. Previous studies have primarily focused on its role in hematopoietic proliferation and leukemia, where it is thought to exert tumor-suppressive effects through inhibition of the JAK-STAT pathway^[24]. However, our results revealed that SH2B3 is highly expressed in GC, and its high expression is significantly associated with shorter overall survival, suggesting a potentially distinct function in solid tumors.

Analysis of immune infiltration showed that SH2B3 expression is significantly positively correlated with CD8⁺ T cells, indicating its potential involvement in recruiting anti-tumor effector cells. Simultaneously, SH2B3 was positively correlated with neutrophils and CAFs, which are known to promote inflammation, extracellular matrix remodeling, and immunosuppression in the tumor microenvironment^[25,26]. Moreover, the positive correlation with M2 macrophages suggests a role in promoting an immunosuppressive microenvironment. Interestingly, SH2B3 was negatively correlated with MDSCs, indicating limited or inhibitory effects on certain immunosuppressive subsets. These observations suggest that SH2B3 may act as a “double-edged sword” in

the GC immune microenvironment: promoting anti-tumor immune responses while simultaneously activating inflammatory and immunosuppressive networks, collectively facilitating tumor progression.

Clinicopathological analysis revealed that SH2B3 expression progressively increased with tumor stage, histologic grade, T stage, lymph node involvement, and distant metastasis, particularly in advanced-stage (Stage III–IV), high-grade (G₂–G₃), deeply invasive (T₃–T₄), extensively lymph node-positive (N₃), and metastatic (M₁) patients. Notably, copy number amplification was associated with significantly higher SH2B3 expression, whereas shallow deletion corresponded to lower levels, indicating that gene dosage effects may be an important driver of aberrant SH2B3 overexpression. Collectively, these results suggest that SH2B3 overexpression is not only closely related to GC occurrence and progression but may also serve as a molecular marker reflecting tumor invasiveness and metastatic potential.

Despite these findings, several limitations exist. First, the study relied primarily on publicly available databases, and the results may be influenced by sample size and inherent biases. Second, MR and bioinformatics analyses reveal associations rather than direct causal relationships. Third, the specific functions of SH2B3 in GC remain unvalidated *in vitro* and *in vivo*. Future studies should combine molecular biology experiments and clinical sample analyses to elucidate the mechanistic role of SH2B3 in GC and assess its potential as a therapeutic target.

In conclusion, this study identified a potential key role for SH2B3 in GC, suggesting that it may modulate the tumor immune microenvironment and disease progression. SH2B3 could serve as a prognostic marker and potential target for immunotherapy in GC. These findings provide new insights into the intrinsic link between autoimmune hypothyroidism and gastric cancer and offer a novel candidate gene for the development of precision therapeutic strategies in GC.

5. Conclusion

This study identified SH2B3 as a potential key gene linking HT and GC. SH2B3 is highly expressed in GC, correlates with poor prognosis, and is associated with tumor stage, histologic grade, metastasis, and immune cell infiltration. Functional analyses suggest that SH2B3 may regulate cytokine responses, angiogenesis, and the tumor immune microenvironment, potentially exerting dual roles in GC progression. These findings highlight SH2B3 as a potential biomarker and therapeutic target, providing new insights into the molecular and immunological connections between HT and GC.

Disclosure statement

The authors declare no conflict of interest.

References

- [1] Zhou L, Han B, Yuan Y, et al., 2025, The Global Burden of Stomach Cancer and Its Risk Factors from 1990 to 2021: Findings from the Global Burden of Disease Study 2021. *BMC Public Health*, 25(1): 2678.
- [2] Zhao L, Liu Y, Zhang S, et al., 2022, Impacts and Mechanisms of Metabolic Reprogramming of Tumor Microenvironment for Immunotherapy in Gastric Cancer. *Cell Death & Disease*, 13(4): 378.
- [3] Vargas-Uricoechea H, Castellanos-Pinedo A, Urrego-Noguera K, et al., 2025, A Scoping Review on the Prevalence of Hashimoto's Thyroiditis and the Possible Associated Factors. *Medical Sciences*, 13(2): 43.

- [4] Wan Y, Li G, Cui G, et al., 2025, Reprogramming of Thyroid Cancer Metabolism: From Mechanism to Therapeutic Strategy. *Molecular Cancer*, 24(1): 74.
- [5] Krashin E, Piekietko-Witkowska A, Ellis M, et al., 2019, Thyroid Hormones and Cancer: A Comprehensive Review of Preclinical and Clinical Studies. *Frontiers in Endocrinology*, 10: 59.
- [6] Puhf H, Wolf P, Berghoff A, et al., 2020, Elevated Free Thyroxine Levels Are Associated with Poorer Overall Survival in Patients with Gastroesophageal Cancer: A Retrospective Single Center Analysis. *Hormones & Cancer*, 11(1): 42–51.
- [7] Dore M, Manca A, Alfonso M, et al., 2020, Male Predominance of Gastric Cancer Among Patients with Hypothyroidism from a Defined Geographic Area. *Journal of Clinical Medicine*, 9(1): 135.
- [8] Zhang T, Qiao J, Wang Y, et al., 2024, Causal Link Between Hypothyroidism and Gastric Cancer Risk: Insights Gained Through Multivariable Mendelian Randomization and Mediation Analysis. *Frontiers in Endocrinology*, 15: 1388608.
- [9] Spudich G, Fernández-Suárez X, 2010, Touring Ensembl: A Practical Guide to Genome Browsing. *BMC Genomics*, 11: 295.
- [10] Tang Z, Kang B, Li C, et al., 2019, GEPIA2: An Enhanced Web Server for Large-Scale Expression Profiling and Interactive Analysis. *Nucleic Acids Research*, 47(W1): W556–W560.
- [11] Zhou Y, Zhou B, Pache L, et al., 2019, Metascape Provides a Biologist-Oriented Resource for the Analysis of Systems-Level Datasets. *Nature Communications*, 10(1): 1523.
- [12] Györfy B, 2021, Survival Analysis Across the Entire Transcriptome Identifies Biomarkers with the Highest Prognostic Power in Breast Cancer. *Computational and Structural Biotechnology Journal*, 19: 4101–4109.
- [13] Cui H, Zhao G, Lu Y, et al., 2025, TIMER3: An Enhanced Resource for Tumor Immune Analysis. *Nucleic Acids Research*, 53(W1): W534–W541.
- [14] Gao J, Aksoy B, Dogrusoz U, et al., 2013, Integrative Analysis of Complex Cancer Genomics and Clinical Profiles Using the cBioPortal. *Science Signaling*, 6(269): p11.
- [15] Qeadan F, Bansal P, Hanson J, et al., 2020, The MK2 Pathway Is Linked to G-CSF, Cytokine Production and Metastasis in Gastric Cancer: A Novel Interrelation Analysis Approach. *Journal of Translational Medicine*, 18(1): 137.
- [16] Lospinoso S, Falco G, Notarangelo T, 2025, Role of Soluble Cytokine Receptors in Gastric Cancer Development and Chemoresistance. *International Journal of Molecular Sciences*, 26(6): 2534.
- [17] Yao Z, Guo F, Tan Y, et al., 2024, Causal Relationship Between Inflammatory Cytokines and Autoimmune Thyroid Disease: A Bidirectional Two-Sample Mendelian Randomization Analysis. *Frontiers in Immunology*, 15: 1334772.
- [18] Hu J, Lei B, Wen D, et al., 2020, IL-2 Enhanced MHC Class I Expression in Papillary Thyroid Cancer with Hashimoto's Thyroiditis Overcomes Immune Escape in Vitro. *Journal of Cancer*, 11(14): 4250–4260.
- [19] Chen S, Zhang X, Peng J, et al., 2016, VEGF Promotes Gastric Cancer Development by Upregulating CRMP4. *Oncotarget*, 7(13): 17074–17086.
- [20] Luidens M, Mousa S, Davis F, et al., 2010, Thyroid Hormone and Angiogenesis. *Vascular Pharmacology*, 52(3–4): 142–145.
- [21] Xiao Z, Wang R, Wang X, et al., 2023, Impaired Function of Dendritic Cells Within the Tumor Microenvironment. *Frontiers in Immunology*, 14: 1213629.
- [22] Shouse A, LaPorte K, Malek T, 2024, Interleukin-2 Signaling in the Regulation of T Cell Biology in Autoimmunity and Cancer. *Immunity*, 57(3): 414–428.

- [23] Pan Z, Bao L, Lu X, et al., 2023, IL2RA+VSIG4+ Tumor-Associated Macrophage Is a Key Subpopulation of the Immunosuppressive Microenvironment in Anaplastic Thyroid Cancer. *Biochimica et Biophysica Acta - Molecular Basis of Disease*, 1869(1): 166591.
- [24] Morris R, Butler L, Perkins A, et al., 2021, The Role of LNK (SH2B3) in the Regulation of JAK-STAT Signalling in Haematopoiesis. *Pharmaceuticals*, 15(1): 24.
- [25] Jia H, Chen X, Zhang L, et al., 2025, Cancer Associated Fibroblasts in Cancer Development and Therapy. *Journal of Hematology & Oncology*, 18(1): 36.
- [26] Liu Z, Zeng H, Jin K, et al., 2022, TIGIT and PD-1 Expression Atlas Predicts Response to Adjuvant Chemotherapy and PD-L1 Blockade in Muscle-Invasive Bladder Cancer. *British Journal of Cancer*, 126(9): 1310–1317.

Publisher's note

Bio-Byword Scientific Publishing remains neutral with regard to jurisdictional claims in published maps and institutional affiliations.



Integrated Services Platform of International Scientific Cooperation

Innoscience Research (Malaysia), which is global market oriented, was founded in 2016. Innoscience Research focuses on services based on scientific research. By cooperating with universities and scientific institutes all over the world, it performs medical researches to benefit human beings and promotes the interdisciplinary and international exchanges among researchers.

Innoscience Research covers biology, chemistry, physics and many other disciplines. It mainly focuses on the improvement of human health. It aims to promote the cooperation, exploration and exchange among researchers from different countries. By establishing platforms, Innoscience integrates the demands from different fields to realize the combination of clinical research and basic research and to accelerate and deepen the international scientific cooperation.

Cooperation Mode



Clinical Workers



In-service Doctors



Foreign Researchers



Hospital



University



Scientific institutions

OUR JOURNALS



The *Journal of Architectural Research and Development* is an international peer-reviewed and open access journal which is devoted to establish a bridge between theory and practice in the fields of architectural and design research, urban planning and built environment research.

Topics covered but not limited to:

- Architectural design
- Architectural technology, including new technologies and energy saving technologies
- Architectural practice
- Urban planning
- Impacts of architecture on environment

Journal of Clinical and Nursing Research (JCNR) is an international, peer reviewed and open access journal that seeks to promote the development and exchange of knowledge which is directly relevant to all clinical and nursing research and practice. Articles which explore the meaning, prevention, treatment, outcome and impact of a high standard clinical and nursing practice and discipline are encouraged to be submitted as original article, review, case report, short communication and letters.

Topics covered by not limited to:

- Development of clinical and nursing research, evaluation, evidence-based practice and scientific enquiry
- Patients and family experiences of health care
- Clinical and nursing research to enhance patient safety and reduce harm to patients
- Ethics
- Clinical and Nursing history
- Medicine



Journal of Electronic Research and Application is an international, peer-reviewed and open access journal which publishes original articles, reviews, short communications, case studies and letters in the field of electronic research and application.

Topics covered but not limited to:

- Automation
- Circuit Analysis and Application
- Electric and Electronic Measurement Systems
- Electrical Engineering
- Electronic Materials
- Electronics and Communications Engineering
- Power Systems and Power Electronics
- Signal Processing
- Telecommunications Engineering
- Wireless and Mobile Communication

